

APPENDIX 2.10.9

TABLE OF CONTENTS

	<u>Page</u>
2.10.9	NUHOMS®-MP197 PACKAGE IMPACT LIMITER TESTING
2.10.9.1	Introduction 2.10.9-1
2.10.9.2	Scaling Relationships..... 2.10.9-3
2.10.9.3	Test Model Description..... 2.10.9-4
2.10.9.4	Test Description..... 2.10.9-6
2.10.9.5	Test Data and Results..... 2.10.9-8
2.10.9.6	Conclusions 2.10.9-17
2.10.9.7	References 2.10.9-18

LIST OF TABLES

2.10.9-1	Comparison of Calculated versus Measured g loads
----------	--

LIST OF FIGURES

- 2.10.9-1 One-Third Scale Test Model
- 2.10.9-2 Accelerometer Locations
- 2.10.9-3 NUHOMS[®]-MP197 Scale Model 0° Slap Down Drop Test Setup
- 2.10.9-4 NUHOMS[®]-MP197 Scale Model 20° End Drop Test Setup
- 2.10.9-5 NUHOMS[®]-MP197 Scale Model 90° Side Drop Test Setup
- 2.10.9-6 NUHOMS[®]-MP197 Scale Model Puncture Drop Test Setup
- 2.10.9-7 Test Article and Accelerometer Locations
- 2.10.9-8 0° Side Drop Test Setup
- 2.10.9-9 Acceleration Time History, with 1,000 Hz. Low-Pass Filter, 0° Side Drop, Accelerometer 1 (Top)
- 2.10.9-10 Acceleration Time History, with 1,000 Hz. Low-Pass Filter, 0° Side Drop, Accelerometer 1 (Top)
- 2.10.9-11 NUHOMS[®]-MP197 Cask Dummy and Impact Limiter After 0° Side Drop
- 2.10.9-12 NUHOMS[®]-MP197 Cask Dummy and Impact Limiter After 0° Side Drop
- 2.10.9-13 20° Side Drop Test Setup
- 2.10.9-14 Acceleration Time History, with 1,000 Hz. Low-Pass Filter, 20° Slap Down Drop, Accelerometer 1 (Top / Second Impact)
- 2.10.9-15 Acceleration Time History, with 1,000 Hz. Low-Pass Filter, 20° Slap Down Drop, Accelerometer 8 (Center of Gravity)
- 2.10.9-16 Acceleration Time History, with 1,000 Hz. Low-Pass Filter, 20° Slap Down Drop, Accelerometer 10 (Bottom / Second Impact)
- 2.10.9-17 NUHOMS[®]-MP197 Cask Dummy and Impact Limiter After 20° Slap Down Drop
- 2.10.9-18 NUHOMS[®]-MP197 Cask Dummy and Impact Limiter After 20° Slap Down Drop
- 2.10.9-19 90° End Drop Test Setup
- 2.10.9-20 Acceleration Time History, with 1,000 Hz. Low-Pass Filter, 90° End Drop, Accelerometer 7 (Center of Gravity)
- 2.10.9-21 Acceleration Time History, with 1,000 Hz. Low-Pass Filter, 90° End Drop, Accelerometer 11 (Bottom / Impact End)
- 2.10.9-22 NUHOMS[®]-MP197 Cask Dummy and Impact Limiter After 90° End Drop
- 2.10.9-23 NUHOMS[®]-MP197 Cask Dummy and Impact Limiter After 90° End Drop
- 2.10.9-24 NUHOMS[®]-MP197 Cask Dummy and Impact Limiter After Puncture Drop

APPENDIX 2.10.9

NUHOMS[®]-MP197 PACKAGE IMPACT LIMITER TESTING

2.10.9.1 Introduction

A series of dynamic tests have been performed on one-third scale models of the NUHOMS[®]-MP197 cask impact limiters. The tests were performed to evaluate the effects of the 30 foot free drop hypothetical accident defined in 10 CFR 71.73(c)(1) [1]. The test results are used to verify the analyses performed for the NUHOMS[®]-MP197 package. The objectives of the NUHOMS[®]-MP197 cask impact limiter test program are:

- Demonstrate that the inertia g values and forces calculated in Appendix 2.10.8 and used in the analyses presented in Appendices 2.10.1 through 2.10.5 are conservative.
- Demonstrate that the extent of crush depths are acceptable, i.e., limiters do not bottom out and the neutron shield does not impact the target.
- Demonstrate the adequacy of the impact limiter enclosure.
- Demonstrate adequacy of the impact limiter attachment design.
- Evaluate the effects of low temperature (-20° F) on the crush strength and dynamic performance of the impact limiters.
- Evaluate the effects (puncture depth and shell damage) of a 40 inch drop onto a scaled six inch diameter puncture bar on a previously crushed impact limiter, as per 10 CFR 71.73(c)(3).

The four 1/3 scale impact limiters that were constructed are identified as 1, 2, 3, and 4. The various drop test orientations were performed in the following sequence.

Test Number	Drop Orientation	Drop Height	Impact Limiter Number	Location of Impact Limiter	Comments
1	0° Side Drop	30 feet	1	Top	
			2	Bottom	
2	20° Slap Down	30 feet	3	Top (2 nd Impact)	Limiter #1 was removed and replaced with limiter #3, entire test article rotates 180°.
			2	Bottom (1 st Impact)	
3	90° End Drop	30 feet	3	Top	Limiter #2 was removed and replaced with limiter #4. Limiter #4 chilled at -20° F for 48 hours before installed to the test body.
			4	Bottom (Impact End)	
4	90° End Drop	40 inches	3	Top	Drop onto scaled 6 inch diameter puncture bar.
			4	Bottom (Puncture End)	

The 0° side drop was performed because this orientation generates the highest transverse acceleration as well as significant deformation. The 0° side drop also provides a reasonable estimate of the likelihood of the neutron shield impacting the target.

The 20° slap down drop was chosen to be performed because the 20° orientation puts the highest load on the impact limiter attachment bolts, and stainless steel shell.

The 90° end drop orientation was chosen to be performed because the 90° orientation causes the highest axial deceleration. For the 90° end drop, the bottom impact limiter was chilled at -20° F for at least 24 hours in order to acquire the most conservative estimate of the highest axial g load.

A 40 inch drop onto a 1/3 scale 6 inch diameter puncture bar was performed in accordance with 10 CFR 71.73(c)(3) in order to evaluate the effects of this drop on the NUHOMS[®]-MP197 transport package. Subsequent to the 30 foot end drop, the test model was dropped in the 90° end drop orientation onto the puncture bar, which was centered over test model's center of gravity. This orientation was chosen because it assures that the puncture impact absorbs 100% of the drop energy. Also the center of the impact limiter outer plate, where the puncture impact occurred, is the weakest portion of the impact limiter since there are no gussets in this location.

2.10.9.2 Scaling Relationships

The NUHOMS®-MP197 cask and impact limiter models are constructed with a geometric scale factor of $1/\lambda = 1/3$. Consequently, the following scale factors apply.

Length:

$$L_p = \lambda L_m$$

Surface area:

$$A_p = \lambda^2 A_m$$

Moment of inertia:

$$I_p = \lambda^4 I_m$$

Section modulus:

$$S_p = \lambda^3 S_m$$

Weight:

$$W_p = \lambda^3 W_m$$

Energy absorbed during drop (from same height h):

$$E_p = W_p h = \lambda^3 W_m h = \lambda^3 E_m$$

Velocity at beginning of impact:

$$V_p = \sqrt{2gh} = V_m$$

where λ is the scale factor, the subscript p refers to the full size, and the subscript m refers to the model.

During impact, the impact limiter materials will deform or crush. Since the model and full size impact limiters are made of the same materials, they deform under the same stress,

$$S_p = S_m.$$

Therefore we have the following relationships.

Force during impact:

$$F_p = S_p A_p = S_m \lambda^2 A_m = \lambda^2 F_m$$

Deformation:

$$D_p = E_p / F_p = \lambda^3 E_m / \lambda^2 F_m = \lambda D_m$$

Impact duration:

$$T_p = D_p / V_p = \lambda D_m / V_m = \lambda T_m$$

Impact deceleration:

$$a_p = V_p / T_p = V_m / \lambda T_m = 1/\lambda a_m$$

2.10.9.3 Test Model Description

The test model for the dynamic tests consists of a solid carbon steel test body with an impact limiter on each end, and a thermal shield located between the bottom impact limiter and the cask body. The test model, shown in Figure 2.10.9-1, is constructed to be as close as possible to one-third of the full size packaging.

2.10.9.3.1 Model Test Body

The model test body provides the proper one-third scale weight, CG location, and dimensions. The test body is 69.33 inches long with a gamma shield outside diameter of 27.33 inches. The reduced diameter portion, located in the axial center of the dummy is not important dimensionally, but is required to provide the proper overall weight and CG location. Important test model and full size packaging dimensions, weight, and CG location are provided below.

Test Model vs. Full Size Packaging

Component	Test Model	Full Size Packaging
Body Length (with spacer)	69.33 in.	208.00 in.
Package Length Including Impact Limiters and Thermal Shield	93.82 in.	281.25 in.
Gamma Shield Diameter	27.33 in.	82.00 in.
Package Outer Diameter Impact Limiters and Thermal Shield	40.67 in.	122 in.
Overall Package Weight	9,750 lb. (measured)	266,300 lb. (calculated)
Overall Package C.G. Location (measured from bottom surface of cask)	34.38 in. (measured)	102.85 in. (calculated)

The 1/3 scale attachment blocks are used to simulate the full scale impact limiter attachment method. The outer shell of the neutron shield is omitted from the 1/3 scale cask body. This omission is conservative, because the out shell structure would strengthen the connection between the attachment blocks and the cask body.

The attachment bolts are made of the same material specified for the full size limiters, but their dimensions are scaled down by a factor of one-third.

2.10.9.3.2 Impact Limiters

The one-third scale model impact limiters are scale models of the full size limiters with some minor exceptions. The steel impact limiter structure is the same as that described in Appendix 2.10.8; stainless steel shells closed off by flat plates and reinforced by twelve (12) radial gussets. The model and full scale configurations are almost identical, except that all linear dimensions in the model are one-third of those in the full scale impact limiter.

The spaces within the steel shells and gussets are filled with wood blocks, which are formed by gluing together a number of smaller pieces of wood. The balsa and redwood used in the model are consistent with that specified for fabrication of the full scale impact limiters. The model contains the same number of wood blocks as the full size impact limiters. The wood blocks are made up of a number of smaller pieces of wood glued together with phenol resorcinol adhesive, using the same procedure to be used on the full size impact limiters.

The differences between the model and full size limiters are as follows:

- a) The nearest standard plate thicknesses corresponding to one-third scale were used. The following dimensions for the scale model impact limiter components do not exactly conform to one-third scaling:

Component	Full-size Thickness	One-third Scale	Model Thickness
Stainless Steel Shell	0.25 in.	0.083 in.	0.0897 (13 Gauge)
12 Radial Gussets	0.19 in.	0.063 in.	0.0598 (16 Gauge)

- b) The support angles used as legs to allow the limiters to stand upright for storage are not included on the models.
- c) The fusible plugs that provide pressure relief during a fire are excluded. Only two openings diametrically opposite from each other are included in the model. Steel plugs are used instead of fusible plugs for sealing these openings and for leak testing.
- d) The lifting lugs are made larger than one-third scale to facilitate lifting.

2.10.9.4 Test Description

The drop tests were performed at the Department of Energy's Hanford Site drop pad facility (Area 300), near Richland Washington. The drop test was performed in accordance with approved written procedures.

The quick release mechanism used to drop the package consists of a hydraulic piston that opens a latch, releasing a shackle that supports the test model via a rigging system. The rigging system consists of nylon straps and padded shackles, which prevent ringing of the cask body during impact.

An inclinometer was placed on the test body to measure the initial angle ($\pm 1^\circ$) of its longitudinal axis with respect to the drop pad (i.e., impact surface). A measured line, 30 feet long (+ 3.0, -0.0 inches), was attached to the lowest point on the test dummy in order to assure the proper drop height.

The impact surface was an unyielding horizontal surface. The drop pad base consisted of an unyielding concrete pad weighing more than 250,000 lb. (weight of test dummy = 9,750 lb.) resting on bedrock. A hot rolled mild steel plate was securely attached to the concrete pad.

Accelerometers were used to measure the inertial g load during impact for the three 30 foot drops performed. The accelerometers were mounted to steel blocks, which were welded to the exterior of the test body at 0° , 90° , 180° , and 270° orientations at the approximate center of gravity location and adjacent to each impact limiter. The twelve (12) accelerometer locations are shown in Figure 2.10.9-2. Accelerometers were not mounted in locations that would result in certain destruction of the accelerometer. However, at least ten (10) accelerometers were used during each 30 foot drop.

The test setup for the 0° side drop is shown in Figure 2.10.9-3. For the side drop test, the accelerometers were oriented to measure accelerations in the drop direction (perpendicular to the drop pad surface).

The test setup for the 20° slap down drop is shown in Figure 2.10.9-4. The accelerometers located at the center of gravity and near the bottom impact limiter (1st impact) were oriented to measure accelerations 70° from the axis of the test model (perpendicular to the drop pad surface when the test model is oriented at a 20° angle). The accelerometers at the CG and near the bottom impact limiter (2nd impact) were oriented to measure accelerations perpendicular to the test model axis (perpendicular to the drop pad surface during slap down when the test modal axis is parallel to the drop pad surface).

The test setup for the end drop is shown in Figure 2.10.9-5. The package was oriented with the cask bottom facing down so that the impact occurred on the bottom end of the package. For the end drop test, the accelerometers were oriented to measure accelerations in the drop (axial) direction. The bottom impact limiter (impact limiter number 4) was kept in a conditioning chamber held at a temperature of -20° F for more than 48 hours. The time between removal of the impact limiter from the conditioning chamber and the test article drop was roughly 2 hours.

The test setup for the 90° puncture drop is shown in Figure 2.10.9-6. During the puncture drop the package was oriented so that the puncture bar impacted on the bottom end of the package. A scaled 6 inch diameter solid cylindrical puncture bar, 18 inches long was used. The puncture bar was constructed from mild steel and was welded to the drop pad with its long axis oriented in the vertical direction. Accelerometer data was not taken during the puncture drop.

PCB Model 350B04 accelerometers were used to measure the cask response. These transducers have a measurement range of $\pm 5000g$, and a shock limit of $\pm 50,000g$. The transducers have both electrical filtering and mechanical filtering, with a nominal frequency response of 1 – 10,000 Hz ($\pm 1dB$).

The lowest natural vibration frequencies of the test body, which are excited during the test, are much lower than this. These body vibrations involve small displacements (low stresses) at high frequencies, which excite the accelerometers and tend to mask the low frequency rigid body acceleration. This low frequency acceleration is masked, because both low frequency rigid body and high frequency natural vibration accelerations superimpose and the net acceleration is recorded. Filtering the data is necessary to remove these high frequency accelerations. A low pass filter is used to eliminate data above a specified cutoff frequency.

A TEAC XR-5000 14-channel instrumentation recorder was used to record the accelerometer signals.

A photograph of the accelerometer locations for each channel are shown in Figure 2.10.9-7. 1-4 are on the front (left side of cask in Figure 1), 5-8 are in the middle, and 9-12 are on the right side of the cask. Note that accelerometers 4, 8 and 12 are not visible in Figure 2.10.9-7.

The following data was measured and recorded before, during, and after each drop test.

1. Prior to each drop test.
 - a. Torque of the impact limiter bolts.
 - b. Impact limiter dimensions.
 - c. Height from test article to drop pad.
 - d. Angular orientation of the test article to the impact surface.
 - e. Atmospheric condition data, *i.e.*, ambient temperature, wind speed, immediately and prior to the release of the test article.

2. During each drop test.
 - a. Test article behavior on videotape.
 - b. Date and time of test.
 - c. Observations of damage or unexpected behavior of the test article
 - d. Impact acceleration time histories and frequency responses (excluding the puncture drop test).

3. Following each drop test.
 - a. Observations of the damage to the test article on features other than the limiters, *i.e.*, attachment bolts.
 - b. Measurements of deformation to each impact limiter to fully describe the extent of the damage. These measurements include:
 - i. Depth of external crushing on the impact limiter.
 - ii. Overall thickness of each impact limiter after each test.
 - iii. Width of impact footprint.

2.10.9.5 Test Data and Results

For purposes of reviewing test results, it should be noted that the energy to be absorbed by the scale model is approximately 1/27 of the full scale NUHOMS[®]-MP197 package value. The acceleration of the model is approximately three times that of the full size cask, and the crush deformation of the model limiter is approximately one-third that of the full size limiter. The impact force applied to the model is determined by multiplying the mass by the rigid body acceleration ($F = ma$). The model force is 1/9 of the full scale force.

2.10.9.5.1 0° Side Drop Test

The first drop test performed was the 0° side drop. Impact limiters 1 and 2 were placed on the top and bottom of the test model respectively. Two straps, connected to the test article and to each other with padded shackles, were used to support the test model. Figure 2.10.9-8 is a photograph of the test package set up just before the 0° drop test.

Accelerometer Data

The acceleration time history plots for the 0° side drop test appeared qualitatively reasonable. The plots generally show a single rounded peak roughly 0.012 s. long, with a high frequency low amplitude signal superimposed on top of it. The measured 1/3 scale impact duration of 0.012 s. corresponds to 0.036 s. for the full size package, which is consistent with the impact duration predicted by ADOC and used to compute the Dynamic Amplification Factor in Appendix 2.10.6.

Recorded Impact Duration (Figure 2.10.9-9)	Predicted Impact Duration From ADOC Computer Run
0.012 seconds (0.012 × 3 = 0.036 seconds)	0.036 seconds

A review of the acceleration data revealed that the accelerometer at location 5 recorded data inconsistent with the other eleven accelerometers. Consequently, the accelerations measured at location 5 are omitted from the data analyses for all three 30 foot drops.

Ten of the twelve accelerometers mounted to the dummy cask properly recorded acceleration data. The following table shows the transverse accelerations measured by the ten accelerometers during the 0° side drop (converted to full scale), as well as the acceleration range predicted by ADOC.

Accelerometer Location (see figure 2.10.9-2)		Measured Transverse Acceleration (gs) (full scale)	Average Measured Transverse Acceleration (gs)	Predicted Transverse Acceleration Range (Gs)
Top	1	61	61	53 - 60
	2	62		
	3	62		
	4	-		
Center of Gravity	5	-		
	6	63		
	7	62		
	8	63		
Bottom	9	57		
	10	61		
	11	58		
	12	62		

The accelerations measured during the side drop are at the high end of the range predicted by the ADOC computer program. The acceleration results presented in the above table are taken from the measured acceleration data filtered with a 1,000 Hz. Low pass filter. Figures 2.10.9-9 and 2.10.9-10 show the filtered acceleration time histories from accelerometers 1 and 10 respectively, which are characteristic of the acceleration plots in general. Note that the accelerations plotted in Figures 2.10.9-9 and 2.10.9-10 are for the 1/3 scale package, which is equivalent to 3 times the full scale accelerations.

Crush Depth Measurements

After the side drop test the top impact limiter (number 1) was removed from the test model body and impact limiter crush depths were measured. There was evidence of both inside and outside crushing. The following table summarizes the measured and predicted crush depths for the bottom impact limiter (slap down impact). A spring back of 0.50 inches is assumed (based of previous crush tests).

	Impact Limiter Number 1 (Top)	Impact Limiter Number 2 (Bottom)
Maximum Inside Crush Depth (in.)	1.44	1.50
Maximum Outside Crush Depth (in.)	0.75	0.75
Spring Back	0.50	0.50
Total Maximum Crush Depth (in.)	2.69	2.75
Predicted Total Maximum Crush Depth $\times 1/3$ (in.)	3.34 – 4.04	

From the above table it can be seen that the measured crush depths are slightly less than those predicted by the ADOC computer program.

It should also be noted that the neutron shield would not contact the target during the impact. The full scale distance between the end of the outer diameter of the neutron shield and the outside diameter of the impact limiter is 15.25 inches. Therefore, a clearance of 7.00 in. (full scale, $15.25 - 2.75 \times 3 = 7.00$) would remain between the crushed plane of the impact limiter and the neutron shield, based on the measured crush depth.

Damage Assessment

Both impact limiters remained attached to the cask during and after the side drop impact. All impact limiter attachment bolts remained intact, except for two bolts on the top impact limiter. These two bolts, located at 15° and 45° with respect to vertical, failed in shear.

Only a single small opening in the stainless steel impact limiter shell was evident. This opening consisted of a tear in the weld between the outer flat plate and the cylindrical shell of the impact limiter. The tear was roughly 0.25 inches wide and 6 inches long. Despite this tear, all impact limiter wood remained completely confined within the shell.

Figures 2.10.9-11 and 2.10.9-12 are photographs of the dummy cask and impact limiters after the 0° side drop.

2.10.9.5.1 20° Slap Down Test

The second drop test performed was the 20° slap down drop. Impact limiters 3 and 2 were placed on the top and bottom of the test model respectively. The cask was oriented such that the bottom end (with thermal shield) impacted the drop pad first. A two point strap rigging system was used to lift the test model by two lifting lugs. The two legs of the rigging system join at a single point that was shackled to the quick release mechanism. Figure 2.10.9-13 is a photograph of the test package set up just before the 20° slap down test.

Accelerometer Data

The acceleration time history plots for the 20° slap down test appeared qualitatively reasonable. The plots measured by the accelerometers located near the bottom impact limiter (first impact) generally show a single rounded peak roughly 0.016s. long, with a high frequency low amplitude signal superimposed on top of it.

The plots measured by the accelerometers located at the package center of gravity generally show two rounded peaks roughly 0.016s. (first impact), and 0.009 s. (second impact) long, with the second peak higher than the first. The plots at the center of gravity also show significant ringing of the cask throughout both impacts.

The plots measured by the accelerometers located near the top impact limiter (second impact) generally show a single rounded peak roughly 0.009s. long, with a high frequency low amplitude signal superimposed on top of it.

The following table shows the transverse accelerations measured by eleven accelerometers during the 20° slap down (converted to full scale), as well as the acceleration ranges predicted by ADOC. The measured and predicted accelerations are broken down into those generated during the initial impact and those generated during the second (slap down) impact. In addition, both the normal acceleration (translational only) at the package CG, and the rotational component of the transverse acceleration at the impact end (top or bottom) are reported.

Measured versus Predicted Accelerations during First Impact

Accelerometer Location (see figure 2.10.9-2)	Measured Acceleration (gs)	Average Measured Acceleration (gs)	Predicted Acceleration Range (gs)	
Normal Transverse Acceleration at Package CG (1 st Impact)	5	-	17	40 - 53
	6	17		
	7	16		
	8	18		
Rotational Acceleration at Bottom Impact Limiter (1 st Impact)	9	13	19	62 - 80
	10	21		
	11	21		
	12	22		

Measured versus Predicted Accelerations during Second Impact

Accelerometer Location (see figure 2.10.9-2)	Measured Acceleration (gs)	Average Measured Acceleration (gs)	Predicted Acceleration Range (gs)	
Normal Transverse Acceleration at Package CG (1 st Impact)	5	-	32	36 - 44
	6	32		
	7	32		
	8	32		
Rotational Acceleration at Top Impact Limiter (2 nd Impact)	1	53	53	69 - 83
	2	52		
	3	56		
	4	51		

The exact locations of the accelerations at the "Top" and "Bottom", reported in the table above, correspond to the locations of the reaction forces applied to the top and bottom impact limiters by the drop pad. These locations are computed by the ADOC computer program, which is described in detail in Appendix 2.10.8. Since the accelerometers mounted near the top and bottom impact limiters are not located at the impact limiter reaction point, the measured top and bottom accelerations, reported in the table above, are adjusted so that a proper comparison with the predicted accelerations can be performed. The locations of the reaction forces with respect to the package center of gravity for both impact limiters are provided in the following table. These locations are computed by the ADOC computer code (see Appendix 2.10.8), and are adjusted to 1/3 scale.

Distance Between Impact Limiter Reaction Forces and Package CG Location

	Maximum Wood Properties (in.)	Minimum Wood Properties (in.)	Average Value (in.)
Bottom Impact Limiter (First Impact)	30.2	30.4	30.3
Top Impact Limiter (Second Impact)	31.3	31.7	31.5

The distance between the accelerometers mounted near the top and bottom impact limiters and the center of gravity of the package are as follows.

Distance between Accelerometer Locations and Package CG Location

	Distance to CG (in)
Bottom Accelerometer (First Impact)	22.38
Top Accelerometer (Second Impact)	22.45

Since the relationship between transverse acceleration and the distance to the rotation point (CG location) is linear ($a = \omega r$), the transverse acceleration at the reaction force locations can be computed by linear interpolation in the following way:

$$\text{acceleration at top reaction location} = \text{measured top acceleration} \times \frac{31.5}{22.45}$$

$$\text{acceleration at bottom reaction location} = \text{measured bottom acceleration} \times \frac{30.3}{22.38}$$

The accelerations measured during the slap down drop are low relative to the range predicted by the ADOC computer program. The acceleration results presented in the above table are taken from the measured acceleration data filtered with a 1,000 Hz. Low pass filter. Figures 2.10.9-14, 2.10.9-15, and 2.10.9-16 show the filtered acceleration time histories from accelerometers 1, 8, and 10 respectively, which depict the general behavior of the acceleration histories at the top,

CG, and bottom of the package. Note that the accelerations plotted in Figures 2.10.9-14, 2.10.9-15 and 2.10.9-16 are for the 1/3 scale package, which is equivalent to 3 times the full scale accelerations.

Crush Depth Measurements

After the slap down test the impact limiters were removed from the test model body and their crush depths were measured. There was evidence of both inside and outside crushing. The following table summarizes the measured and predicted crush depths for the top and bottom impact limiter. A spring back of 0.50 inches is assumed (based of previous crush tests).

	Impact Limiter Number 3 (Top)	Impact Limiter Number 2 (Bottom)
Maximum Inside Crush Depth (in.)	2.42	0.42
Maximum Outside Crush Depth (in.)	1.80	4
Spring Back	0.50	0.50
Total Maximum Crush Depth (in.)	4.72	4.92
Predicted Total Maximum Crush Depth \times 1/3 (in.)	7.47 - 7.61	6.05 - 6.65

From the above table it can be seen that the measured crush depths are less that those predicted by the ADOC computer program.

It should also be noted that the neutron shield would not contact the target during the impact. Since the crush pattern on the top and bottom impact limiters occur at a 20° angle, and only at the outer edge, there is no possibility of the neutron shield impacting the target during the slap down impact.

Damage Assessment

Both impact limiters remained attached to the cask during and after the slap down impact. All impact limiter attachment bolts remained intact, except for four bolts on the top impact limiter (slap down side). Four bolts located 90° apart from each other, starting with the bolt located 45° from vertical, failed in shear. No two adjacent bolts failed.

No openings in the stainless steel impact limiter shell were evident, and no welds in the shell failed. The impact limiter wood remained completely confined within the shell.

Figures 2.10.9-17 and 2.10.9-18 are photographs of the dummy cask and impact limiters after the 20° slap down drop.

2.10.9.5.2 90° End Drop Test

The third drop test performed was the 90° end drop. Impact limiters 3 and 4 were placed on the top and bottom of the test model respectively. The cask was oriented such that the bottom end impacted the drop pad. Two straps were attached to the test article's top two lifting lugs and to the quick release mechanism with padded shackles. Figure 2.10.9-19 is a photograph of the test package set up just before the 90° end drop test.

Accelerometer Data

The acceleration time history plots for the 90° end drop test appeared qualitatively reasonable. The plots generally show a single rounded peak 0.010 s. long, with a high frequency low amplitude signal superimposed on top of it. The measured 1/3 scale impact duration of 0.010 s. corresponds to 0.030 s. for the full size package, which is consistent with the impact duration predicted by ADOC and used to compute the Dynamic Amplification Factor in Appendix 2.10.6.

The following table shows the axial acceleration measured by nine accelerometers, during the 90° end drop, as well as the range of axial acceleration predicted by ADOC (accelerometers at locations 1 and 3 were removed from the package, because of interference with the rigging system in the vertical orientation).

Accelerometer Location (see figure 2.10.9-2)	Measured Axial Acceleration (gs)	Average Measured Axial Acceleration (gs)	Predicted Axial Acceleration Range (gs)		
Top	1	-	65		
	2	63			
	3	-			
	4	68			
Center of Gravity	5	-		44 - 50	
	6	65			
	7	66			
	8	66			
Bottom	9	63			65
	10	63			
	11	62			
	12	70			

The higher than predicted accelerations are attributed to the fact that the bottom impact limiter was chilled to -20° F prior to the drop test. The crush strength of balsa and redwood increases as temperature decreases.

The acceleration results presented in the above table are taken from the measured acceleration data filtered with a 1,000 Hz. Low pass filter. Figures 2.10.9-20 and 2.10.9-21 show the filtered acceleration time histories from accelerometers 7 and 11 respectively, which are characteristic of the acceleration plots in general. Note that the accelerations plotted in Figures 2.10.9-20 and 2.10.9-21 are for the 1/3 scale package, which is equivalent to 3 times the full scale accelerations.

Crush Depth Measurements

After the end drop test the crush depths of the bottom impact limiter were measured. There was evidence of both inside and outside crushing. The following table summarizes the measured and predicted crush depths for the bottom impact limiter (impact limiter 4). A springback of 0.50 inches is assumed.

	Impact Limiter Number ? (Top)
Maximum Inside Crush Depth (in.)	1.75
Maximum Outside Crush Depth (in.)	0.25
Spring Back	0.50
Total Maximum Crush Depth (in.)	2.50
Predicted Total Maximum Crush Depth \times 1/3 (in.)	3.51 – 4.48

The relatively low crush depth measured after the 90° end drop, compared with predicted values can be attributed to the fact that the bottom impact limiter was chilled to -20° F prior to the drop test.

Damage Assessment

Both impact limiters remained attached to the cask during and after the end drop impact, and all impact limiter attachment bolts remained intact.

No openings in the stainless steel impact limiter shell were evident, and no welds in the shell failed. The impact limiter wood remained completely confined within the shell.

Figures 2.10.9-22 and 2.10.9-23 are a photographs of the test dummy and impact limiters after the 90° end drop.

2.10.9.5.4 Puncture Drop Test

The final drop test performed was the puncture drop. In order to simulate the proper sequence of accident events specified in 10 CFR 71.73, the impact limiters used for the end drop test were left on the dummy cask without adjustment or tightening of the attachment bolts. Two straps, attached to top two lifting lugs, were used to support the test model in the 90° vertical orientation with the test model's bottom end facing down. The puncture bar impacted impact limiter 4, which was previously crushed during the 90° end drop. No accelerometer data was taken, since the purpose of the puncture drop is to obtain impact limiter damage only. Figure 2.10.9-6 depicts the test setup up for the 90° puncture drop test.

Test Results

The puncture bar impacted the test package squarely in the center of the outer flat surface of the bottom impact limiter shell. The puncture bar cleanly punched through the outer stainless steel shell of the impact limiter and was imbedded in the impact limiter wood. The test package came to rest in the vertical position, perfectly balanced on top of the puncture bar.

The puncture bar sheared a circular section, roughly 2 inches in diameter, of the outer shell of the bottom impact limiter. No other sections of the impact limiter were damaged, and no welds on the impact limiter shell were broken. The impact limiter wood remained completely contained by the impact limiter shell, and no impact limiter wood could be seen at the puncture point.

The puncture bar was stopped by a thin wedge of impact limiter wood that was compacted between the top of the puncture bar and the inner shell of the impact limiter. The puncture bar did not penetrate the inner stainless steel shell of the impact limiter or the aluminum thermal shield.

Both impact limiters remained attached to the cask during the puncture drop event, and no additional impact limiter attachment bolts were damaged.

Figure 2.10.9-24 is a photograph of the test dummy and impact limiters after the puncture drop.

2.10.9.6 Conclusions

The predicted performance of the impact limiters in terms of accelerations and crush depths agrees well with the measured data. Table 2.10.9-1 summarizes the maximum inertial loads measured during the dynamic testing program, as well as the maximum inertial loads computed by ADOC and used in the NUHOMS[®]-MP197 transport package structural analysis. Table 2.10.9-1 demonstrates that the inertial loads calculated in Appendix 2.10.8 are reasonable and that the inertial loads used in the analyses in Appendices 2.10.1 through 2.10.5 are conservative.

The results of the dynamic tests demonstrate that:

- The crush depths do not result in lockup of the wood in the limiters.
- The crush depths for the 0° side drop case would not result in the neutron shield impacting the target.
- The predicted performance of the impact limiters in terms of decelerations and crush depths agrees well with the measured data.
- The impact limiter enclosure is structurally adequate in that it successfully confines the wood inside the steel shell.
- The impact limiter attachment design is structurally adequate in that the attachment bolts hold the impact limiters on the ends of the cask during all drop orientations.
- The effects of low temperature (-20° F) on the crush strength of the impact limiters is minor, and is bounded by the conservative accelerations and forces used in the analysis in Appendices 2.10.1 through 2.10.5.
- A 40 inch drop onto a scaled six inch diameter puncture bar, as per 10 CFR 71.73(c)(3), does not significantly destroy the impact limiter. The impact limiter and attachments remain firmly secured to the cask, and the impact limiter wood is confined.

2.10.9.7 References

1. 10 CFR PART 71, Packaging and Transportation of Radioactive Material.

TABLE 2.10.9-1

Comparison of Calculated vs. Measured g loads

30 foot Drop Orientation	Average g Load Measured by Drop Test (Appendix 2.10.9)	g Load Computed by ADOC (Appendix 2.10.9)	Input Loading Used in Stress Analysis** (Appendix 2.10.1)
0° Side Drop	61g Transverse	53g – 60g Transverse	75g Transverse
20° Side Drop	32g Normal	36g – 44g Normal	60g Normal
	53g Rotational	69g – 83g Rotational	196g Rotational
90° End Drop	65g Axial	46g – 50g Axial	75g Axial

** Conservatively Using Higher g loads

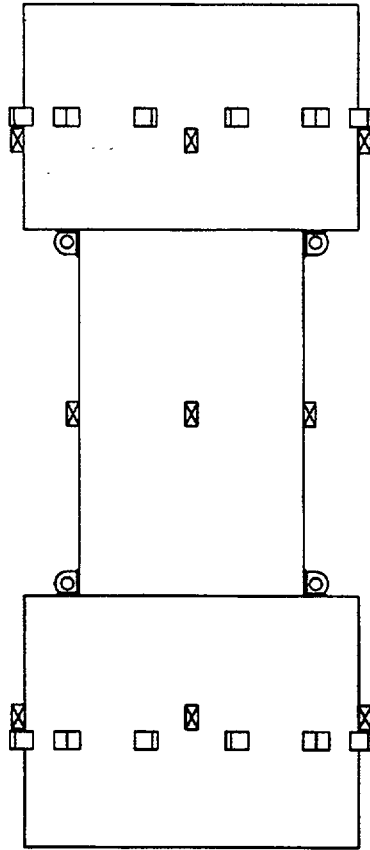
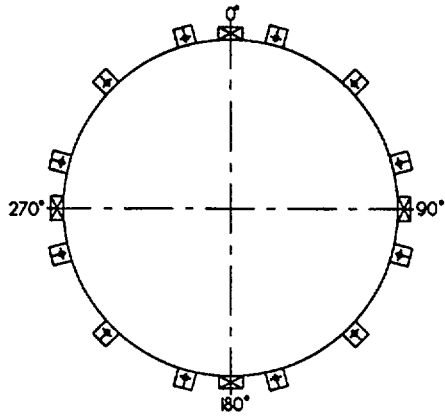
Figure 2.10.9-1

One-Third Scale Test Model

**FIGURE WITHHELD AS SENSITIVE
UNCLASSIFIED INFORMATION**

Figure 2.10.9-2

Accelerometer Locations



☒ ACCELEROMETER

Figure 2.10.9-3

NUHOMS[®]-MP197 Scale Model 0° Side Drop Test Setup

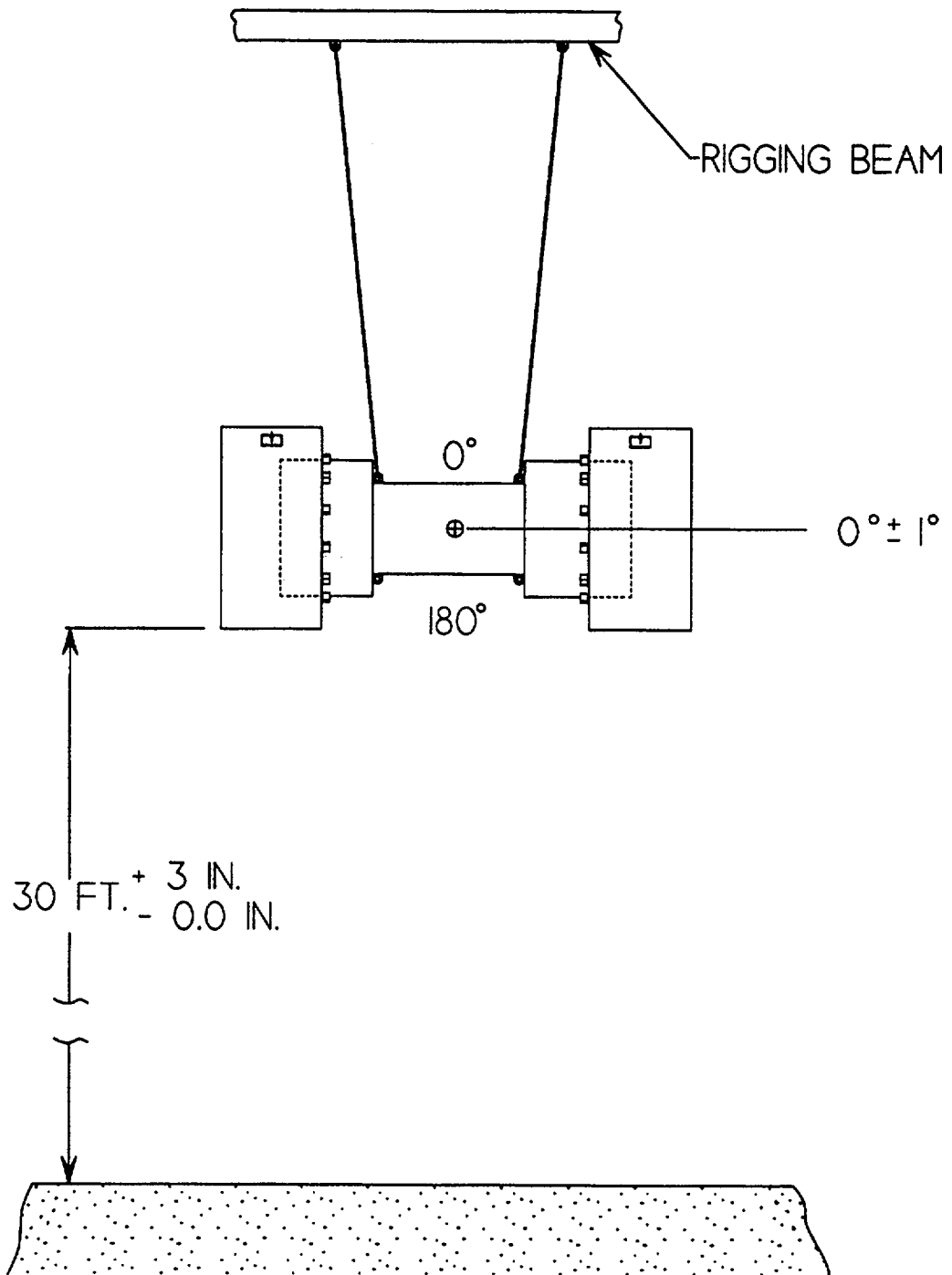


Figure 2.10.9-4

NUHOMS[®]-MP197 Scale Model 20° Slap Down Test Setup

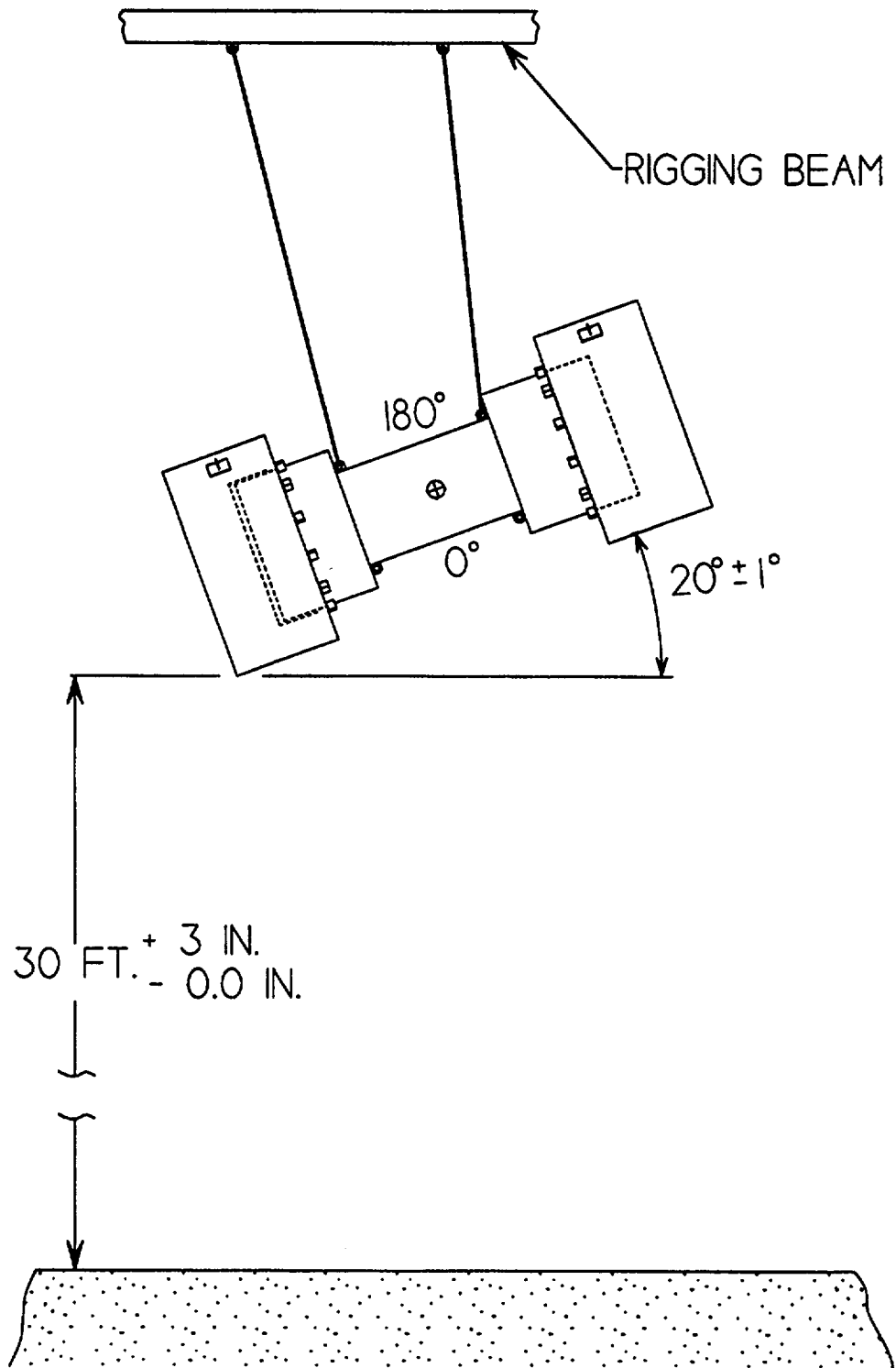


Figure 2.10.9-5

NUHOMS[®]-MP197 Scale Model 90° End Drop Test Setup

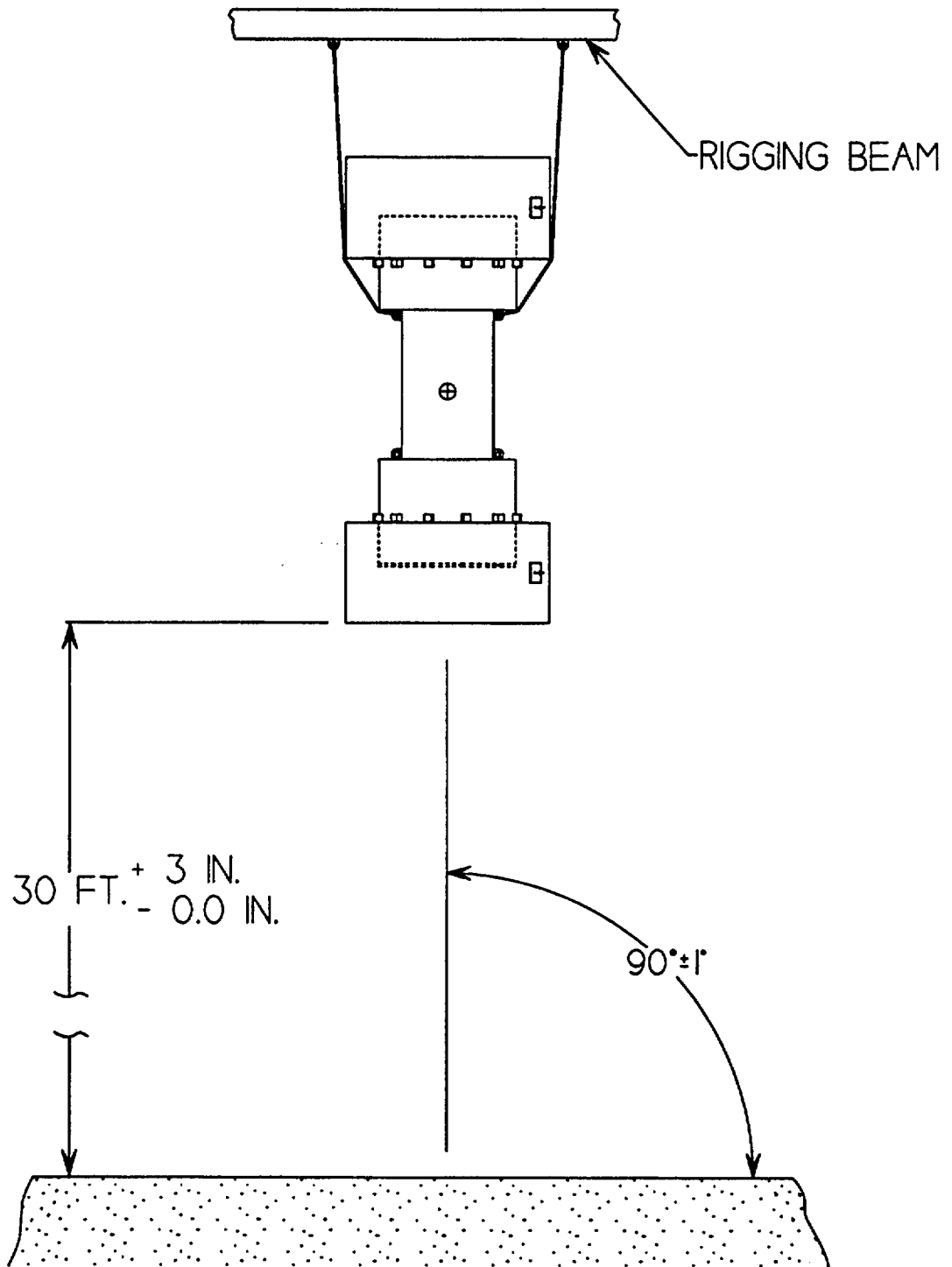


Figure 2.10.9-6

NUHOMS[®]-MP197 Scale Model Puncture Drop Test Setup

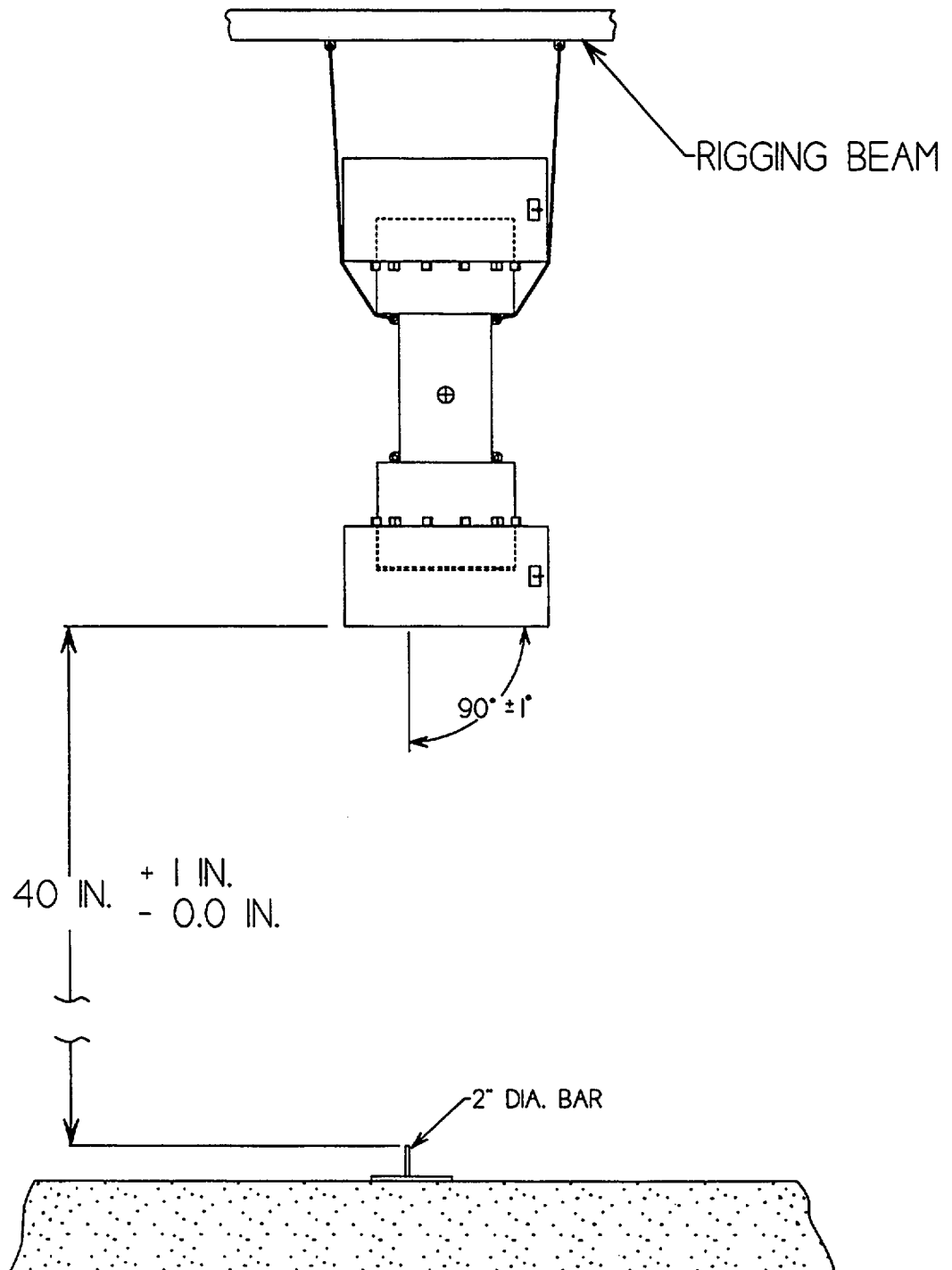


Figure 2.10.9-7

Test Article and Accelerometer locations

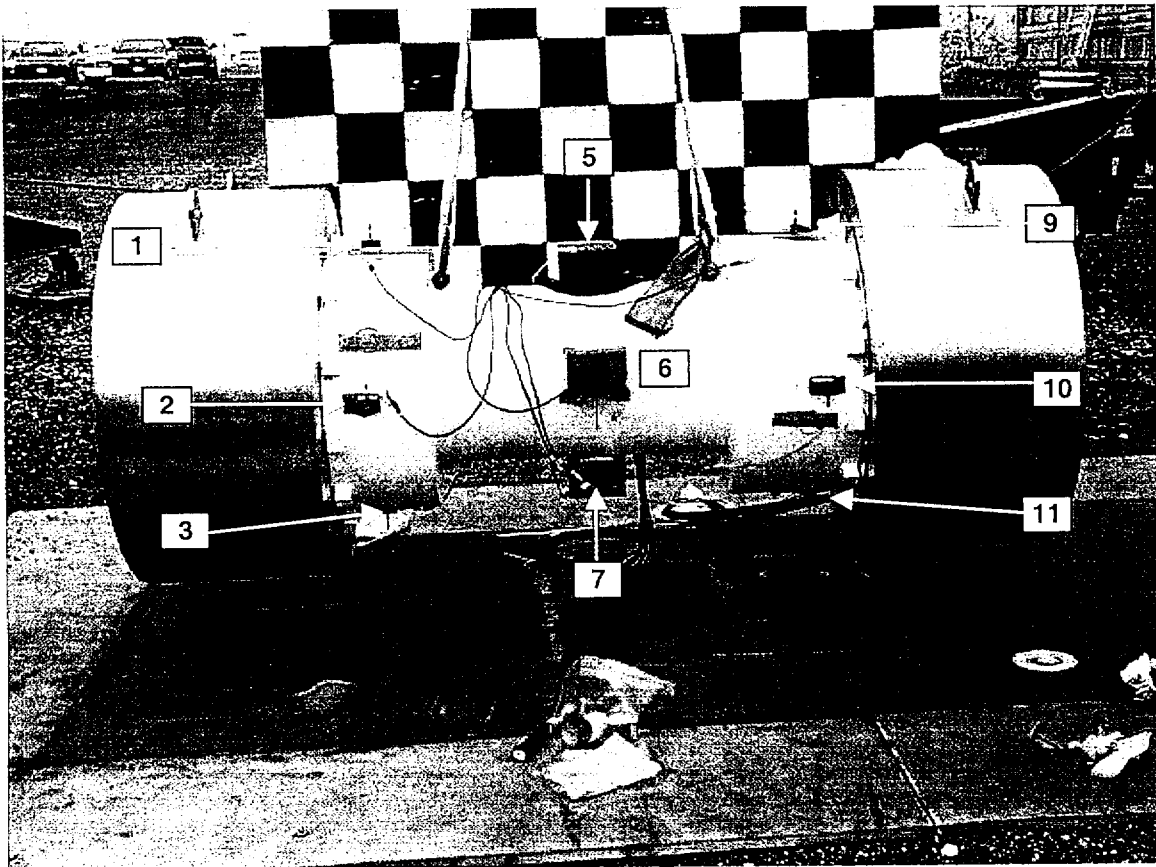


Figure 2.10.9-8

0° Side Drop Test Setup



Figure 2.10.9-9

Acceleration Time History, with 1,000 Hz. Low-Pass Filter, 0° Side Drop,
Accelerometer 1 (Top)

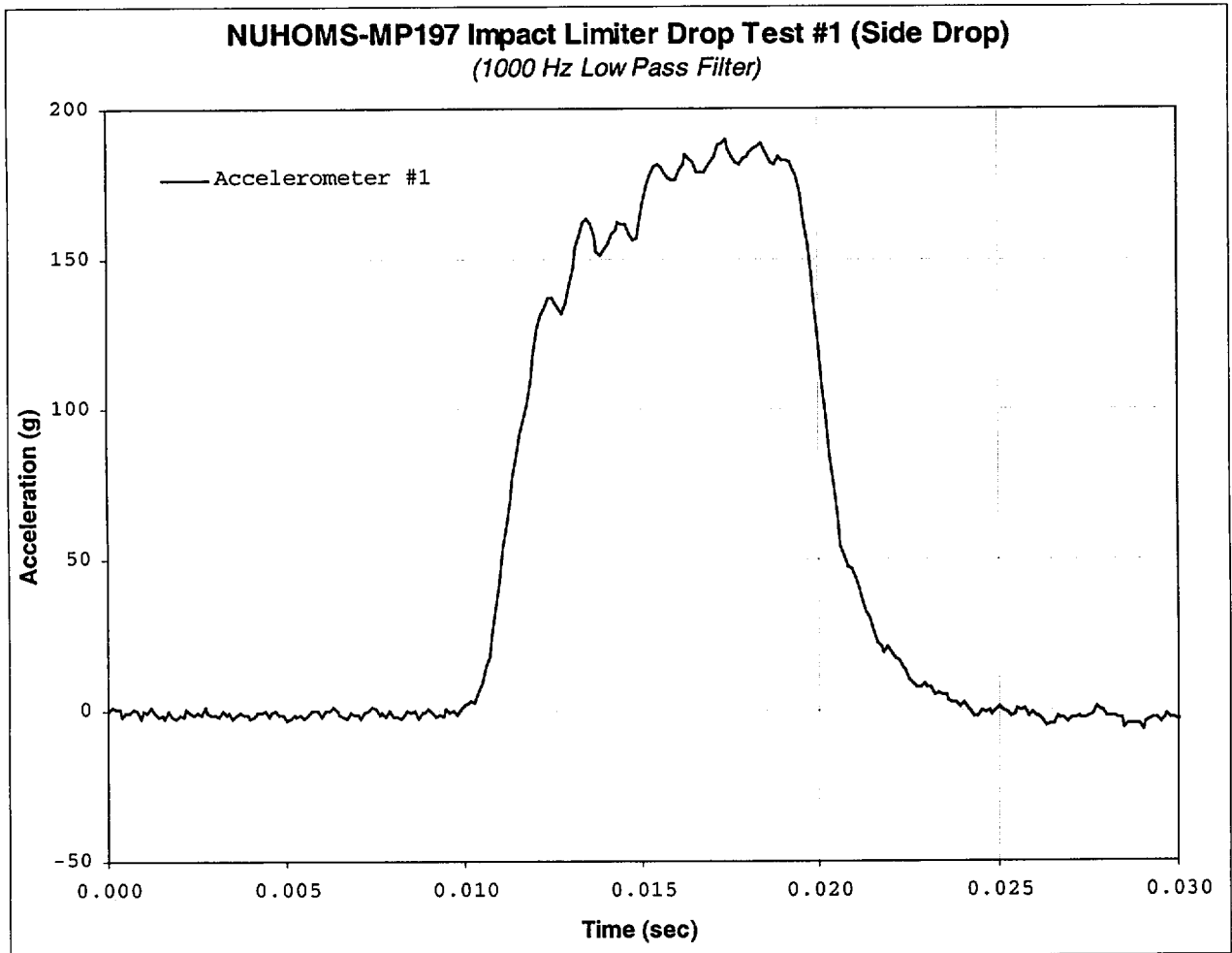


Figure 2.10.9-10

Acceleration Time History, with 1,000 Hz. Low-Pass Filter, 0° Side Drop,
Accelerometer 10 (Bottom)

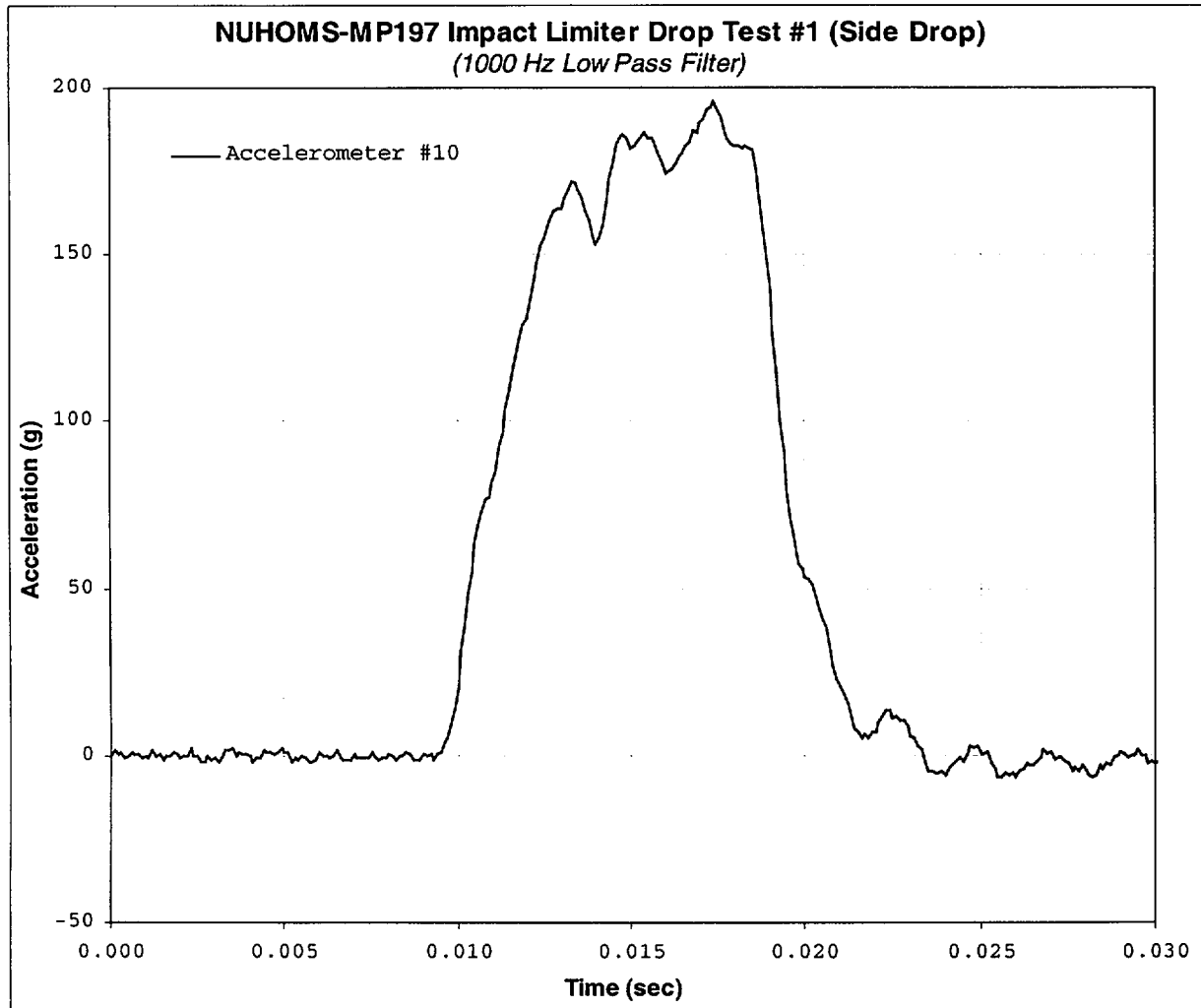


Figure 2.10.9-11

NUHOMS[®]-MP197 Cask Dummy and Impact Limiters After 0° Side Drop

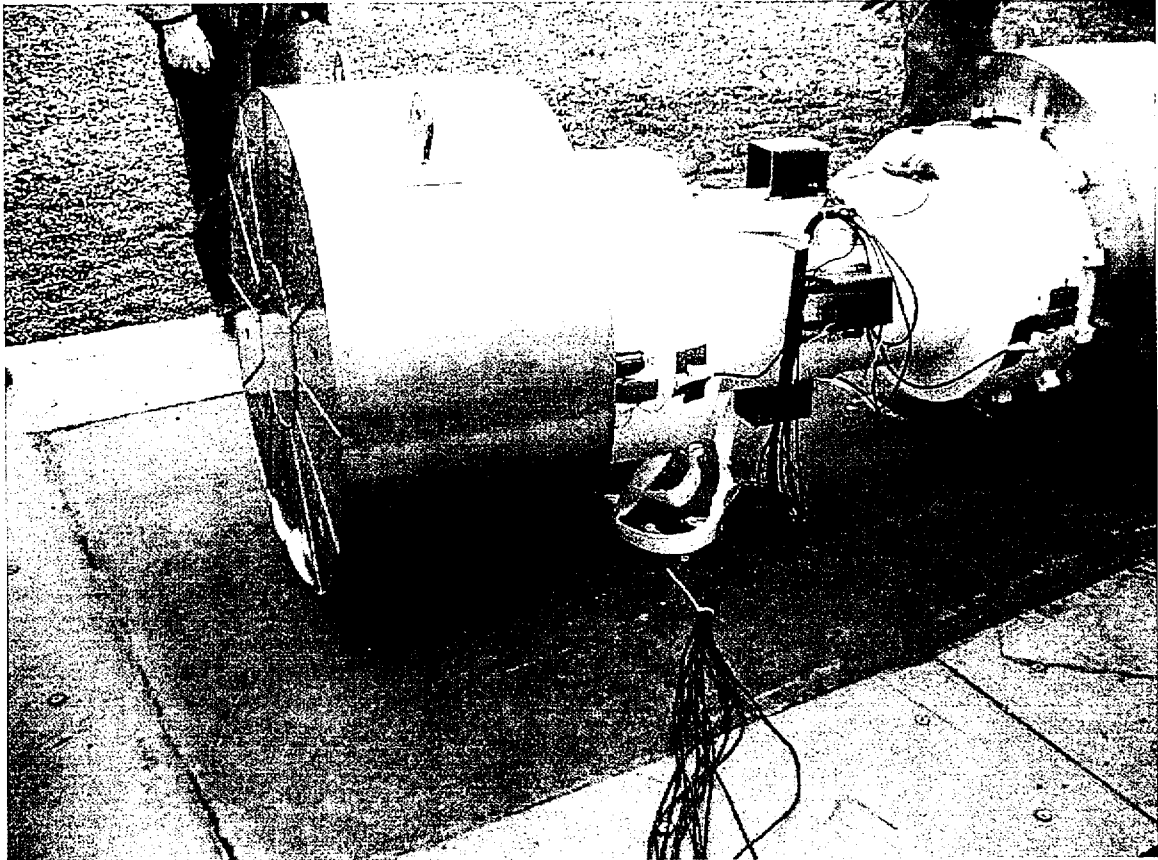


Figure 2.10.9-12

NUHOMS[®]-MP197 Cask Dummy and Impact Limiters After 0° Side Drop

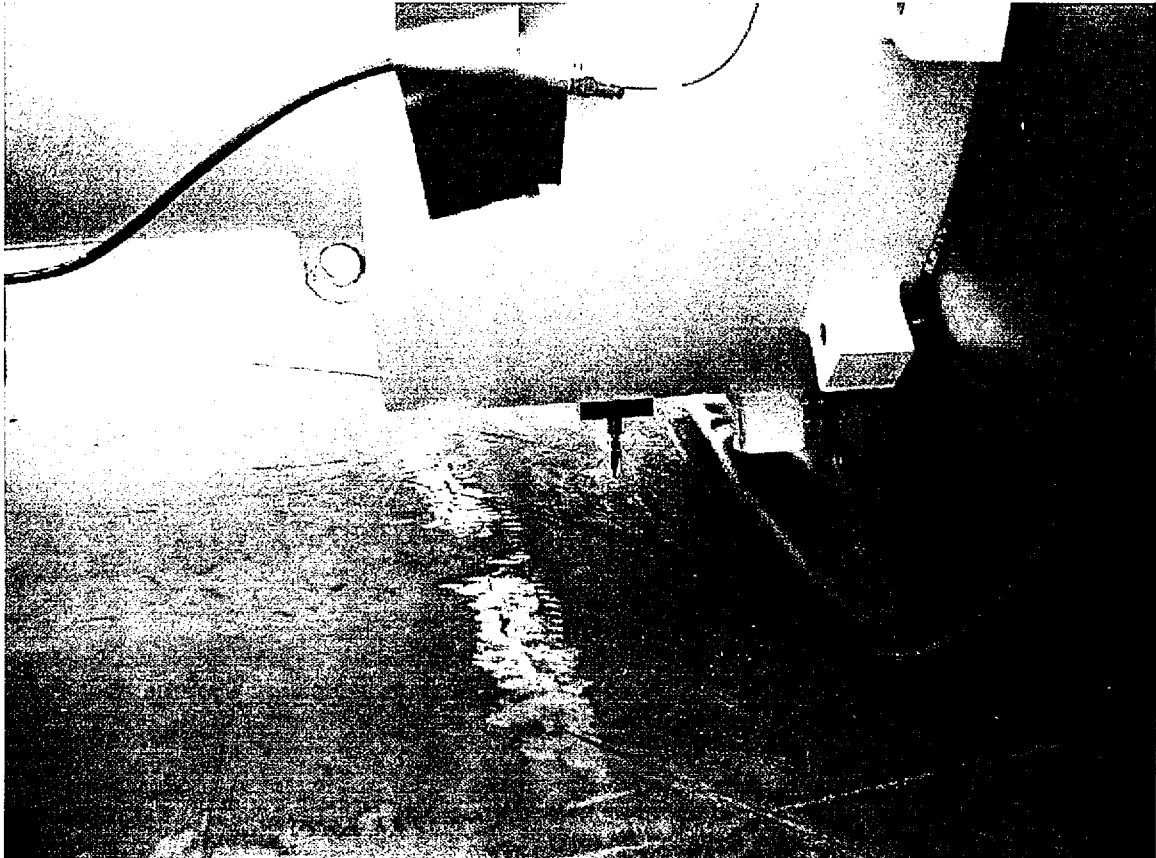


Figure 2.10.9-13

20° Slap Down Test Setup

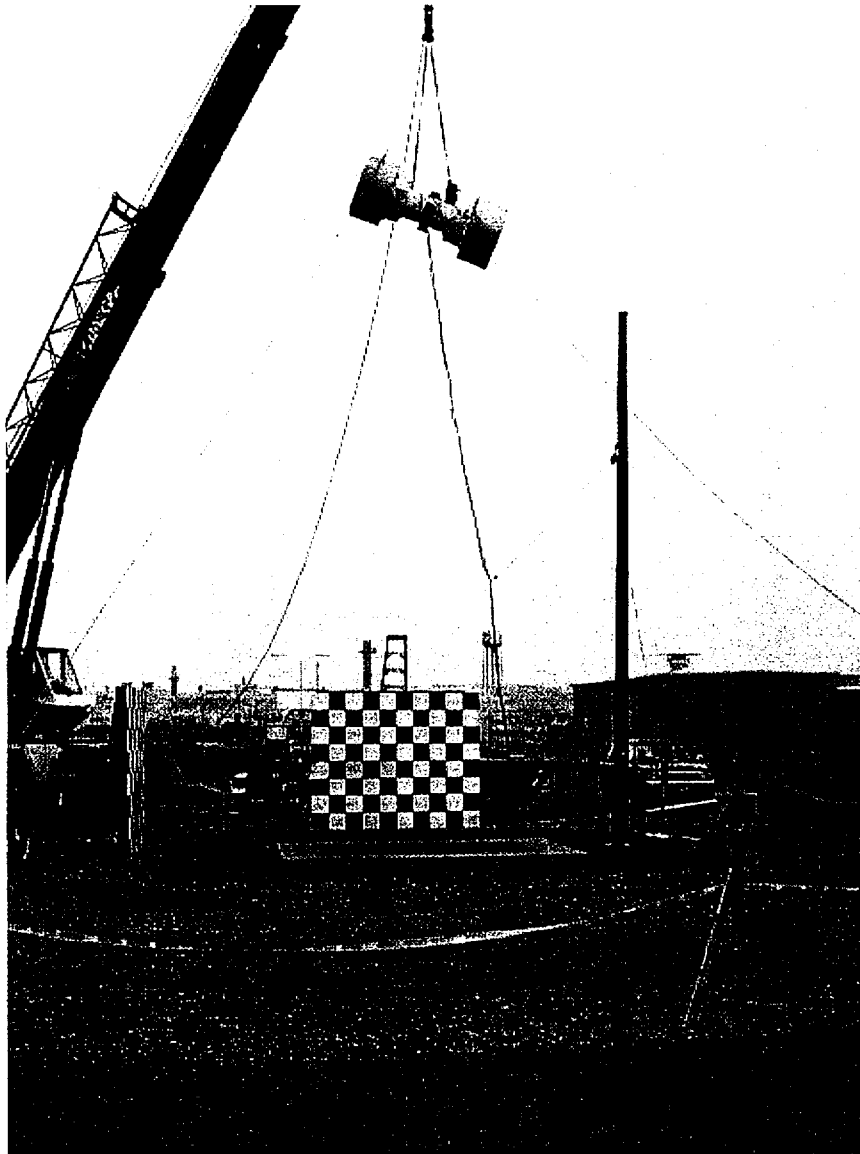


Figure 2.10.9-14

Acceleration Time History, with 1,000 Hz. Low-Pass Filter, 20° Slap Down Drop,
Accelerometer 1 (Top / Second Impact)

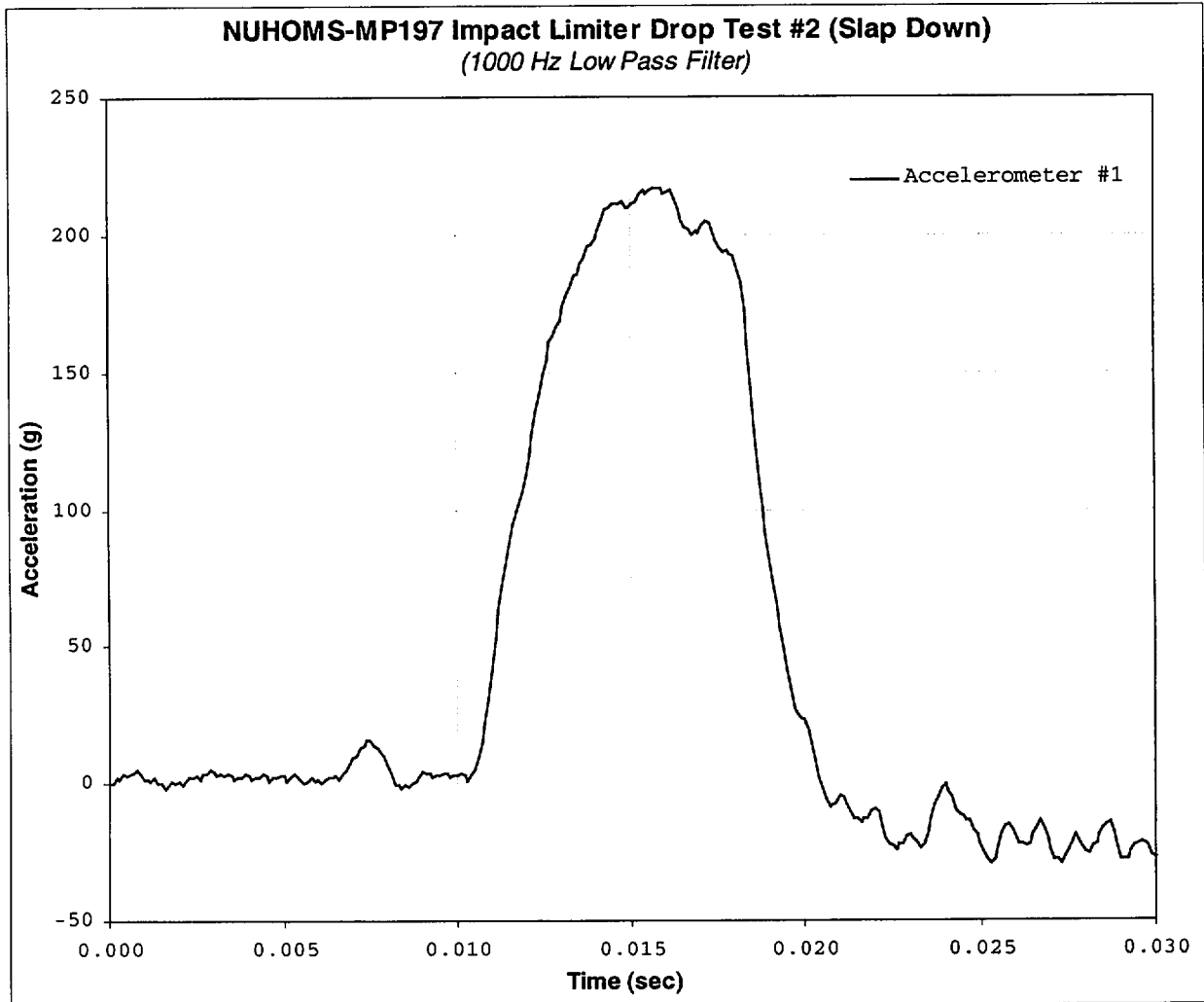


Figure 2.10.9-15

Acceleration Time History, with 1,000 Hz. Low-Pass Filter, 20° Slap Down Drop,
Accelerometer 8 (Center of Gravity)

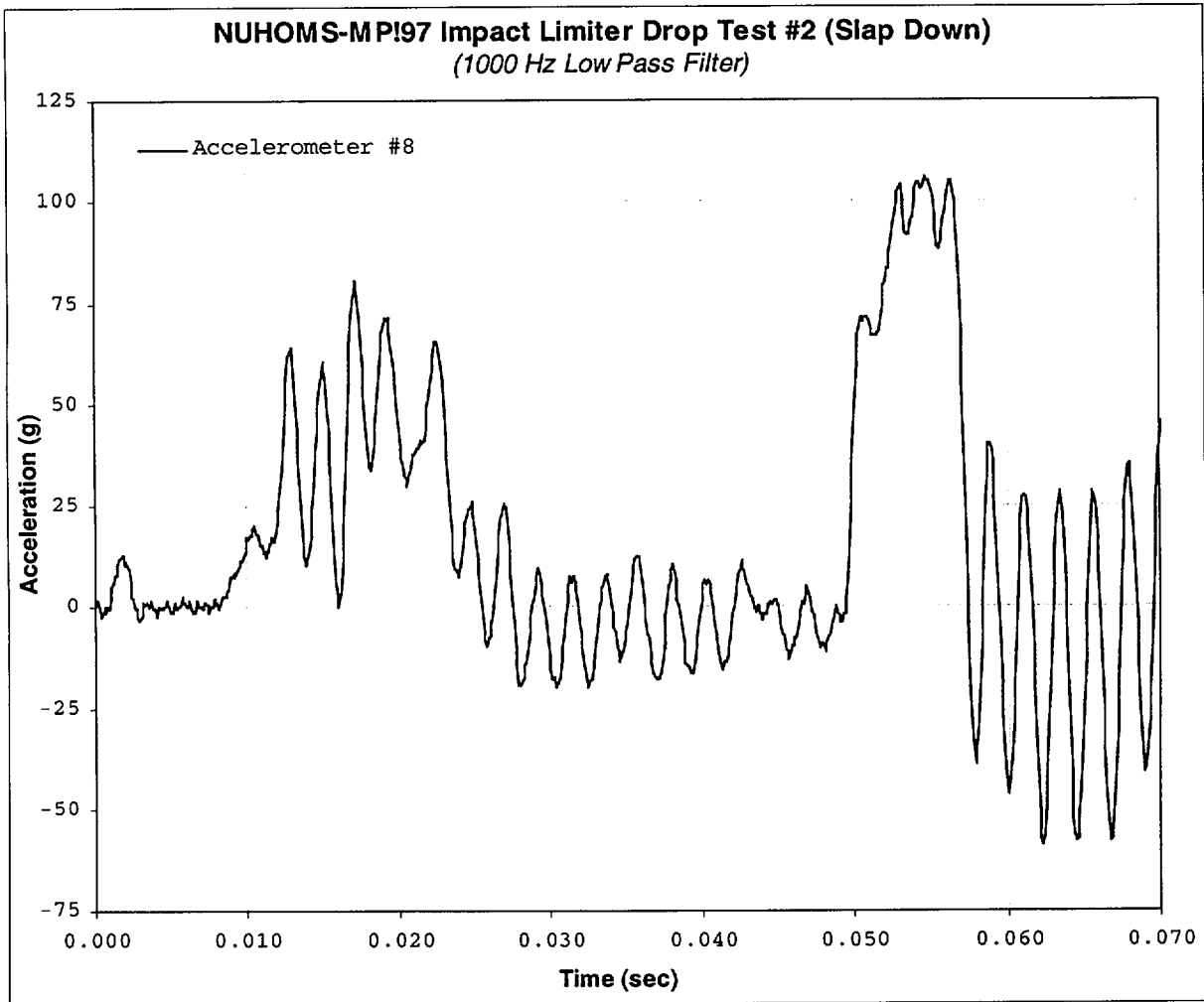


Figure 2.10.9-16

Acceleration Time History, with 1,000 Hz. Low-Pass Filter, 20° Slap Down Drop,
Accelerometer 10 (Bottom / First Impact)

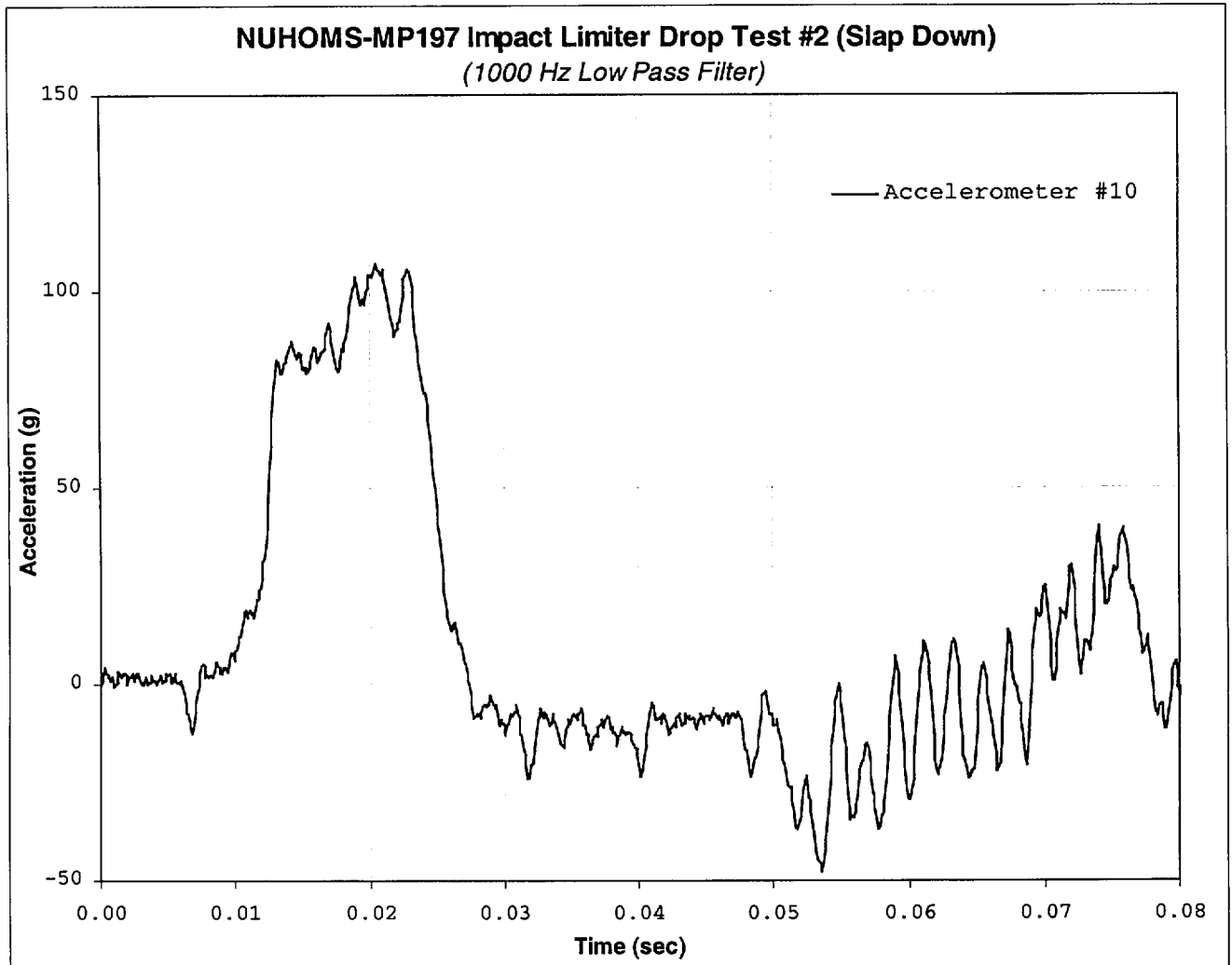


Figure 2.10.9-17

NUHOMS[®]-MP197 Cask Dummy and Impact Limiters After 20° Slap Down Drop

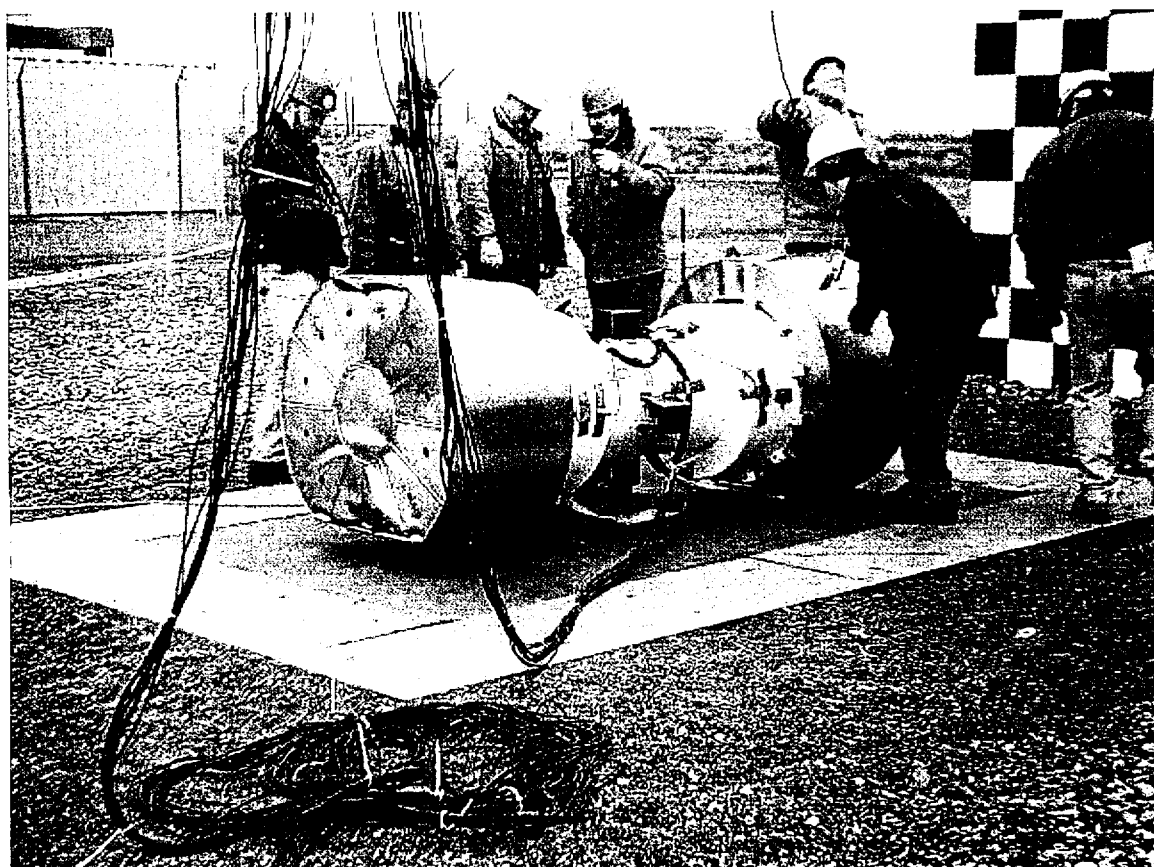


Figure 2.10.9-18

NUHOMS[®]-MP197 Cask Dummy and Impact Limiters After 20° Slap Down Drop

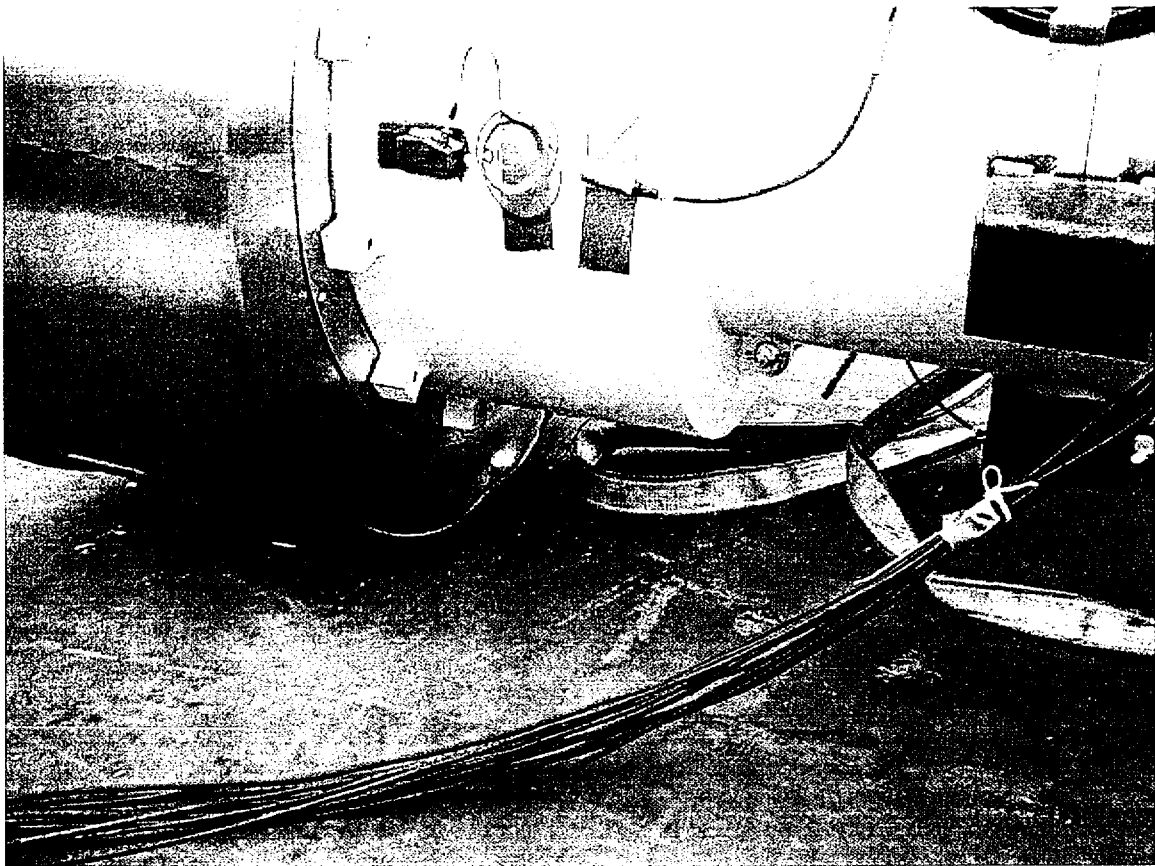


Figure 2.10.9-19

90° End Drop Test Setup

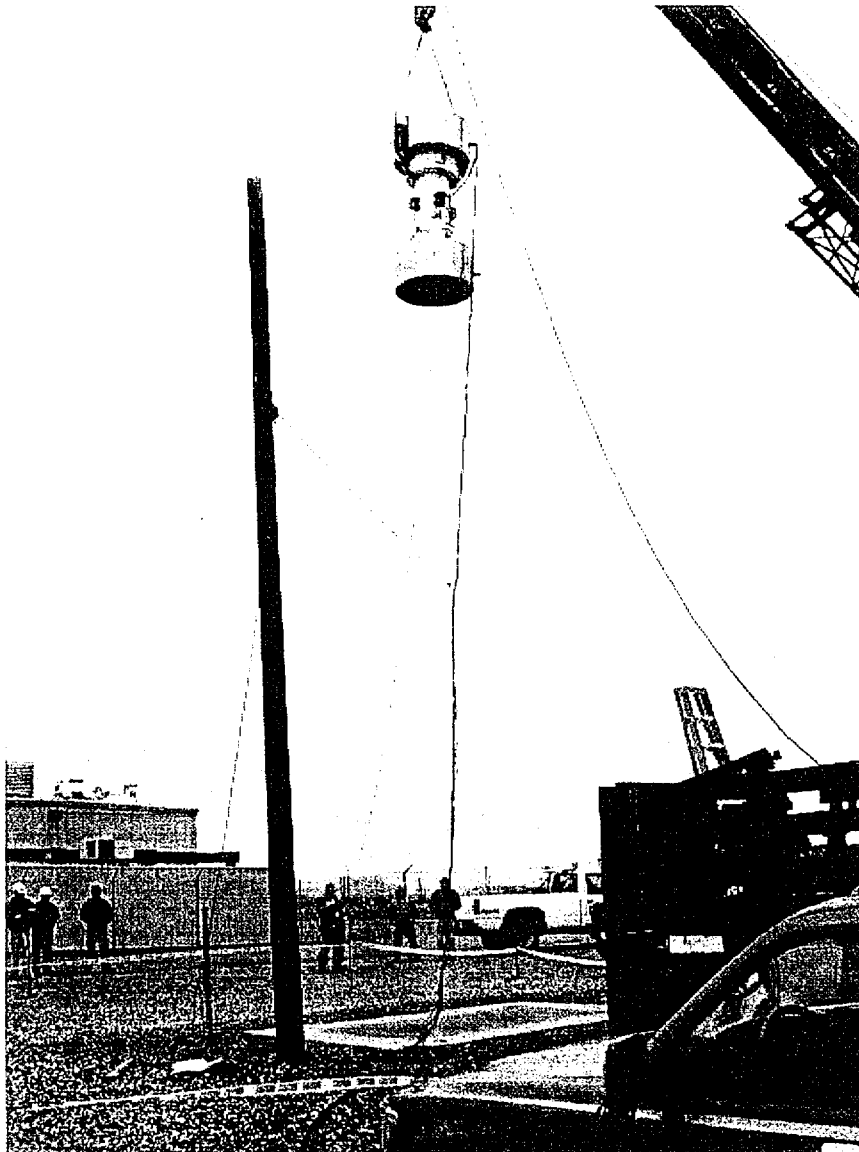


Figure 2.10.9-20

Acceleration Time History, with 1,000 Hz. Low-Pass Filter, 90° End Drop,
Accelerometer 7 (Center of Gravity)

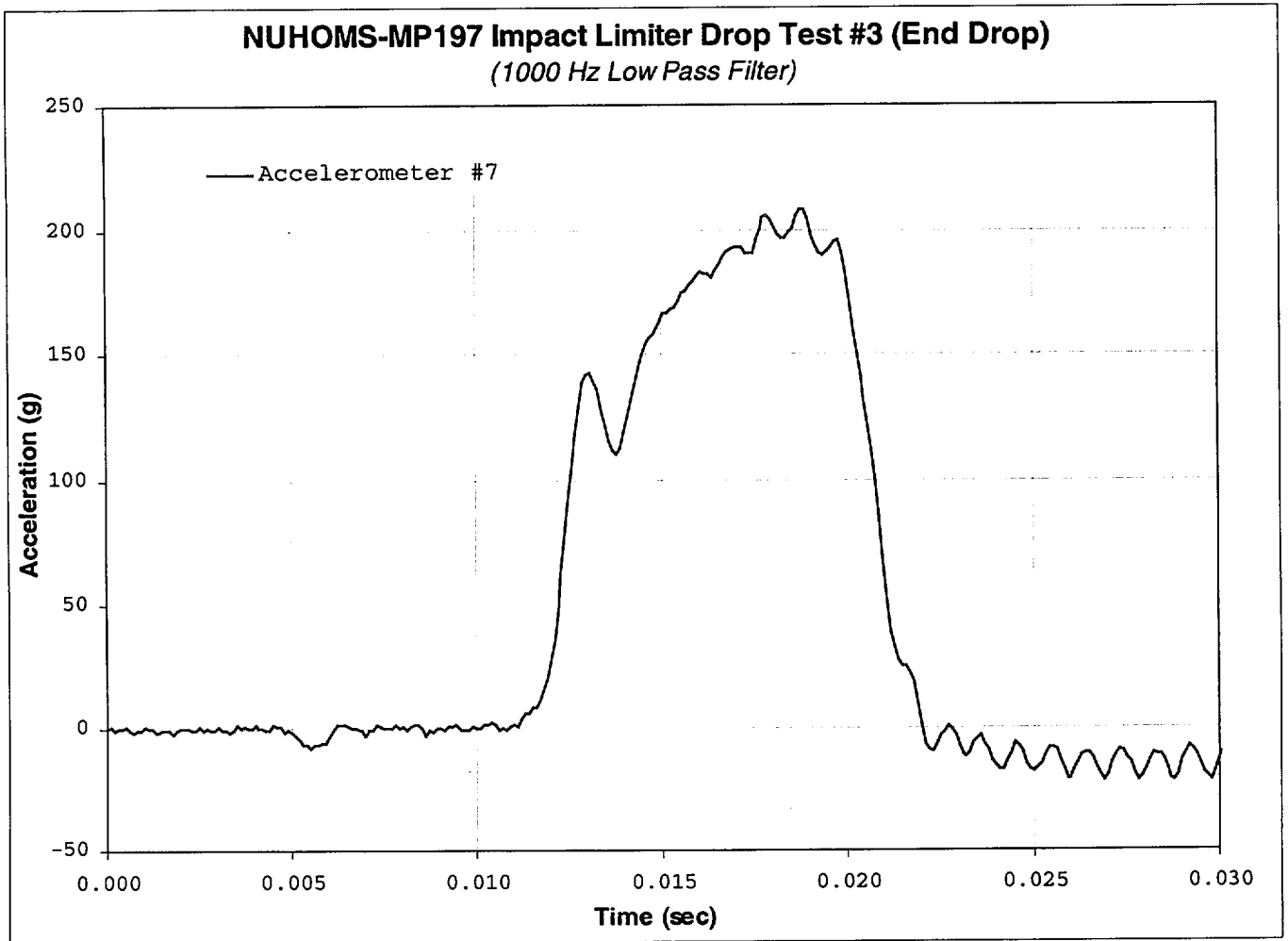


Figure 2.10.9-21

Acceleration Time History, with 1,000 Hz. Low-Pass Filter, 90° End Drop,
Accelerometer 11 (Bottom / Impact End)

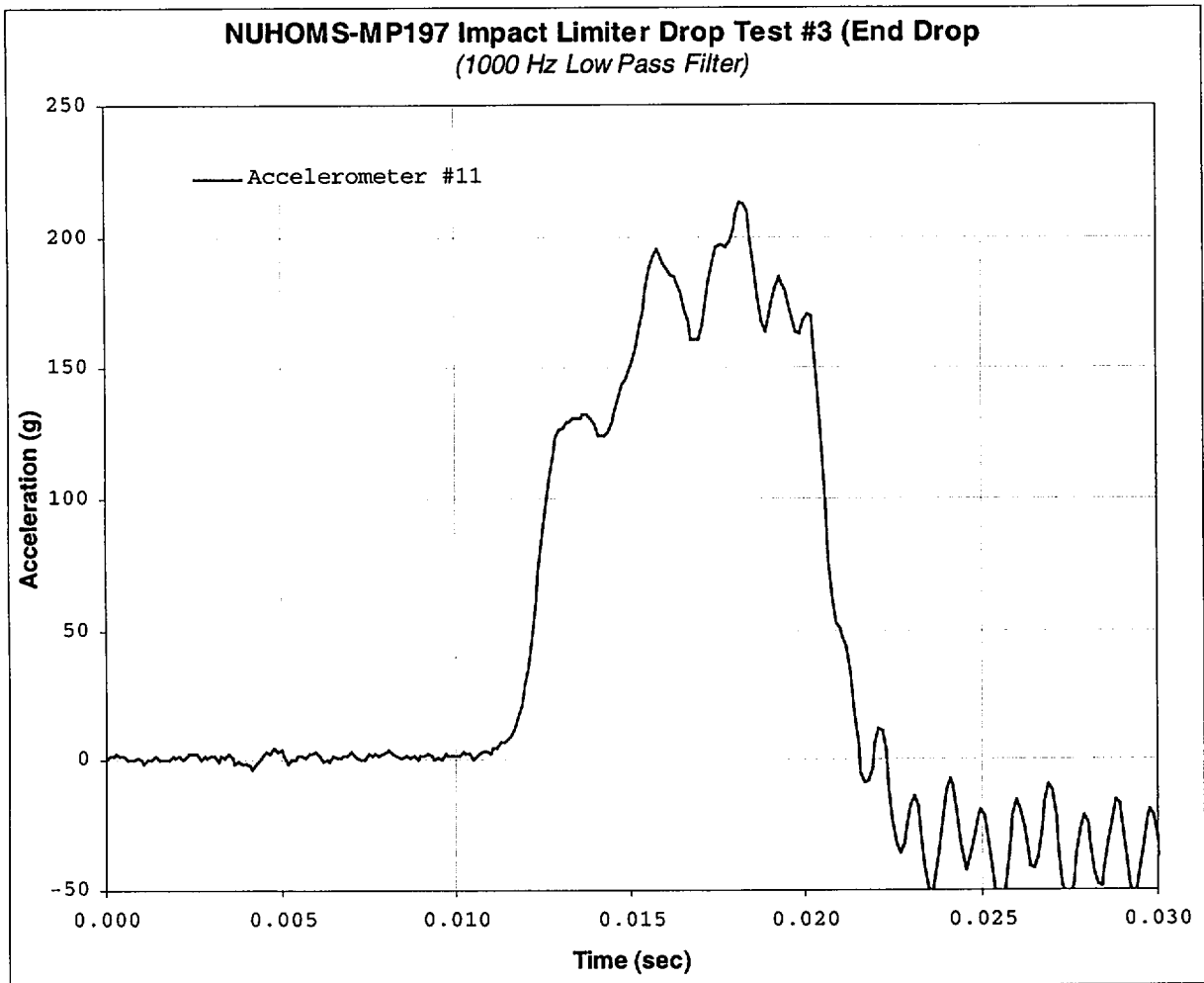


Figure 2.10.9-22

NUHOMS[®]-MP197 Cask Dummy and Impact Limiters After 90° End Drop

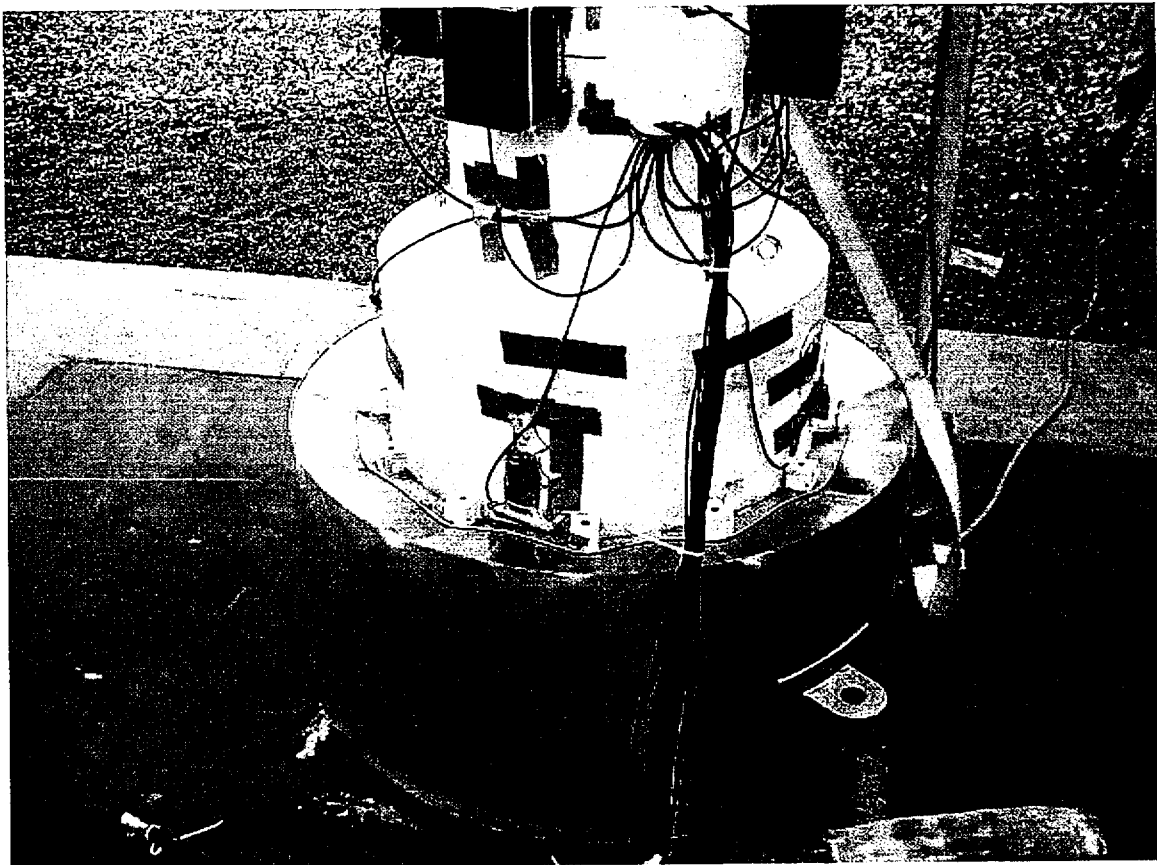


Figure 2.10.9-23

NUHOMS[®]-MP197 Cask Dummy and Impact Limiters After 90° End Drop

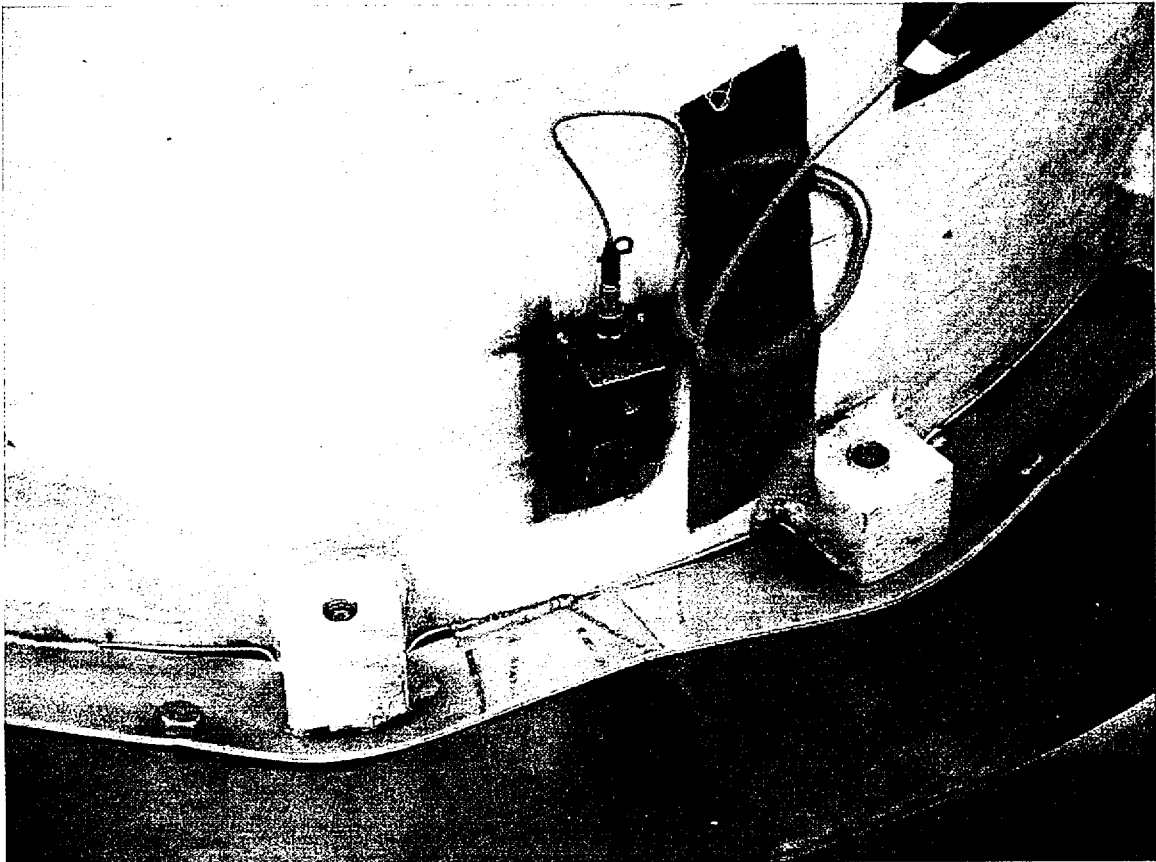
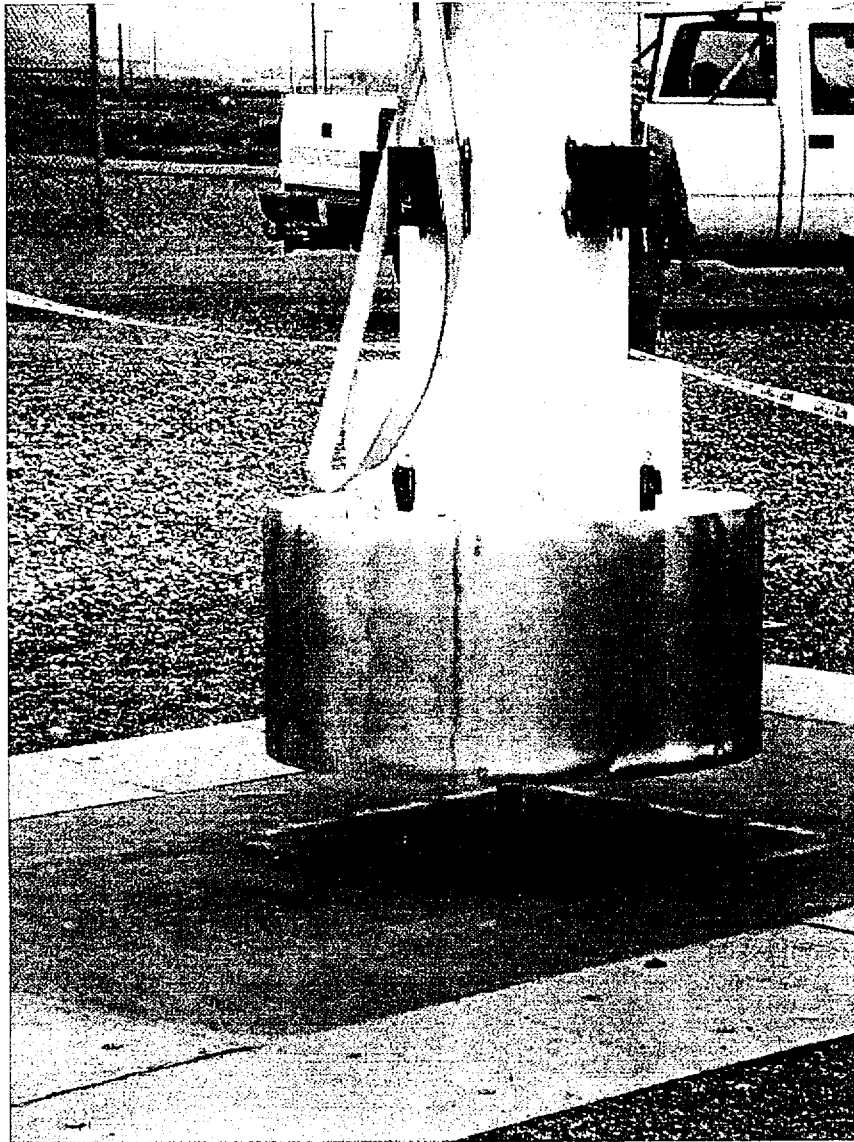


Figure 2.10.9-24

NUHOMS®-MP197 Cask Dummy and Impact Limiters After Puncture Drop



APPENDIX 3.7.1

TABLE OF CONTENTS

3.7.1	EFFECTIVE THERMAL CONDUCTIVITY FOR THE FUEL ASSEMBLY	3.7.1-1
3.7.1.1	Discussion	3.7.1-1
3.7.1.2	Summary of Material Properties	3.7.1-2
3.7.1.3	Effective Fuel Conductivity	3.7.1-3
	3.7.1.3.1 Transverse Effective Conductivity.....	3.7.1-3
	3.7.1.3.2 Axial Effective Conductivity	3.7.1-4
3.7.1.4	Effective Fuel Density.....	3.7.1-5
3.7.1.5	Effective Fuel Specific Heat	3.7.1-6
3.7.1.6	Conclusion.....	3.7.1-7
3.7.1.7	References	3.7.1-8

LIST OF TABLES

3.7.1-1	Fuel Assembly Parameters
---------	--------------------------

LIST OF FIGURES

3.7.1-1	Finite Element Model of 7x7 (GE2, GE3) Fuel Assembly
3.7.1-2	Finite Element Model of 9x9 (GE11, GE13) Fuel Assembly
3.7.1-3	Finite Element Model of 10x10 (GE12) Fuel Assembly
3.7.1-4	Finite Element Model of 8x8 (GE4) Fuel Assembly
3.7.1-5	Finite Element Model of 8x8 (GE5, GE8-Type I) Fuel Assembly
3.7.1-6	Finite Element Model of 8x8 (GE8-Type II) Fuel Assembly
3.7.1-7	Finite Element Model of 8x8 (GE9, GE10) Fuel Assembly

APPENDIX 3.7.1

EFFECTIVE THERMAL CONDUCTIVITY FOR THE FUEL ASSEMBLY

3.7.1.1 Discussion

The transportable NUHOMS[®]-MP197 finite element models simulate the effective thermal properties of the fuel with a homogenized material occupying the volume within the basket where the active fuel lengths are stored. Effective values for density, specific heat, and conductivity are determined for this homogenized material for use in the finite element models.

The NUHOMS[®]-MP197 shall be capable of handling a wide variety of spent BWR fuel assemblies. In order to determine the appropriate effective thermal properties of the fuel assembly, a study was performed of the BWR fuel assemblies to be stored in the NUHOMS[®]-MP197 packaging. The lowest effective thermal conductivity, density, and specific heat of the studied fuel assemblies are selected to apply in the finite element model. Use of these properties would conservatively predict bounding maximum temperatures for the components of the NUHOMS[®]-MP197.

Parameters of the fuel assemblies to be stored in the NUHOMS[®]-MP197 are listed in Table 3.7.1-1.

3.7.1.2 Summary of Material Properties

a. UO₂ Fuel

Thermal Conductivity [2] (Btu/hr-in-°F)	Specific Heat [1] (Btu/lbm-°F)	Density [1] (lbm/in ³)
0.1926 ⁽ⁱ⁾	0.0560 ⁽ⁱⁱ⁾	0.396

(i) bounds values for temperatures below 750 K (890 °F)

(ii) bounds values found in reference

b. Zircaloy-2

Thermal Conductivity [2] (Btu/hr-in-°F)	Specific Heat [2] (Btu/lbm-°F)	Density [1] (lbm/in ³)	Emissivity [2] (---)
0.6019 ⁽ⁱ⁾	0.0657 ⁽ⁱ⁾	0.237	0.74 ⁽ⁱ⁾

(i) bounds values found in reference

c. Helium

Temperature [3] (K)	Thermal Conductivity [3] (W/m-K)	Temperature (°F)	Thermal Conductivity (Btu/hr-in-°F)
200	0.1151	-100	0.0055
250	0.1338	-10	0.0064
300	0.150	80	0.0072
400	0.180	260	0.0087
500	0.211	440	0.0102
600	0.247	620	0.0119
800	0.307	980	0.0148
1000	0.363	1340	0.0175

d. Stainless Steel SA-240, Type 304

A stainless steel emissivity of 0.2, a measured value from Reference 5, is used in the analysis.

3.7.1.3 Effective Fuel Conductivity

3.7.1.3.1 Transverse Effective Conductivity

The purpose of the effective conductivity in the transverse direction of a fuel assembly is to relate the temperature drop of a homogeneous heat generating square to the temperature drop across an actual assembly cross section for a given heat load. This relationship is established by the following equation obtained from Reference 4:

$$k_e = \frac{Q}{4L_a(T_o - T_s)} (0.2947)$$

where:

k_e = Effective thermal conductivity (Btu/hr-in.-°F)

Q = Assembly head generation (Btu/hr)

L_a = Assembly active length (in.)

T_o = Maximum temperature (°F)

T_s = Surface temperature (°F)

Discrete finite element models of the fuel assemblies to be transported in the NUHOMS[®]-MP197 packaging are developed using the ANSYS computer code [6]. These two-dimensional models simulate heat transfer by radiation and convection and include the geometry of the fuel rods and fuel pellets. Helium is used as the fill gas in the fuel assembly. A fuel assembly decay heat load of 264 W is used for heat generation. An active length of 144 in. is assumed.

The finite element models are used to calculate the maximum radial temperature difference with isothermal boundary conditions. All components are modeled using 2-D PLANE55 thermal solid elements. LINK32 elements are placed on the exteriors of the fuel assembly components to set up the creation of the radiation super-element. The compartment wall is modeled using LINK32 elements and used only to set up the surrounding surface for the creation of the radiation matrix super-element using the /AUX12 processor in ANSYS. All LINK32 elements are unselected prior to solution of the thermal problem. The thermal properties used are as described in Section 3.7.1.2, and the fuel assembly geometries are as described in Section 3.7.1.1. The ANSYS finite element models of the assemblies are shown in Figures 3.7.1-1 through 3.7.1-7.

The effect of radial gaps between the fuel pellets and the fuel rods on the temperature distributions is negligible. These thermal gaps are not included in the finite element models.

Several computational runs were made for each model using isothermal boundary temperatures ranging from 100 to 600°F. In determining the temperature dependent effective conductivities of the fuel assemblies an average temperature, equal to $(T_o + T_s)/2$, is used for the fuel temperature.

3.7.1.3.2 Axial Effective Conductivity

The backfill gas, fuel pellets, and zircaloy behave like resistors in parallel. However, due to the small conductivity of the fill gas and the axial gaps between fuel pellets, credit is only taken for the zircalloy in the determination of the axial effective conductivities.

$$K_{axl} = (K_{zirc})(A_{zirc}/A_{eff})$$

$$K_{zirc} = 0.6019 \text{ Btu/hr-in-}^{\circ}\text{F}$$

$$A_{eff} = (6.00'') \times (6.00'') = 36.00 \text{ in}^2$$

Assembly Type	GE2, GE3	GE11, GE13	GE 12
Fuel Array	7x7	9x9	10x10
Fuel Rod Outer Diameter, in.	0.563	0.440	0.404
Fuel Rod Clad Thickness, in.	0.032	0.028	0.026
$A_{zirc}, \text{ in}^2$	2.616	2.683	2.842
$K_{axl}, \text{ Btu/hr-in-}^{\circ}\text{F}$	0.0437	0.0449	0.0475

Assembly Type	GE4	GE5, GE8-Type I	GE8-Type II	GE9, GE10
Fuel Array	8x8	8x8	8x8	8x8
Fuel Rod Outer Diameter, in.	0.493	0.483	0.483	0.483
Fuel Rod Clad Thickness, in.	0.034	0.032	0.032	0.032
$A_{zirc}, \text{ in}^2$	3.089	2.812	2.722	2.722
$K_{axl}, \text{ Btu/hr-in-}^{\circ}\text{F}$	0.0516	0.0470	0.0455	0.0455

A bounding axial conductivity of 0.0437 Btu/hr-in-^oF is used in the thermal analyses.

3.7.1.4 Effective Fuel Density

The mass of the zircalloy and fuel pellets within the 144 inch active length of the fuel assemblies is homogenized over the volume of the fuel elements:

$$\rho_{\text{fuel}} = (\rho_{\text{UO}_2} V_{\text{UO}_2} + \rho_{\text{zirc}} V_{\text{zirc}}) / V_{\text{fuel}}$$

$$\rho_{\text{UO}_2} = 0.396 \text{ lbm/in}^3$$

$$\rho_{\text{zirc}} = 0.237 \text{ lbm/in}^3$$

$$V_{\text{fuel}} = (6.00 \text{ in})^2 (144 \text{ in}) = 5,184 \text{ in}^3$$

Assembly Type	GE2, GE3	GE11, GE13	GE 12
Fuel Array	7x7	9x9	10x10
Fuel Rod Outer Diameter, in.	0.563	0.440	0.404
Fuel Rod Clad Thickness, in.	0.032	0.028	0.026
Fuel Pellet Outer Diameter, in.	0.487	0.376	0.345
V_{UO_2} , in ³	1,314.34	1,183.20	1,238.45
V_{zirc} , in ³	376.66	386.37	409.22
ρ_{eff} , lbm/in ³	0.118	0.108	0.113

Assembly Type	GE4	GE5, GE8-Type I	GE8-Type II	GE9, GE10
Fuel Array	8x8	8x8	8x8	8x8
Fuel Rod Outer Diameter, in.	0.493	0.483	0.483	0.483
Fuel Rod Clad Thickness, in.	0.034	0.032	0.032	0.032
Fuel Pellet Outer Diameter, in.	0.416	0.410	0.410	0.411
V_{UO_2} , in ³	1,233.05	1,178.72	1,140.70	1,146.27
V_{zirc} , in ³	444.83	404.90	391.93	391.90
ρ_{eff} , lbm/in ³	0.115	0.109	0.105	0.106

The bounding density of 0.105 lbm/in³ is used in the thermal analyses.

3.7.1.5 Effective Fuel Specific Heat

A mass weighted average is used in determination of the fuel assemblies effective specific heats:

$$C_{p,\text{fuel}} = (C_{p,\text{UO}_2}M_{\text{UO}_2} + C_{p,\text{zirc}}M_{\text{zirc}}) / M_{\text{tot}}$$

$$C_{p,\text{UO}_2} = 0.0560 \text{ Btu/lbm-}^\circ\text{F}$$

$$C_{p,\text{zirc}} = 0.0657 \text{ Btu/lbm-}^\circ\text{F}$$

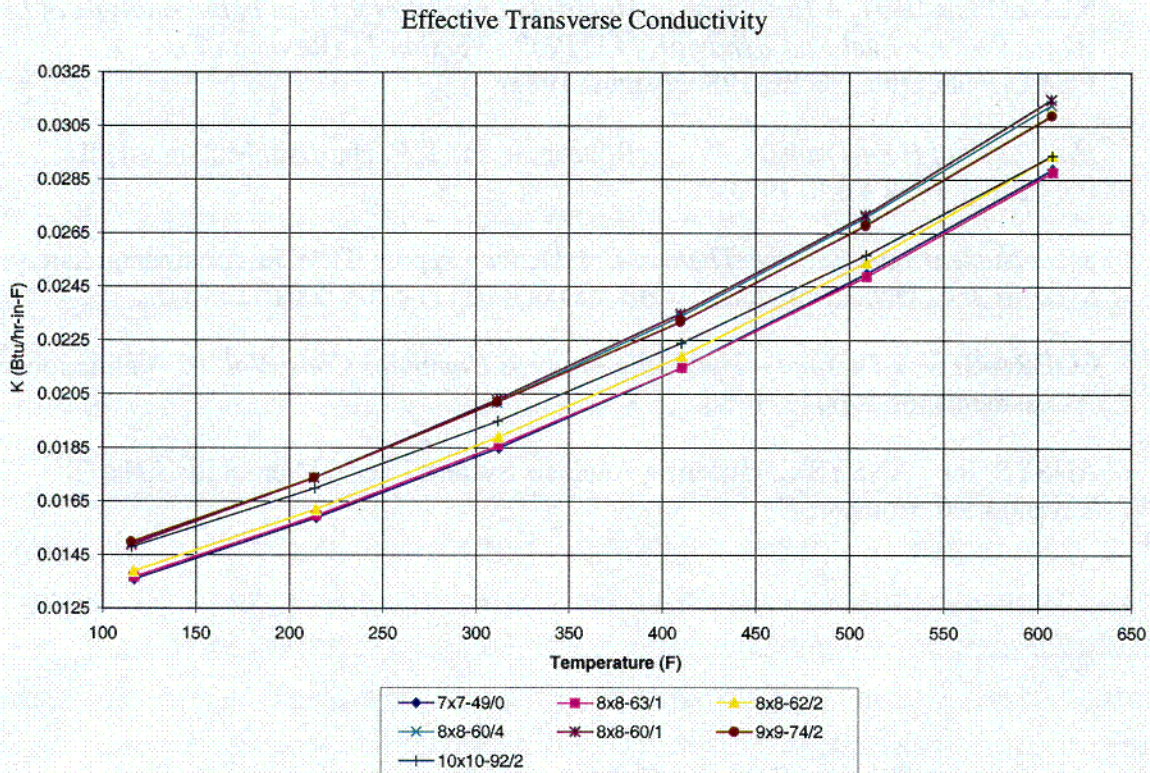
Assembly Type	GE2, GE3	GE11, GE13	GE 12
Fuel Array	7x7	9x9	10x10
M_{UO_2} , lbm	520.5	468.5	490.4
M_{zirc} , lbm	89.3	91.6	97.0
M_{tot} , lbm	609.7	560.1	587.4
$C_{p,\text{fuel}}$, Btu/lbm- $^\circ\text{F}$	0.0574	0.0576	0.0576

Assembly Type	GE4	GE5, GE8-Type I	GE8-Type II	GE9, GE10
Fuel Array	8x8	8x8	8x8	8x8
M_{UO_2} , lbm	488.3	466.8	451.7	453.9
M_{zirc} , lbm	105.4	96.0	92.9	92.9
M_{tot} , lbm	593.7	562.8	544.6	546.8
$C_{p,\text{fuel}}$, Btu/lbm- $^\circ\text{F}$	0.0577	0.0577	0.0577	0.0576

The bounding specific heat of 0.0574 is used in the thermal analyses.

3.7.1.6 Conclusion

The transverse effective conductivities for the fuel assemblies configurations are plotted below. For temperatures above 400°F, the 8x8 (GE4) fuel assembly has the lowest conductivity.



The transverse effective conductivity of the 8x8 (GE4) fuel assembly, and the bounding axial conductivity, density, and specific heat calculated in Sections 3.7.1.2 through 3.7.1.5 are used in the thermal analysis.

Average Fuel Temperature (°F)	Thermal Conductivity (Btu/hr-in-°F)		Density (lbm/in ³)	Specific Heat (Btu/lbm-°F)
	Transverse	Axial		
116.8	0.0137	0.0437	0.105	0.0574
214.4	0.0160
312.4	0.0186
410.7	0.0215
509.3	0.0249
608.0	0.0288	0.0437	0.105	0.0574

3.7.1.7 References

1. NUREG/CR-0200, Vol. 3, Rev. 6, SCALE, A Modular Code System for Performing Standardized Computer Analyses for Licensing Evaluation.
2. NUREG/CR-0497, *A Handbook of Materials Properties for Use in the Analysis of Light Water Reactor Fuel Rod Behavior, MATPRO - Version 11* (Revision 2), EG&G Idaho, Inc., TREE-1280, August 1981.
3. *Handbook of Heat Transfer*, W. M. Rohsenow and J. P. Hartnett, McGraw-Hill Publishing, New York, 1973.
4. *Spent Nuclear Fuel Effective Thermal Conductivity Report*, TRW Environmental Safety Systems, Inc., Document Identifier BBA000000-01717-5705-00010 Rev 00.
5. *COBRA-SFS: A Thermal – Hydraulic Analysis Computer Code, Vol. III, Validation Assessments*, PNL-6049, 1986.
6. ANSYS, Inc., ANSYS Engineering Analysis System User's Manual for ANSYS Revision 5.6, Houston

TABLE 3.7.1-1

FUEL ASSEMBLY PARAMETERS

Assembly Type	GE2, GE3	GE11, GE13	GE 12
Fuel Array	7x7	9x9	10x10
Number of Fuel Rods	49	74	92
Fuel Rod Outside Diameter, in.	0.563	0.440	0.404
Fuel Rod Clad Thickness, in.	0.032	0.028	0.026
Fuel Pellet Outer Diameter, in.	0.487	0.376	0.345
Rod Pitch, in.	0.738	0.566	0.510
Number of Water Rods	0	2	2
Water Rod Outer Diameter, in.	N/A	0.980	0.980
Water Rod Inner Diameter, in.	N/A	0.920	0.920
Fuel Rod Material	Zr-2	Zr-2	Zr-2
Fuel Pellet Material	UO ₂	UO ₂	UO ₂
Active Fuel Length, in.	144	146*	150*

Assembly Type	GE4	GE5, GE8-Type I	GE8-Type II	GE9, GE10
Fuel Array	8x8	8x8	8x8	8x8
Number of Fuel Rods	63	62	60	60
Fuel Rod Outside Diameter, in.	0.493	0.483	0.483	0.483
Fuel Rod Clad Thickness, in.	0.034	0.032	0.032	0.032
Fuel Pellet Outer Diameter, in.	0.416	0.410	0.410	0.411
Rod Pitch, in.	0.640	0.640	0.640	0.640
Number of Water Rods	1	2	4	1
Water Rod Outer Diameter, in.	0.493	0.591	2 @ 0.591 2 @ 0.483	1.340
Water Rod Inner Diameter, in.	0.425	0.531	2 @ 0.531 2 @ 0.419	1.260
Fuel Rod Material	Zr-2	Zr-2	Zr-2	Zr-2
Fuel Pellet Material	UO ₂	UO ₂	UO ₂	UO ₂
Active Fuel Length, in.	146*	150*	150*	150*

* Conservatively taken as 144 inches in the analyses.

FIGURE 3.7.1-1

FINITE ELEMENT MODEL OF 7x7 FUEL ASSEMBLY

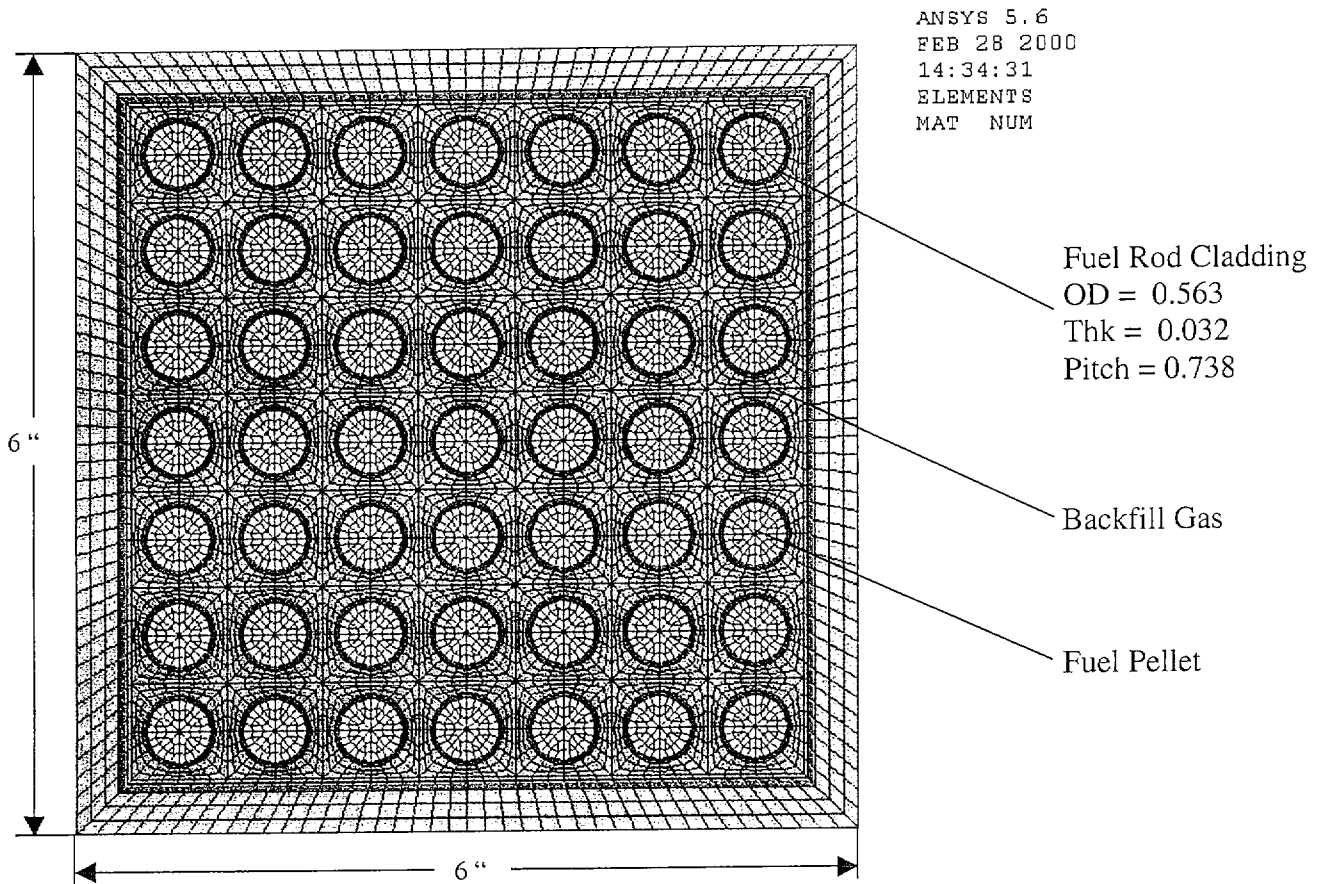


FIGURE 3.7.1-2

FINITE ELEMENT MODEL OF 9x9 FUEL ASSEMBLY

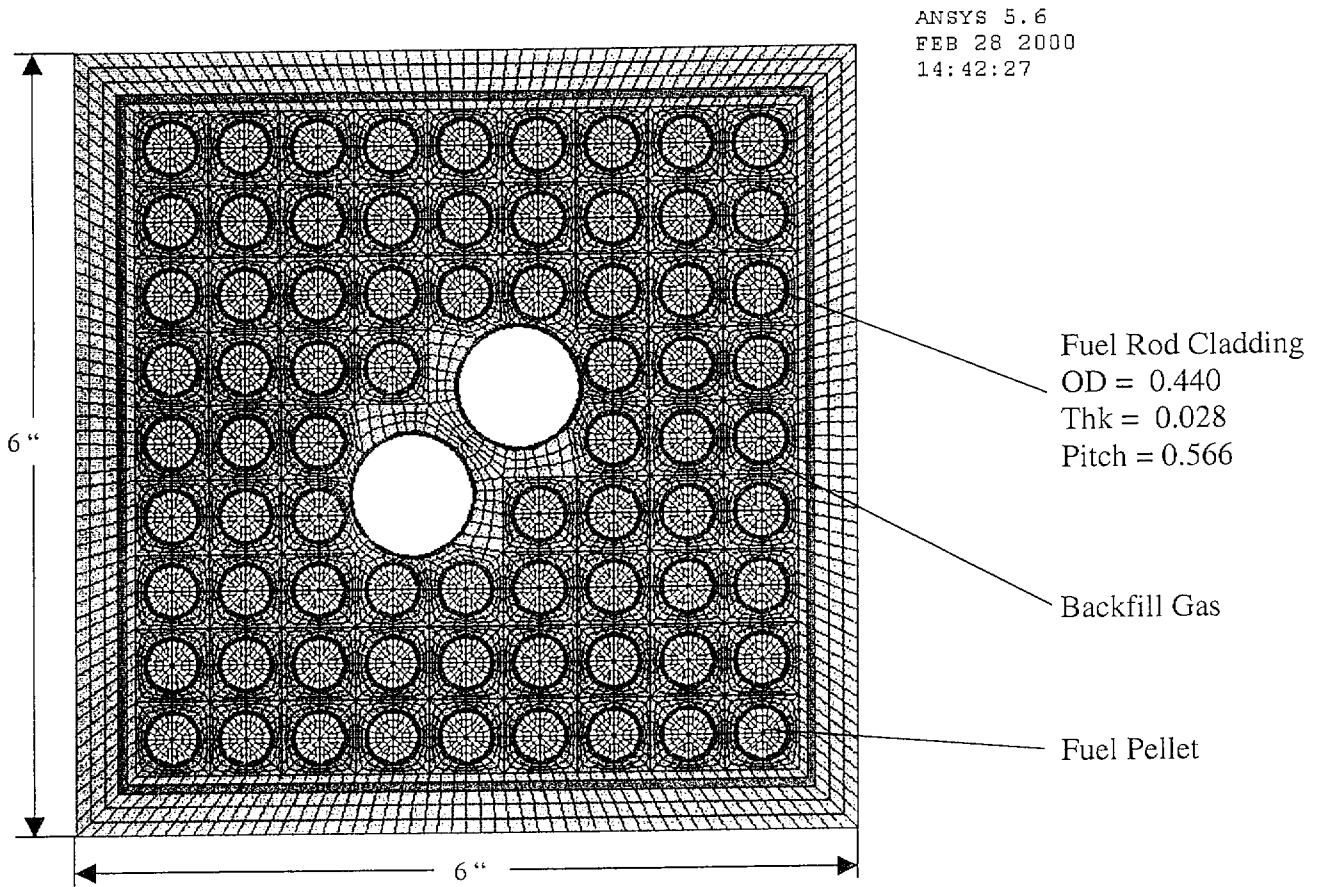


FIGURE 3.7.1-3

FINITE ELEMENT MODEL OF 10x10 FUEL ASSEMBLY

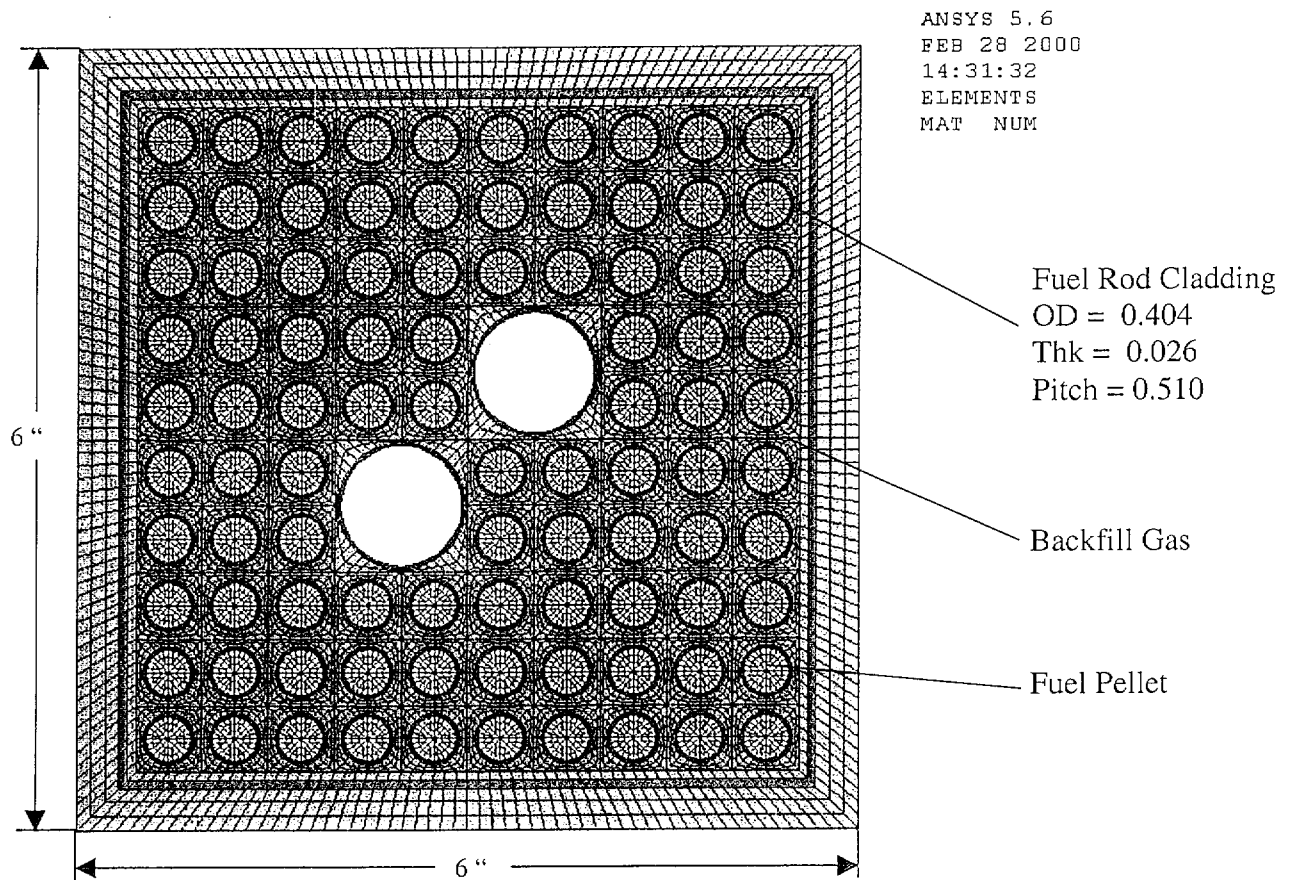


FIGURE 3.7.1-4

FINITE ELEMENT MODEL OF 8x8 (GE4) FUEL ASSEMBLY

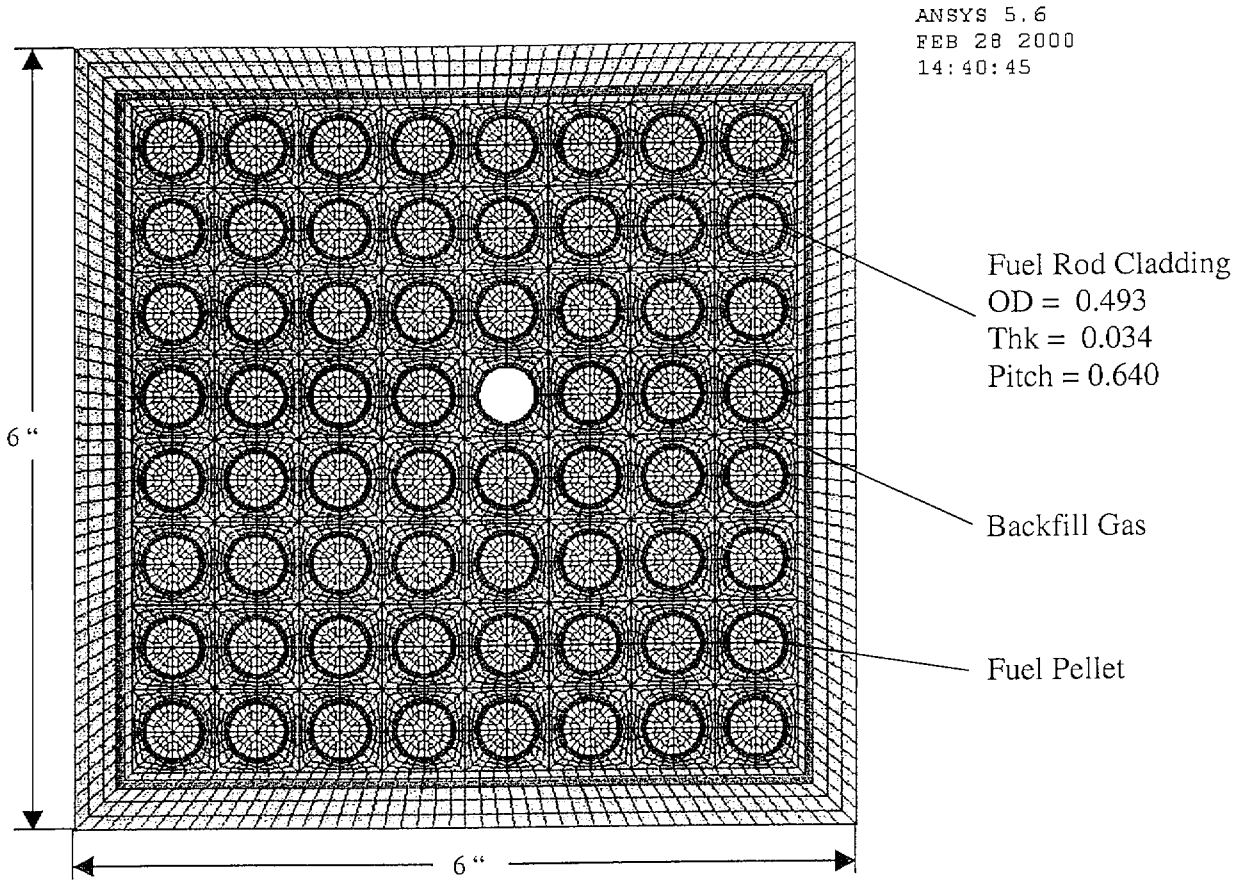


FIGURE 3.7.1-5

FINITE ELEMENT MODEL OF 8x8 (GE5, GE8-Type I) FUEL ASSEMBLY

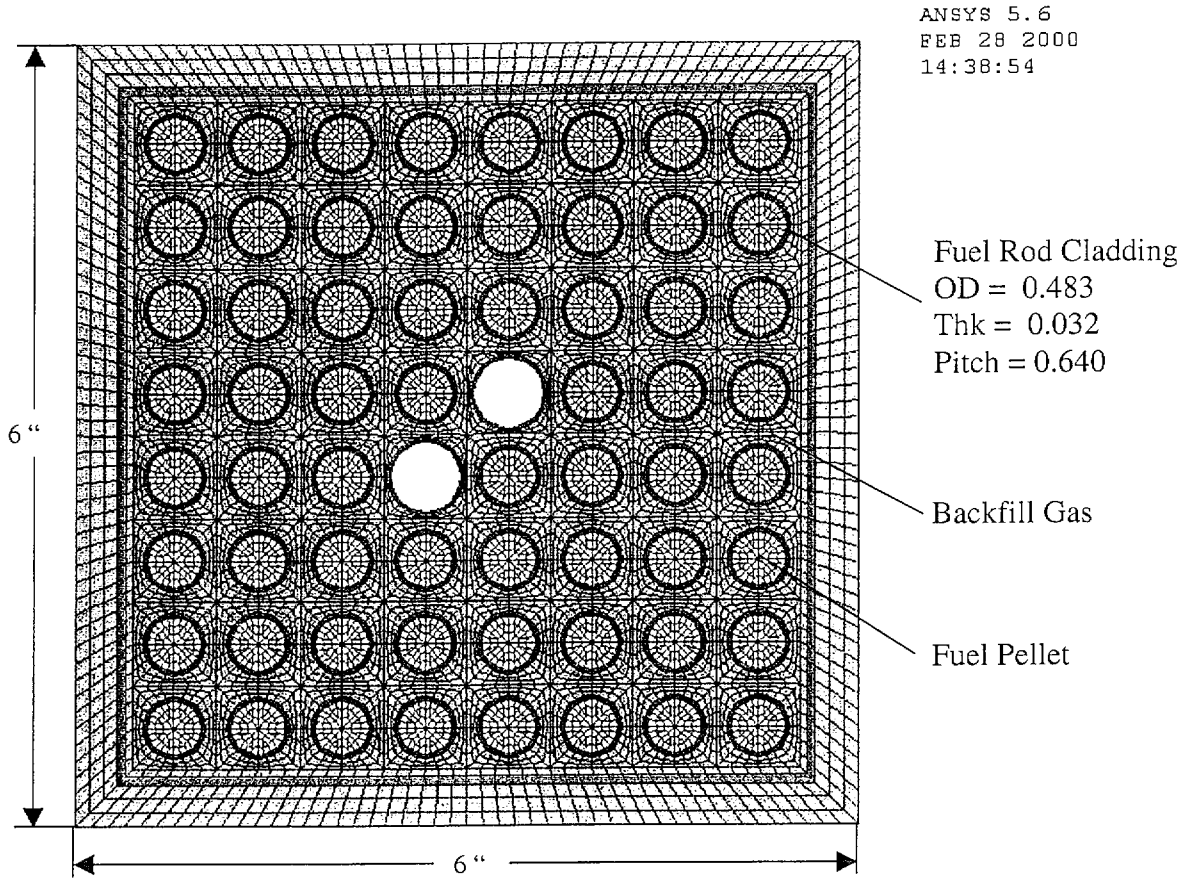


FIGURE 3.7.1-6

FINITE ELEMENT MODEL OF 8x8 (GE8-Type II) FUEL ASSEMBLY

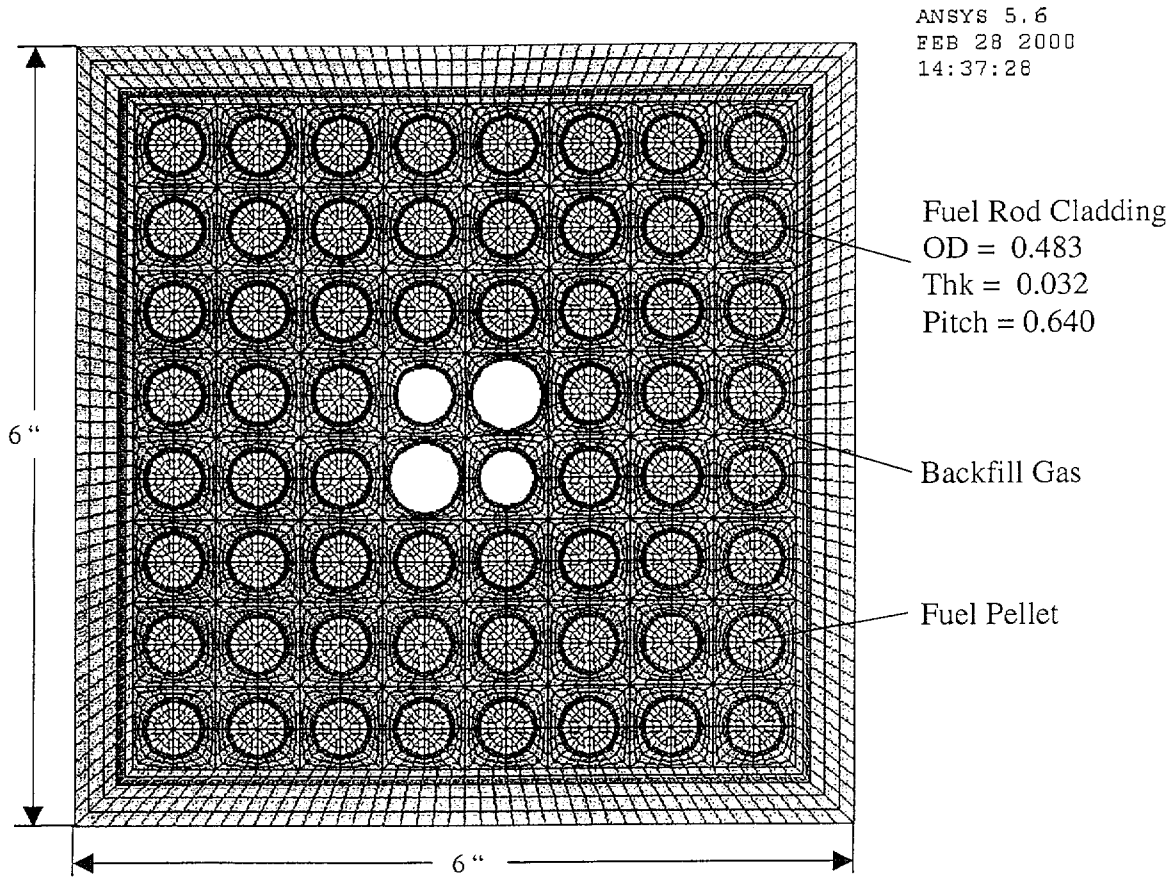
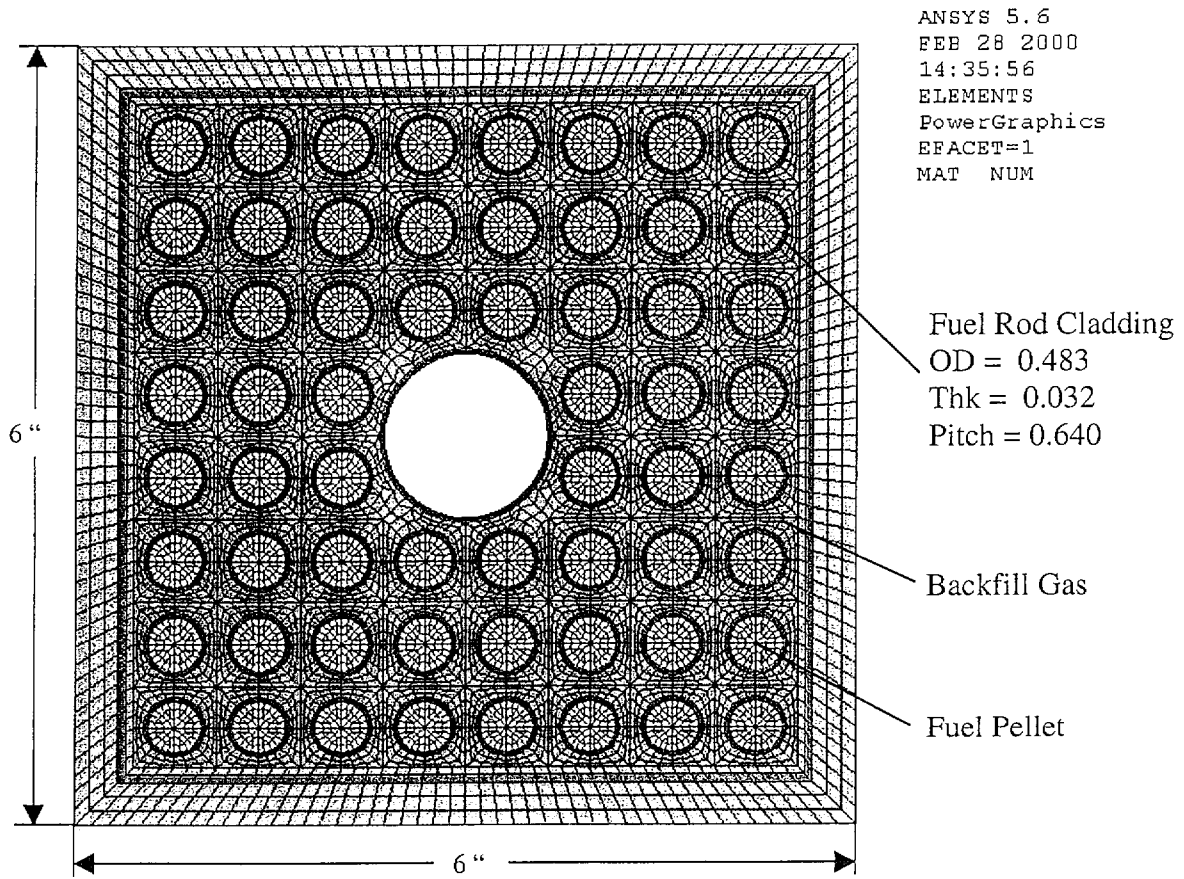


FIGURE 3.7.1-7

FINITE ELEMENT MODEL OF 8x8 (GE9, GE10) FUEL ASSEMBLY



APPENDIX 3.7.2

TABLE OF CONTENTS

3.7.2	AVERAGE CONVECTIVE HEAT TRANSFER COEFFICIENT FOR FIRE ACCIDENT CONDITIONS	3.7.2-1
3.7.2.1	Discussion	3.7.2-1
3.7.2.2	Material Properties for Air	3.7.2-1
3.7.2.3	Average Convective Heat Transfer Coefficient	3.7.2-1
3.7.2.4	References	3.7.2-2

APPENDIX 3.7.2

AVERAGE CONVECTIVE HEAT TRANSFER COEFFICIENT FOR FIRE ACCIDENT CONDITIONS

3.7.2.1 Discussion

The NUHOMS[®]-MP197 finite element models for the fire accident conditions use an average convection heat transfer coefficient. This coefficient is determined assuming an average flame velocity of 15 m/s and an ambient fire temperature of 1475 °F.

3.7.2.2 Material Properties for Air

Temperature		ν ^[1] (m ² /kg)	μ ^[1] (Pa-s)	Pr ^[1] (---)	Conductivity		Kin. Visc. (ft ² /s)
(K) ^[1]	(°F)				(W/m-K) ^[1]	(Btu/hr-ft-°F)	
200	-100	0.573	1.33E-5	0.740	0.0181	0.0105	8.203E-05
300	80	0.861	1.85E-5	0.708	0.0263	0.0152	1.715E-04
400	260	1.148	2.30E-5	0.694	0.0336	0.0194	2.842E-04
500	440	1.436	2.70E-5	0.688	0.0404	0.0233	4.173E-04
600	620	1.723	3.06E-5	0.690	0.0466	0.0269	5.675E-04
800	980	2.298	3.70E-5	0.705	0.0577	0.0333	9.152E-04
1000	1340	2.872	4.24E-5	0.707	0.0681	0.0393	1.311E-03

3.7.2.3 Average Convection Heat Transfer Coefficient

From Reference 1, the skin friction coefficient for a flat plate with constant fluid properties is:

$$\frac{C_f}{2} = \frac{0.185}{(\log_{10} Re)^{2.584}} \quad (3.1)$$

For Pr near unity:

$$\frac{C_f}{2} = \frac{Nu}{(Re Pr)} \quad (3.2)$$

From equations (3.1) and (3.2):

$$h = \frac{\left(\frac{k}{L}\right)(0.185)(Re Pr)}{(\log_{10} Re)^{2.584}}$$

Properties are evaluated at the average temperature between the ambient fire and ambient cool-down condition temperatures. The length of the cask is taken to be 13 ft.

$$T_{\text{avg}} = (1475 + 100)/2 = 788 \text{ }^\circ\text{F}$$

$$U = 15 \text{ m/s} = 49.21 \text{ ft/s}$$

$$L = 13 \text{ ft}$$

$$\text{Pr} = 0.697$$

$$k = 0.0299 \text{ Btu/hr-ft-}^\circ\text{F}$$

$$\nu = 7.294\text{E-}04 \text{ ft}^2/\text{s}$$

(via linear interpolation)

(via linear interpolation)

(via linear interpolation)

$$\text{Re} = (UL/\nu) = 877,010$$

$$h_{\text{avg}} = 2.601 \text{ Btu/hr-ft}^2\text{-}^\circ\text{F}$$

For additional conservatism, a value of $2.750 \text{ Btu/hr-ft}^2\text{-}^\circ\text{F}$ is used in the analysis.

3.7.2.4 References

1. *Handbook of Heat Transfer*, W. Rohsenow and J. Harnett, McGraw-Hill Publishing, New York, 1973.

APPENDIX 3.7.3

TABLE OF CONTENTS

3.7.3 MAXIMUM INTERNAL OPERATING PRESSURES 3.7.3-1

3.7.3.1 Discussion 3.7.3-1

3.7.3.1.1 Average Cavity Gas Temperatures 3.7.3-1

3.7.3.1.2 Amount of Initial Helium Backfill 3.7.3-2

3.7.3.1.3 Free Gas within Fuel Assemblies 3.7.3-2

3.7.3.1.4 Total Amount of Gases within Canister 3.7.3-3

3.7.3.2 Maximum Pressures 3.7.3-3

3.7.3.3 Results and Conclusions 3.7.3-4

3.7.3.4 References 3.7.3-4

APPENDIX 3.7.3

MAXIMUM INTERNAL OPERATING PRESSURES

3.7.3.1 Discussion

The following approach is used in the determination of maximum pressures within the cask body and canister during normal and hypothetical accident conditions of transport:

- First, average cavity gas temperatures are derived from component temperatures.
- Next, the amount of helium present within the canister and cask body after the initial backfilling of each is determined via the ideal gas law.
- Then, the total amount of free gas within the fuel assemblies, including both fill and fission gases, is calculated.
- Using the prescribed percentage of fuel rods that develop cladding breaches from the Standard Review Plan, the total amount of gas within the canister is determined
- Finally, the maximum cavity pressures are determined via the ideal gas law.

3.7.3.1.1 Average Cavity Gas Temperatures

For simplicity, the average cavity gas temperatures within the canister is taken to be the average of the maximum steady state or peak transient fuel cladding and canister wall temperatures. Within the cask body the average cavity gas temperature is taken to be the average of the maximum steady state or peak transient cask body and canister wall temperatures.

Component	Max. Temperature (°F)	
	Normal Conditions	Accident Conditions
Fuel Cladding	598	680
Canister Wall	388	485
Cask Body	302	522
Average Cavity Gas, Canister	493	583
Average Cavity Gas, Cask Body	345	504

3.7.3.1.2 Amount of Initial Helium Backfill

The amounts of helium present within the DSC and the cask body are calculated using the ideal gas law and a maximum initial helium fill of 3.5 psig within the canister and cask body. The initial fill temperature is assumed to be 273 °F; the value used within the NUHOMS®-MP197 Storage Application [1].

From the backfill pressure and average gas temperatures the amounts of helium backfill gas can be calculated.

$$n = (PV)/(RT)$$

P = initial fill pressure = 3.5 psig = 1.24 atm

V = Free volume (ft³)

T = initial fill temperature = 273 °F = 733 R

R = universal gas constant = 0.730 atm-ft³/lbmoles-R

	Canister	Cask Body
Free Volume, V	214.86 ft ³	9.03 ft ³
Amount of backfill, n	0.498 lbmoles	0.021 lbmoles

3.7.3.1.3 Free Gas within Fuel Assemblies

The amount of fission and fill gases within each of the fuel assembly types is taken from Reference 2. The amounts of fission gases tabulated below were determined from SAS2H/ORIGEN-S computer runs. I, Kr, and Xe gases are considered following irradiation. These numbers include the 30 percent release fraction for fission gases due to cladding breaches specified in the Standard Review Plan for Transportation (Reference 3).

Fuel Design	Fill Gas ^[5]	Fission Gas ^[6]	Total	Total
(---)	(kg moles/rod)	(kg moles/rod)	(kg moles/rod)	(lb moles/assy)
7x7-49-0	5.489E-06	6.640E-05	7.189E-05	7.767E-03
8x8-63-1	3.842E-06	4.889E-05	5.273E-05	7.325E-03
8x8-62-2	8.176E-06	4.923E-05	5.741E-05	7.848E-03
8x8-60-4	8.177E-06	5.016E-05	5.834E-05	7.718E-03
8x8-60-1	8.247E-06	5.041E-05	5.866E-05	7.760E-03
9x9-74-2	1.800E-05	3.927E-05	5.727E-05	9.345E-03
10x10-92-2	1.492E-05	3.318E-05	4.810E-05	9.758E-03

The General Electric 10x10 fuel assembly is the bounding case and is used in the determination of the cavity pressures.

3.7.3.1.4 Total Amount of Gases within Canister

The total amount of gas within the canister is equal to the amount of initial helium fill plus any free gases within the assemblies that are released.

The Standard Review Plan for Transportation prescribes the percentage of fuel rods that develop cladding breaches during normal conditions of transport and hypothetical accident conditions. All free gases within fuel rods that develop breaches will be released into the canister.

$$n_{total} = 0.498 \text{ lbmoles} + (f_B)(61 \text{ assemblies})(9.758E-03 \text{ lb moles/assy})$$

n_{total} = total amount of gases

f_B = fraction of fuel rods that develop cladding breaches

= 0.03 for Normal Conditions of Transport [3]

= 1.00 for Hypothetical Accident Conditions [3]

	Normal Conditions	Accident Conditions
f_B	0.03	1.00
n_{total}	0.516 lbmoles	1.093 lbmoles

3.7.3.2 Maximum Pressures

Maximum cavity pressures are determined via the ideal gas law:

$$P = (nRT)/V$$

P = pressure (atm)

V = Free volume (ft³)

T = average cavity gas temperature (R)

R = universal gas constant = 0.730 (atm-ft³/lbmoles-R)

n_{total} = total amount of gases (lbmoles)

	Canister		Cask Body	
	N.C.T.	H.A.C	N.C.T.	H.A.C.
n_{total} (lbmoles)	0.516	1.093	0.021	0.021
T (R)	953	1043	805	964
V (ft ³)	214.86	214.86	9.03	9.03
Cavity Pressure (atm)	1.67	3.87	1.37	1.64

3.7.3.3 Results and Conclusions

During normal operating conditions the maximum pressure within the canister is 1.67 atm (9.8 psig). Within the cask body the maximum normal operating pressure is 1.37 atm (5.4 psig).

During hypothetical accident conditions the maximum pressure within the canister is 3.87 atm (42.2 psig). Within the cask body the maximum accident operating pressure is 1.64 atm (9.4 psig).

3.7.3.4 References

1. NUHOMS COC 1004 Amendment No. 3, 2000
2. *TN-68 Dry Storage Cask Final Safety Analysis Report*, Transnuclear Inc., Revision 0, Hawthorne, NY, 2000.
3. *Standard Review Plan for Transportation Packages for Spent Nuclear Fuel*, NUREG-1617, 2000.
4. ANSYS Engineering Analysis System, *User's Manual for ANSYS Revision 6*, ANSYS, Inc., Houston, PA.

APPENDIX 3.7.4

TABLE OF CONTENTS

3.7.4	THERMAL EVALUATION FOR VACUUM DRYING CONDITIONS.....	3.7.4-1
3.7.4.1	Discussion.....	3.7.4-1
3.7.4.2	Finite Element Model.....	3.7.4-1
3.7.4.3	Material Properties.....	3.7.4-2
3.7.4.4	Transient Analysis.....	3.7.4-2
3.7.4.5	Steady-State Analysis.....	3.7.4-2
3.7.4.6	References.....	3.7.4-2

APPENDIX 3.7.4

THERMAL EVALUATION FOR VACUUM DRYING CONDITIONS

3.7.4.1 Discussion

All fuel transfer operations occur when the packaging is in the spent fuel pool. The fuel is always submerged in free-flowing pool water permitting heat dissipation. After fuel loading is complete, the packaging is removed from the pool, drained and dried.

The loading condition evaluated is the heatup of the cask before its cavity can be backfilled with helium. This typically occurs during the performance of the vacuum drying operation of the cask cavity. Two thermal analyses are performed of the vacuum drying process:

- A transient analysis to determine component temperatures after 36 hours of vacuum drying with the maximum decay heat load.
- A steady state analysis to determine component temperatures with a total decay heat load of 6.5 kW.

3.7.4.2 Finite Element Model

The cask cross-section finite element model developed in Section 3.5.2 is modified for this transient analysis. The vacuum drying of the cask generally does not reduce the pressure sufficiently to reduce the thermal conductivity of the air in the cask cavity. All gaseous heat conduction within the cask cavity is through air instead of helium. Radiation heat transfer within the cask cavity is neglected. The fuel properties were recalculated using air properties instead of helium. All temperatures in the cask are initially assumed to be at 100°F. Radiation and natural convection heat transfer are from the cask outer surface to the building environment at a temperature of 100°F.

3.7.4.3 Material Properties

BWR Fuel w/ Air Backfill

Temperature (°F)	Thermal Conductivity (Btu/hr-in-°F)		Specific Heat (Btu/lbm-F)	Density (lbm/in ³)
	Transverse	Axial		
150.796	0.0045	0.0437	0.105	0.0574
239.954	0.0058
331.555	0.0073
425.095	0.0092
520.134	0.0114
616.315	0.0141
713.356	0.0173
811.049	0.0209
909.232	0.0250	0.0437	0.105	0.0574

3.7.4.4 Transient Analysis

The modified cask-cross section model was run to determine maximum component temperatures after 36 hours of vacuum drying. At that time all temperatures remain below those during normal conditions of transport and are well below all thermal design limits discussed within Section 3.1.

3.7.4.5 Steady-State Analysis

The modified cask-cross section model was run to determine maximum component temperatures using a total decay heat load of 6.5 kW. At that heat load all temperatures remain below those during normal conditions of transport and are well below all thermal design limits discussed within Section 3.1.

3.7.4.6 References

1. ANSYS Engineering Analysis System, *User's Manual for ANSYS Revision 6*, ANSYS, Inc., Houston, PA.

NUHOMS® -MP197 TRANSPORT PACKAGING

CHAPTER 4

TABLE OF CONTENTS

	<u>Page</u>
4. CONTAINMENT	
4.1 Containment Boundary.....	4-1
4.1.1 Containment Vessel.....	4-1
4.1.2 Containment Penetrations.....	4-2
4.1.3 Seals and Welds.....	4-2
4.1.4 Closure.....	4-3
4.2 Requirements for Normal Conditions of Transport.....	4-4
4.2.1 Containment of Radioactive Material.....	4-4
4.2.2 Pressurization of Containment Vessel.....	4-4
4.2.3 Containment Criterion.....	4-4
4.3 Containment Requirements for Hypothetical Accident Conditions.....	4-5
4.3.1 Fission Gas Products.....	4-5
4.3.2 Containment of Radioactive Material.....	4-5
4.3.3 Containment Criterion.....	4-5
4.4 Special Requirements.....	4-6
4.5 References.....	4-7

LIST OF TABLES

4-1	Radionuclide Inventory
4-2	Activity Concentration by Source

LIST OF FIGURES

4-1	NUHOMS® - MP197 Containment Boundary Components
-----	---

CHAPTER 4

CONTAINMENT

4.1 CONTAINMENT BOUNDARY

The containment boundary consists of a cylindrical inner shell, a bottom end (closure) plate with a ram access penetration with seal, a cask body flange, a top lid with seal, and vent and drain port closure bolts and seals. The containment boundary is shown in Figure 4-1. The construction of the containment boundary is shown on the drawings provided in Appendix 1.4. The containment vessel prevents leakage of radioactive material from the cask cavity. It also maintains an inert atmosphere (helium) in the cask cavity.

Additionally, the NUHOMS[®] -61BT DSC welded canister contains helium. Thus, the welded canister also provides a containment function. Helium assists in heat removal and provides a non-reactive environment to protect fuel assemblies against fuel cladding degradation which might otherwise lead to gross rupture.

4.1.1 Containment Vessel

The NUHOMS[®] -MP197 containment vessel consists of the inner shell, a 6.50 inch thick bottom plate with a 23.88 inch diameter, 2.5 inch thick RAM access closure, a top closure flange, a 4.50 inch thick top closure lid with closure bolts, vent and drain port closures and bolts, and double O-ring seals for each of the penetrations. A 68 inch diameter, 197 inch long cavity is provided.

The inner containment shell is SA-240, Type XM-19, and the bottom, and top flange materials are SA-182, Type FXM19. The top closure lid is constructed from SA-705, Type 630, H1100. The NUHOMS[®] -MP197 packaging containment vessel is designed, fabricated, examined and tested in accordance with the requirements of Subsection NB of the ASME Code [1] to the maximum practical extent. In addition, the design meets the requirements of Regulatory Guides 7.6 [2] and 7.8 [3]. Exceptions to the ASME Code are discussed in Section 2.11 of Chapter 2. The construction of the containment boundary is shown in drawings 1093-71-2, -3 and -4 provided in Appendix 1.4. The design of the containment boundary is discussed in Chapter 2.

The cask design, fabrication and testing are performed under Transnuclear's Quality Assurance Program which conforms to the criteria in Subpart H of 10CFR71.

The materials of construction meet the requirements of Section III, Subsection NB-2000 and Section II, Material specifications or the corresponding ASTM Specifications. The containment vessel is designed to the ASME Code, Section III, Subsection NB, Article 3200.

The containment vessel is fabricated and examined in accordance with NB-2500, NB-4000 and NB-5000. Also, weld materials conform to NB-2400 and the material specification requirements of Section II, Part C of ASME B&PV.

The containment vessel is hydrostatically tested in accordance with the requirements of the ASME B&PV Code, Section III, Article NB-6200.

Even though the code is not strictly applicable to transport casks, it is the intent to follow Section III, Subsection NB of the Code as closely as possible for design and construction of the containment vessel. The casks may, however, be fabricated by other than N-stamp holders and materials may be supplied by other than ASME Certificate Holders. Thus the requirements of NCA are not imposed. TN's quality assurance requirements, which are based on 10CFR71 Subpart H and NQA-1 are imposed in lieu of the requirements of NCA-3850. This SAR is prepared in place of the ASME design and stress reports. Surveillances are performed by TN and utility personnel rather than by an Authorized Nuclear Inspector (ANI).

Paragraph NB-4213 requires the rolling process used to form the inner vessel be qualified to determine that the required impact properties of NB-2300 are met after straining by taking test specimens from three different heats. If the plates are made from less than three heats, each heat will be tested to verify the impact properties.

The materials of the NUHOMS[®] -MP197 packaging will not result in any significant chemical, galvanic or other reaction as discussed in Chapter 2.

4.1.2 Containment Penetrations

The only penetrations into the containment boundary are the drain and vent ports, ram closure plate and the top closure plate (lid). Each penetration is designed to maintain a leak rate not to exceed 1×10^{-7} ref cc/sec, defined as "leak tight" per ANSI N14.5 [4]. To obtain these seal requirements, each penetration has an O-ring face seal type closure. Additionally, each penetration has a double O-ring configuration.

4.1.3 Seals and Welds

All containment boundary welds are full penetration bevel or groove welds to ensure structural and sealing integrity. These full penetration welds are designed per ASME III Subsection NB and are fully examined by radiography or ultrasonic methods in accordance with Subsection NB. Additionally, a liquid penetrant examination is performed on these welds.

Containment seals are located at the ram access port closure plate, the top closure (lid) plate, the drain plug and the vent plug. The inner seal in all cases is the primary containment seal. The outer, secondary seals, facilitate leak testing of the inner containment seal of the ram closure plate and the lid. There are also test ports provided for these two closures. The test ports are not part of the containment boundary.

All the seals use in the NUHOMS[®] -MP197 cask containment boundary are static face seals. The seal areas are designed for no significant plastic deformation under normal and accident loads as shown in Chapter 2. The bolts are torqued to maintain a seal load during all load conditions as shown in Appendix 2.10.2. The seals used for all of the penetrations are fluorocarbon elastomer O-rings. All seal contact surfaces are stainless steel and are machined to a 16 microinch (maximum) R_a surface finish. The dovetail grooves in the cask lid and the ram closure plate are intended to retain the seals during installation. The volume of the grooves is controlled to allow the mating metal surfaces to contact under bolt loads, thereby providing uniform seal deformation in the final installation condition.

Fluorocarbon has good sealing properties from -15°F up to 400°F for the seal configuration used in the cask, and it can withstand a maximum temperature of 700°F for the accident conditions [5]. At temperatures below -15°F , some fluorocarbon compounds (V0835-75) can maintain a sealing ability to approximately -40°F .

4.1.4 Closure

The containment vessel contains an integrally-welded bottom closure and a bolted and flanged top closure plate (lid). The lid plate is attached to the cask body with forty eight (48), SA-540, Grade B24, Class 1, 1 1/2" diameter bolts. Closure of the ram closure plate is accomplished by twelve (12), SA-540, Grade B24, Class 1, 1 inch diameter bolts. The bolt torque required for the lid and ram closure plate are provided in Drawing 1093-71-3 in Appendix 1.4 . The closure bolt analysis is presented in Appendix 2.10.2.

Closure of each of the vent and drain ports is accomplished by a single 3/4 inch SA-540, Grade B24, Class 1 bolt with seals under the head of the bolt tightened to the values shown in Drawing 1093-71-3.

4.2 REQUIREMENTS FOR NORMAL CONDITIONS OF TRANSPORT

4.2.1 Containment of Radioactive Material

As described earlier, the NUHOMS[®]-MP197 cask is designed and tested for a leak rate of 1×10^{-7} ref cc/s, defined as "leak tight" per ANSI N14.5. Additionally, The structural and thermal analyses presented in Chapters 2 and 3 , respectively, verify that there is no release of radioactive materials under any of the normal conditions of transport.

4.2.2 Pressurization of Containment Vessel

The NUHOMS[®]-MP197 cask contains a sealed (welded) canister which has been tested to a "leak tight" criteria. Therefore, the pressure in the MP197 cask is from helium that has been backfilled into an evacuated cask cavity to a pressure of 3.5 psig at the end of loading. If the MP197 cask contains design basis fuel at thermal equilibrium, the cask cavity helium temperature with 100°F ambient air and maximum solar load is 345°F. The maximum normal operating pressure is calculated in Appendix 3.7.3 to be 5.4 psig. The analyses in Chapter 2 and 3 demonstrate that the MP-197 cask effectively maintains containment integrity with a cavity pressure of 50 psig.

4.2.3 Containment Criterion

The NUHOMS[®]-MP197 cask is design to be "leak tight". The acceptance criterion for fabrication verification and periodic verification leak test of the MP197 containment boundary shall be 1.0×10^{-7} ref cm³/s. The test must have a sensitivity of at least one half the acceptance criterion, or 5×10^{-8} ref cm³/s.

4.3 CONTAINMENT REQUIREMENTS FOR HYPOTHETICAL ACCIDENT CONDITIONS

4.3.1 Fission Gas Products

The following equations from NUREG/CR-6487 [6] are used to determine the source term available for release.

$$\begin{aligned}C_{\text{volatiles}} &= \{N_A f_B A_V f_V\} / V \\C_{\text{gases}} &= \{N_A f_B A_F f_F\} / V \\C_{\text{fines}} &= \{N_A f_B A_F f_F\} / V \\C_{\text{crud}} &= \{f_C S_C N_R N_A S_{AR}\} \\C_{\text{total}} &= C_{\text{crud}} + C_{\text{volatiles}} + C_{\text{gases}} + C_{\text{fines}}\end{aligned}$$

Table 4-1 shows the free activity available for release from typical BWR spent fuel rods. Table 4-2 shows the activity concentration from each of the sources available for release. The release fractions for the radionuclides are taken from NUREG/CR-6487. Under hypothetical accident conditions, the cladding of 100% of the fuel rods is assumed to fail ($f_B=1.0$).

4.3.2 Containment of Radioactive Material

The NUHOMS[®]-MP197 cask is designed and tested to be "leak tight". The MP197 contains a sealed (welded) canister (DSC) which is also tested to a "leak tight" criteria. The results of the structural and thermal analyses presented in Chapters 2 and 3, respectively, verify the package will meet the leakage criteria of 10CFR71.51 for the hypothetical accident scenario.

4.3.3 Containment Criterion

This package has been designed and is verified by leak testing, to meet the "leak tight" criteria of ANSI N14.5.

4.4 SPECIAL REQUIREMENTS

Solid plutonium in the form of reactor elements is exempt from the double containment requirements of 10 CFR 71.63.

4.5 REFERENCES

1. American Society of Mechanical Engineers, ASME Boiler and Pressure Vessel Code, Section III, Division 3, Subsection WB, 1998 including 1999 addenda.
2. USNRC Regulatory Guide 7.6, "Design Criteria for the Structural Analysis of Shipping Cask Containment Vessel", Rev. 1, March 1978.
3. USNRC Regulatory Guide 7.8, "Load Combinations for the Structural Analysis of Shipping Cask", Rev. 1, March 1989.
4. ANSI N14.5-1997, "American National Standard for Radioactive Material – Leakage Tests on Packages for Shipment," February 1998.
5. "Parker O-Ring Handbook", Publication No. ORD-5700, Parker Seals.
6. NUREG/CR-6487, "Containment Analysis for Type B Packages used to Transport Various Contents," Lawrence Livermore National Laboratory, 1996.

TABLE 4-1
RADIONUCLIDE INVENTORY

	Ci/assembly ¹
Volatiles	
Sr 90	1.36E+04
Cs134	1.30E+03
Cs137	2.02E+04
Total - Volatiles	3.51E+04
Gases	
H 3	6.40E+01
Kr 85	1.03E+03
I129	7.62E-03
Total - Gases	1.09E+03
Fines	
Pu238	8.19E+02
Pu239	6.32E+01
Pu240	1.09E+02
Pu241	1.81E+04
Am241	4.06E+02
Cm244	6.25E+02
Y 90	1.36E+04
Ru106	1.15E+02
Sb125	1.32E+02
Pm147	2.10E+03
Sm151	7.57E+01
Eu154	1.32E+03
Eu155	4.61E+02
Total - Fines	3.79E+04

¹ Values are based on a 7x7 fuel assembly (40,000 MWD/MTU burnup, 3.3 wt% U-235 initial bundle average enrichment, and 10 year cooled).

² Ba137m and Rh106 contribute 20.4% and 0.1%, respectively, to the total design basis activity. Ba137m and Rh106 are daughters of Cs137 and Ru106, respectively, with half lives of 2.6 min and 30 sec, respectively. In accordance with 10CFR71 Appendix A Note III, these radionuclides are evaluated with the parent nuclide.

TABLE 4-2

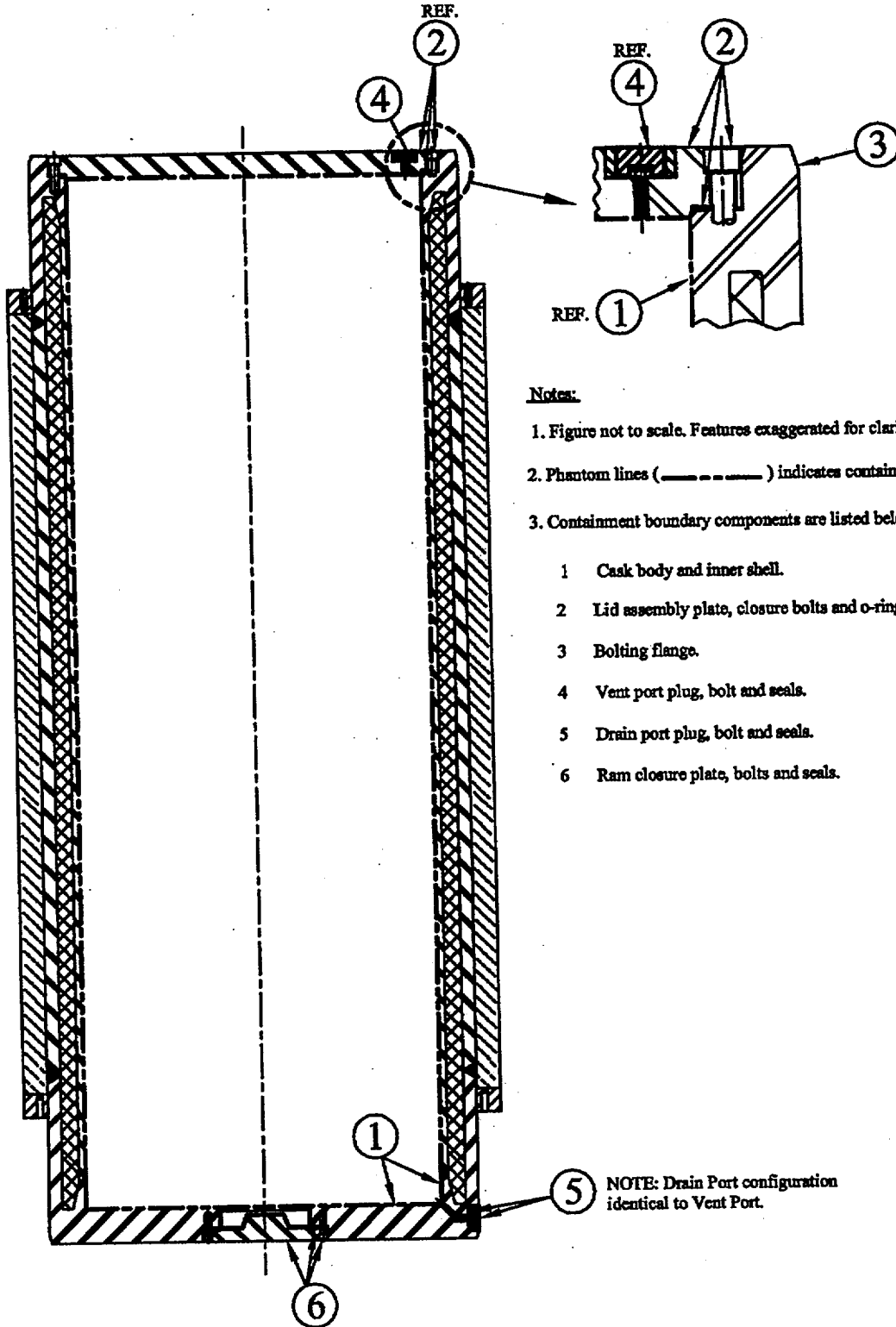
ACTIVITY CONCENTRATION BY SOURCE

<u>Source</u>	<u>Fraction available for release from the fuel rod⁽¹⁾ ($f_V / f_G / f_F / f_C$)</u>	<u>Fraction of rods that develop cladding breach⁽¹⁾</u>
Normal Transport Conditions		
Volatiles	2E-04	0.03
Gases	0.3	0.03
Fines	3E-05	0.03
Crud ⁽⁵⁾	0.15	not applicable
Hypothetical Accident Conditions		
Volatiles	2E-04	1.0
Gases	0.3	1.0
Gases - Kr-85 only	0.3	1.0
Fines	3E-05	1.0
Crud	1.0	not applicable

¹ Values taken from NUREG/CR-6487 [6]

FIGURE 4-1

NUHOMS®-MP197 CONTAINMENT BOUNDARY COMPONENTS



Notes:

- 1. Figure not to scale. Features exaggerated for clarity.
- 2. Phantom lines (-----) indicates containment boundary.
- 3. Containment boundary components are listed below:

- 1 Cask body and inner shell.
- 2 Lid assembly plate, closure bolts and o-rings.
- 3 Bolting flange.
- 4 Vent port plug, bolt and seals.
- 5 Drain port plug, bolt and seals.
- 6 Ram closure plate, bolts and seals.

NOTE: Drain Port configuration identical to Vent Port.

NUHOMS® -MP197 TRANSPORT PACKAGING

CHAPTER 5

TABLE OF CONTENTS

	<u>Page</u>
5. SHIELDING EVALUATION	
5.1 Discussion and Results	5-1
5.2 Source Specification.....	5-2
5.2.1 Axial Source Distribution	5-4
5.2.2 Gamma Source	5-4
5.2.3 Neutron Source.....	5-5
5.3 Model Specification	5-6
5.3.1 Description of Radial and Axial Shielding Configuration.....	5-6
5.3.2 Shield Regional Densities	5-7
5.4 Shielding Evaluation	5-8
5.5 References.....	5-10
5.6 Appendix.....	5-11
5.6.1 SAS2H/ORIGENS Input File.....	5-11
5.6.2 MCNP Neutron Model Input File.....	5-13
5.6.3 MCNP Primary Gamma Input File (Preferential Loading).....	5-21

LIST OF TABLES

- 5.1-1 NUHOMS® MP-197/61B Shield Materials
- 5.1-2 Summary of Dose Rates
- 5.2-1 BWR Fuel Assembly Design Characteristics
- 5.2-2 BWR Fuel Assembly Hardware Characteristics
- 5.2-3 Material Compositions For Fuel Assembly Hardware Materials
- 5.2-4 BWR Fuel Assembly Source (With Channels) Bundle Average Enrichment 3.3 Wt%
U235, 40,000 MWD/MTU, 10 Year Cooling Time
- 5.2-5 Primary Gamma Source Spectrum Scale 18 Group Structure
General Electric 7x7, Bundle Average Enrichment 2.65wt% U235,
35,000 MWD/MTU, And 12 Year Cooling Time With Channels
- 5.2-6 Primary Gamma Source Spectrum Scale 18 Group Structure
General Electric 7x7, Bundle Average Enrichment 2.65wt% U235,
35,000 MWD/MTU, And 12 Year Cooling Time With Channels

LIST OF TABLES (continued)

- 5.2-7 Source Term Summary
- 5.3-1 Materials Input For MCNP
- 5.4-1 Response Functions For Gamma
- 5.4-2 Response Functions For Neutron

LIST OF FIGURES

- 5.1-1 NUHOMS[®]-MP197 Cask Shielding Configuration
- 5.2-1 Axial Burnup Profile For Design Basis Fuel
- 5.3-1 MCNP Top Half Model
- 5.3-2 MCNP Bottom Half Model
- 5.4-1 NUHOMS[®]-MP197 Radial Gamma Dose Rate Profile
- 5.4-2 NUHOMS[®]-MP197 Radial Neutron Dose Rate Profile
- 5.4-3 NUHOMS[®]-MP197 Gamma Dose Rate Impact Limiter Surface
- 5.4-4 NUHOMS[®]-MP197 Neutron Dose Rate Impact Limiter Surface

CHAPTER 5

SHIELDING EVALUATION

5.1 DISCUSSION AND RESULTS

Shielding for the NUHOMS[®]-MP197 cask is provided mainly by the cask body. Gamma-ray shielding is provided mainly by the lead and stainless steel shells that comprise the cask wall. For the neutron shielding, a borated polyester resin compound surrounds the cask body radially. Gamma shielding in the cask ends is provided mainly by the steel top and bottom assemblies of the NUHOMS[®]-61BT DSC.

For transport, wood filled impact limiters are installed on the top and bottom of the cask and provide additional shielding for the top and bottom ends in addition to some radial shielding for the areas above and below the radial neutron shield. Figure 5.1-1 shows the configuration of shielding in the cask. Table 5.1-1 lists the compositions of the shielding materials.

The fuel assemblies acceptable for storage in the NUHOMS[®]-MP197 are listed in Section 1.2.3. This listing of fuel assemblies was collapsed into seven basic designs. Using the SAS2H/ORIGEN-S modules of SCALE [1], source terms for the seven basic fuel designs are calculated. Each basic group has an initial bundle-average enrichment of 3.3 wt% and a total maximum bundle average burnup of 40,000 MWD/MTU. The most conservative source/configuration is used in the subsequent shielding calculations.

Through this analysis, the GE 7x7 fuel array is identified as the most conservative source/configuration, due mainly to the mass of uranium. Additional SAS2H/ORIGENS analyses are performed for four different fuel burnup/enrichment groups using the bounding 7x7 fuel assembly. Through these analyses, the Group 2 source was identified as having the bounding gamma and neutron source. Section 5.2 describes the source specification and Section 5.4 describes the shielding analysis performed for the NUHOMS[®]-MP197 cask containing the 61BT canister.

Normal conditions are modeled with the NUHOMS[®]-MP197 intact. This shielding calculation is performed using the Monte Carlo computer code MCNP [5]. Dose rates on the side, top and bottom of the MP197 cask are calculated for the various sources (active fuel-gamma and neutron and irradiated hardware-gamma) and summed to a total gamma and neutron dose rate.

Accident conditions assume that the neutron shield, and shield shell are removed. A gap(s) is also modeled in the lead shield to account for lead slump in the accident. Shielding calculations for accident conditions are also performed using MCNP.

The expected maximum dose rates (for normal and accident conditions) from the MP197 cask are provided in Table 5.1-2. These dose rates are calculated for a NUHOMS[®]-MP197 cask containing the 61BT DSC filled with Group 2 fuel assemblies cooled for 12 years.

5.2 SOURCE SPECIFICATION

There are five principal sources of radiation associated with cask storage that are of concern for radiation protection:

- Primary gamma radiation from spent fuel;
- Primary neutron radiation from spent fuel (both alpha-n reactions and spontaneous fission);
- Gamma radiation from activated fuel structural materials;
- Capture gamma radiation produced by attenuation of neutrons by shielding material of the cask; and
- Neutrons produced by sub-critical fission in fuel.

The NUHOMS[®]-MP197 is designed to transport GE BWR fuel types; from the GE Series 2 and 3 (7x7 fuel array), the GE Series 4 through 10 (8x8 fuel array), the current GE Series 12 (10x10 fuel array), and the current GE Series 11 and 13 (9x9 fuel array). The fuel assemblies acceptable for transport in the MP197 are described in Section 1.2.3. This listing of fuel assemblies was collapsed into seven basic designs provided below. The various fuel assembly designs were separated according to fuel assembly array, the maximum metric tons of uranium, and the number of water rods. These three parameters are the significant contributors to the SAS2H/ORIGEN-S model. The largest uranium loading results in the largest source term at the design basis enrichment and burnup.

<u>Fuel Array Type</u>	<u>Number of Fueled Rods</u>	<u>Number of Water Rods</u>	<u>Metric Tons Uranium per Assembly</u>
7 x 7	49	0	0.1977
8 x 8	63	1	0.1880
8 x 8	62	2	0.1856
8 x 8	60	4	0.1825
8 x 8	60	1	0.1834
9 x 9	74	2	0.1766
10 x 10	92	2	0.1867

Table 5.2-1 provides additional fuel assembly design characteristics for the seven basic fuel designs. The SAS2H/ORIGEN-S modules of the SCALE code are used to generate a gamma and neutron source term for each fuel assembly design. Each basic design has an initial bundle-average enrichment of 3.3 wt% U235 and the fuel zone is irradiated at a constant specific power of 5 MW/assembly to a total bundle average burnup of 40,000 MWD/MTU.. A conservative three-cycle operating history is utilized with 30 day down time each cycle except for no down time in the last cycle.

The source terms are generated for the active fuel regions, the plenum region, and the end regions. Irradiation of the fuel assembly structural materials (including the channel, plenum, and end fittings) are included in the irradiation of the fuel zone. The fuel assembly hardware materials and masses on a per assembly basis are listed in Table 5.2-2. Table 5.2-3 provides the material composition of fuel assembly hardware materials. Cobalt impurities are included in the SAS2H model. In particular, the cobalt impurities in Inconel, Zircaloy and Stainless Steel are 0.649%, 0.001% and 0.08%, respectively [2].

The masses for the materials in the top end fitting, the plenum, and the bottom fitting regions are multiplied by 0.1, 0.2 and 0.15, respectively [4]. These factors are used to correct for the spatial and spectral changes of the neutron flux outside of the fuel zone. The material compositions of the fuel assembly hardware are included in the SAS2H/ORIGEN-S model on a per assembly basis.

Axial variation in the moderator density along the BWR fuel assembly was considered by including a volume averaged density for the moderator around the fuel pins. The following axial variation of temperatures and moderator densities were used to calculate the volume average moderator density for use in the BWR source term models [1]:

<u>Distance from bottom of Active Fuel Length</u>	<u>Average Density in Zone (g/cc)</u>	<u>Average Water Temp (K)</u>
30.83	0.743	552
43.17	0.600	558
55.5	0.494	558
67.83	0.417	558
80.17	0.360	558
98.67	0.309	558
123.33	0.264	558
148	0.234	558
Assembly data -water, volume-average density	0.4234 g/cc	558 K

Gamma and neutron source terms are calculated for each of the four groups. Table 5.2-4 presents the gamma and neutron source terms for a 10 year cooling time. The 7x7 fuel assembly is the most conservative source/configuration and is utilized to determine the bounding source terms for the NUHOMS[®]-MP197 shielding analysis.

As shown in Section 1.2.3, four different groups of fuel assembly parameters are chosen as representative of the fuel to be transported in the MP197. SAS2H/ORIGEN-S analyses are performed for each of these four groups of fuel assemblies and the bounding source term identified and chosen for the shielding analysis. The Group 2 fuel assembly (lattice enrichment 2.65 wt% and 35,000 MWD/MTU burnup) with a cooling time of 12 years is selected as the bounding source for the shielding analysis.

5.2.1 Axial Source Distribution

Axial source term peaking factors are determined based on typical axial burnup distributions for BWR assemblies and based upon typical axial water density distribution that occurs during core operation. Using the base SAS2H/ORIGEN-S input for the 7x7 BWR, selected as the design basis assembly above, neutron and gamma source terms are generated for axial zones as a function of burnup and moderator density. This estimates both the non-linear behavior of the neutron source with burnup and the core operating moderator density effects on the actinide isotopics (neutron source).

In-core data from an operating BWR facility forms the basis for the evaluation. The data provided the burnup and moderator density for 25 axial locations along the fuel assembly. Five assemblies located in different locations in the reactor core were utilized to generate a burnup (peaking factor) distribution for the assembly. Figure 5.2-1 represents this distribution.

For water densities, the nodal data provided was examined and 7 assemblies with the lowest densities were selected for evaluation. Of these seven, the assembly with the lowest densities was chosen. The water density data provided shows densities ranging from 0.7608 g/cc at the bottom node to 0.3607 at the top node.

The peaking factors and water densities for the 25 axial locations were collapsed into 12 axial zones and utilized in determining the source terms and axial profiles of the sources for the shielding evaluation. The top and bottom 10% of the assembly was divided into two zones each and the middle 80% divided into 8 equal zones. The peaking factors ranged from 0.2357 and 0.2410 at the bottom and top respectively, to a maximum of 1.20 just below the middle. The water densities ranged from 0.3609 at the top zone to 0.7603 at the bottom.

The burnup and water density axial distribution data was utilized to prepare a 12 axial zone fuel assembly model. Twelve SAS2H calculations were performed for the design basis fuel with the power and water density being variables for each zone. The specific power input was the product of the nominal specific power, (5 MW) and the peaking factor. The water density was that value calculated for the zone as described above. Therefore, the fuel assembly was divided into 12 zones, with each zone having a unique gamma and neutron source term, specifically calculated for the burnup and water density in that zone. This data is presented in Table 5.2-11. (Note: the axial profile data is for 10 year cooled fuel, but the profile is equally applicable for longer cooled fuel.)

5.2.2 Gamma Source

The primary gamma source spectrum for the Group 2 fuel assembly is provided in Tables 5.2-5. Table 5.2-5 present spectra for a 7x7 assembly with an initial bundle average enrichment of 2.65wt%, maximum bundle-average burnup of 35,000 MWD/MTU and 12 year decay. The gamma source spectra are presented in the 18-group structure consistent with the SCALE 27n-18 γ cross section library.

The conversion of the source spectra from the default ORIGEN-S energy grouping to the SCALE 27n-18 γ energy grouping is performed directly through the ORIGEN-S code. The SAS2H/ORIGEN-S input file for the Group 2 7x7 fuel assembly is provided in Section 5.5.

The gamma source for the fuel assembly hardware is primarily from the activation of cobalt. This activation contributes primarily to SCALE Energy Groups 36 and 37. Based on the weight fraction of cobalt in each zone of the fuel assembly model (as adjusted by the appropriate flux ratio), the gamma source term in SCALE Energy Groups 36 and 37 are redistributed accordingly. The gamma source for the plenum region, the top fitting region and the bottom fitting region is provided in Tables 5.2-6.

An axial burnup profile has been developed as discussed in Section 5.2.1 above. Table 5.2-7 provides design axial gamma peaking factors and source terms that were utilized in the MCNP shielding model.

5.2.3 Neutron Source

Tables 5.2-7 provides the total neutron source spectra for the Group 2 fuel assembly under the irradiation/decay history described above in 5.2.2. The SAS2H/ORIGEN-S code provides the neutron spectra in the SCALE 27n-18 γ energy groups. The SAS2H/ORIGEN-S input file for the 7x7 fuel assembly is provided in Section 5.5.

The neutron source is not linearly dependent with burnup, and therefore analyses were performed to determine the axial neutron source distribution (Section 5.2.1). The axial neutron source distribution as a function of burnup and water density is shown in Table 5.2-7.

5.3 MODEL SPECIFICATION

The monte carlo code MCNP is used for calculating the gamma and neutron doses immediately around the cask.

5.3.1 Description of Radial and Axial Shielding Configuration

A single geometric model was developed for MCNP. This model was used to calculate both the axial and radial dose rates. In order to determine the total dose rate around a single cask, three separate runs were performed, each with a different source; 1) primary gamma, 2) neutron and 3) hardware gamma (end fittings).

Sections 5.3.1.1 and 5.3.1.2 describe the shielding model (for the vicinity immediately around the cask) developed for the NUHOMS[®]-MP197 under normal, off-normal and accident conditions.

5.3.1.1 Radial and Axial Shielding Configuration under Normal Conditions of Transport

Under normal conditions, one shielding configuration is used for the NUHOMS[®]-MP197 design. The model is illustrated in Figures 5.3-1 and 5.3-2 for the transport configuration of the MP197. The dimensions of this shielding model correspond to the dimensions of the MP197 design. The metal trunnions are replaced with the trunnion plugs. The impact limiter wood is assumed to all be balsa. The hold down ring was not included in the model. A 0.06" radial air gap is assumed at the lead (gamma shield) and outer shell interface to account for possible lead shrinkage during fabrication.

The axial locations of the plenum and the end fittings for the fuel assembly are taken from Reference 3; these are the same regardless of fuel assembly type.

The modeled active fuel length is 144 inches and the plenum length is 16.5 inches. The stainless steel rails are included as an equivalent layer of material (0.44") within the canister.

The impact limiters are modeled as wood surrounded by a 0.25" thick steel shell. The interior steel gussets are neglected. The wood is assumed to be balsa. The thermal shield under the bottom impact limiter is not included in the model, this is conservative since shielding material is neglected.

The fuel region is assumed to consist of uranium dioxide. The fuel cladding and one half of the steel and aluminum basket mass are included in the homogenized fuel region. The fuel channels are not included in the homogenization. (However, the fuel channels are included in the source term.) The fuel and basket region are modeled as a cylinder within the DSC. The actual DSC ID is reduced by the 0.44" equivalent steel rail layer so that the homogenized source region is modeled with a reduced diameter of 65.37".

The plenum region is assumed to consist of the cladding, plenum springs and the steel and aluminum basket. The hydrogen getters within the plenum are neglected. One-half of the basket mass in this region is homogenized through the plenum region.

Similarly, the bottom fitting region is homogenized with one-half the basket. The top fitting hardware with one-half of the basket mass is homogenized through the same reduced canister diameter as the other regions.

The key-way at the bottom of the cask that interfaces the cask to the transporter is included in the model. The key-way is assumed to be filled with the steel "key" on the transporter since the cask in normal transport mode is modeled. Voids are neglected within the fuel assembly. The voids within the cask cavity are modeled.

5.3.1.2 Radial and Axial Shielding Configuration under Hypothetical Accident Conditions of Transport

For accident conditions, it is assumed the neutron shield and shield shell are removed. The accident model also includes a 3.5" air gap at the top and bottom of the lead shield to account for the lead slump calculated in Chapter 2. The model utilizes the same regional densities and shield thickness as the model for normal conditions.

5.3.2 Shield Regional Densities

For the MCNP model, four source areas, shown in Figures 5.3-1 and Figure 5.3-2 are utilized: fuel zone, plenum, upper fitting and lower fitting. The sources are uniformly homogenized over the reduced canister diameter (65.37") and the appropriate length. One-half of the fuel basket mass is homogenized over the source diameter and appropriate length (of the fuel zone, plenum and bottom fitting).

The radial resin and aluminum boxes are homogenized into a single composition based on the mass of each component. Measured dose rates around the TN-24P [7], the TN-40, and the TN-32 casks have shown no streaming effects around the neutron shield. This is because the neutrons will not generally travel in a direct path, but scatter, such that the majority of the neutrons will not be able to travel through the aluminum box wall for the full 6 inches of resin box thickness. The material input for the MCNP model is listed in Table 5.3-1.

5.4 SHIELDING EVALUATION

Dose rates around the MP-197 are determined by choosing the most conservative source and using it within a three dimensional MCNP model. The MCNP dose is calculated as surface flux (F2) tallies and converted into dose rates using energy dependent dose conversion factors [6], (Tables 5.4-1 and 5.4-2). The shielding evaluation accounts for subcritical neutron multiplication. The generation of secondary gamma dose due to neutron interactions in the shielding materials, principally the neutron shield resin, is neglected because the resin is surrounded by a steel shell and previous evaluations have shown the secondary gamma dose to be small fraction (< 3%) of the total calculated contact dose.

For the doses around the NUHOMS[®]-MP197, the source is divided into four separate regions: fuel, plenum, top fitting, and bottom fitting. The model is utilized in three separate computer runs consisting of contributions from the following sources:

- Primary gamma radiation from the active fuel (axial and radial directions).
- Neutron radiation from the active fuel region (axial and radial directions).
- Gamma radiation from activated hardware within the top fitting, plenum region and bottom fitting (axial and radial directions).

The sources in the active fuel region (gamma and neutron) are uniform radially but vary axially. The sources in the structural hardware regions (plenum, top fitting, and bottom fitting) are uniform both radially and axially. The results from the individual runs are summed to provide the total gamma, neutron and total dose for the cask.

Detector surfaces were placed in several radial and axial locations in order to evaluate the dose rate around the cask body. These surfaces provide an averaged surface dose rate based on the size of the detector (surface). The surfaces are subdivided into segments in order to determine the location and magnitude of maximum dose rates. Approximately 25 cm length "detector" segments were utilized both axially and radially.

For normal conditions, the contribution of each source to each dose point is summed to calculate the total gamma and/or neutron dose for each location. Table 5.1-2 presents the maximum calculated dose at contact, at the vehicle's outer edge (assumed 10 ft wide vehicle), and at 2 m from the vehicle's outer edge. The calculated neutron and gamma dose rates at the various dose points are illustrated in Figures 5.4-1 through 5.4-4.

For accident conditions, Table 5.1-2 also presents the maximum calculated doses at 1 m from the cask body.

The source term evaluation was performed using SCALE 4.4, "Modular Code System for Performing Standardized Computer Analyses for Licensing Evaluation for Workstations and Personal Computers" [1] by Oak Ridge National Laboratory. The dose rate analysis was performed using MCNP, "MCNP4B2 Monte Carlo N-Particle Transport Code System" [5] by Los Alamos National Laboratory. SCALE 4.4 and MCNP are implemented on Pentium based PCs using Windows NT. These program(s) have been verified in accordance with the Transnuclear quality assurance program.

Selected input for MCNP are included in Section 5.6.

5.5 REFERENCES

1. SCALE 4.4, "Modular Code System for Performing Standardized Computer Analyses for Licensing Evaluation for Workstations and Personal Computers," CCC-545, ORNL, NUREG/CR-0200, September 1998.
2. Croff, et al, "Revised Uranium-Plutonium Cycle PWR and BWR Models for the ORIGEN Computer Codes," ORNL/TM-6051, Oak Ridge National Laboratories, September 1978.
3. Moore and Notz, "Physical Characteristics of GE BWR Fuel Assemblies," ORNL-TM-10902, June 1989.
4. Luksic, 'Spent Fuel Assembly Hardware: Characterization and 10 CFR 61 Classification for Waste Disposal,' PNL-6906, UC-85, June 1989.
5. MCNP4B2, "Monte Carlo N-Particle Transport Code System." Los Alamos National Laboratory, CCC-660, RSIC.
6. "Data for Use in Protection Against External Radiation," Publication 51, International Commission on Radiological Protection, Annals of the ICRP, 17, No. 2/3, Pergamon Press, Oxford, 1987.
7. EPRI-NP-5128, "The TN-24P PWR Spent-Fuel Storage Cask: Testing and Analyses," prepared by Pacific Northwest Laboratory, Virginia Power Company and EG&G Idaho National Engineering Laboratory, April 1987.

5.6 APPENDIX

5.6.1 SAS2H/ORIGENS Input File

```

=sas2h      parm=(halt03,skipshipdata)
7x7-49.inp, 2.65 w/o U235, 35,000 MWD/MTU, 8-60 year cooling
27groupndf4 latticecell
uo2        1      0.95  840 92234 0.0294 92235 2.65 92236 0.0152
92238 97.3055 end
zircalloy  2      1.0      620  end
h2o        3  den=0.432  1.0  558  end
zircalloy  5      1.0      552  end
h2o        11  den=0.669  1.0  552  end
end comp
squarepitch 1.8745 1.23698 1 3 1.43002 2 1.26746 0 end
npin/assm=49 fuelength=365.76 ncycles=3 nlib/cyc=1 printlevel=10
lightel=10  inplevel=2 numzones=5 end
3 1.0E-10 500 7.4031 3 7.5091 5 7.7957 11 8.5982
power=5.00  burn=461.3  down=30  end
power=5.00  burn=461.3  down=30  end
power=5.00  burn=461.3  down=1461 end
n 0.0432  si 0.0106  ti 0.0106  cr 0.375  mn 0.0228  fe 0.854
co 0.00456  ni 0.422  sn 1.30  zr 84.9
end
=origens
0$$ a4 21 a8 26 a10 51 71 e
1$$ 1 1t
cooling to 18 years and fission product gamma reordering
3$$$ 21 0 1 a33 -86 e
54$$$ a8 1 e t
35$$$ 0 t
56$$$ 0 8 a13 -2 5 3 e
57** 4.0 e t
cooling to 18 years and fission product gamma re-ordering
single reactor assembly
60** 8.0 9.0 10.0 11.0 12.0 14.0 16.0 18.0
65$$$ a4 1 a7 1 a10 1 a25 1 a28 1 a31 1 a46 1 a49 1 a52 1 e
61** f.0000001
81$$$ 2 51 26 1 e
82$$$ f6 t
fission product gamma spectra in scale 18 groups
56$$$ f0 t
end
=origens
0$$ a4 21 a8 26 a10 51 71 e
1$$ 1 1t
cooling to 18 years and actinide gamma re-ordering
3$$$ 21 0 1 a33 -86 e
54$$$ a8 1 e t

```

```

35$$ 0 t
56$$ 0 8 a13 -2 5 3 e
57** 4.0 e t
cooling to 18 years and actinide gamma re-ordering
single reactor assembly
60** 8.0 9.0 10.0 11.0 12.0 14.0 16.0 18.0
65$$ e
61** f.0000001
81$$ 2 51 26 1 e
82$$ f5 t
actinide gamma spectra in scale 18 groups
56$$ f0 t
end
=origens
0$$ a4 21 a8 26 a10 51 71 e
1$$ 1 1t
cooling to 18 years and light element gamma re-ordering
3$$ 21 0 1 a33 -86 e
54$$ a8 1 e t
35$$ 0 t
56$$ 0 8 a13 -2 5 3 e
57** 4.0 e t
cooling to 18 years and light element gamma re-ordering
single reactor assembly
60** 8.0 9.0 10.0 11.0 12.0 14.0 16.0 18.0
65$$ e
61** f.0000001
81$$ 2 51 26 1 e
82$$ f4 t
light element scale group structure
56$$ f0 t
end

```

5.6.2 MCNP Neutron Model Input File

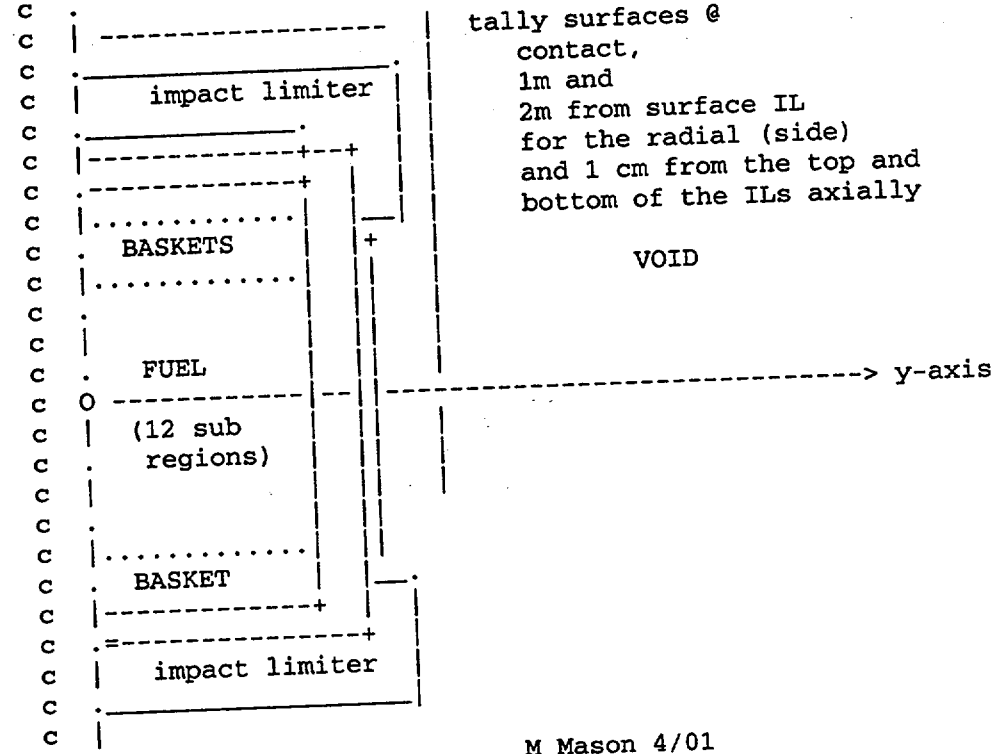
TransNuclear NU-61B cask: Near-Field model

c This model calculates doses for neutrons

c ***** BLOCK 1: CELL CARDS *****

c GEOMETRY (r-z)

c ^ z-axis



M Mason 4/01

c ***** Cask cells

1	8	-7.92	1	-2	-260	#35	imp:n,p=1	\$ Fe cask bottom			
2	8	-7.92	2	-12	25	-21	imp:n,p=1	\$ Inner shell			
3	7	-1.284	18	-5	-28		imp:n,p=1	\$ bottom basket			
4	6	-0.790	7	-8	-28		imp:n,p=1	\$ top plenum basket			
5	5	-0.836	8	-11	-28		imp:n,p=1	\$ top fitting			
8	1	-0.0013	11	-19	-28		imp:n,p=1	\$ Void between top and canister			
9	1	-0.0013	20	-12	-27		imp:n,p=1	\$ Void between canister and lid			
10	8	-7.92	2	-18	-27		imp:n,p=1	\$ bottom of canister			
11	8	-7.92	12	-14	-260		imp:n,p=1	\$ Fe cask lid - part1			
12	8	-7.92	19	-20	-27		imp:n,p=1	\$ top of canister			
25	8	-7.92	18	-19	28	-27	imp:n,p=1	\$ The canister			
26	1	-0.0013	2	-12	27	-25	imp:n,p=1	\$ Void between canister and inner shell			
27	16	-11.34	333	-12	21	-222	332	-17	2	imp:n,p=1	\$ Gamma shield
627	1	-0.0013	333	-12	-22	222	332	-17	2	imp:n,p=1	\$ gap at gamma shield
16	8	-7.92	21	2	-12	-22	#27	#627	imp:n,p=1	\$ Gamma shield CS	

```

28 8 -7.92 2 -12 22 -260 imp:n,p=1 $ Outer shell
c 29 12 -1.687 149 -166 260 -202 #37 #38 #39 #99 #240 #241 #242 #243
c #260 #261 #262 #263 imp:n,p=1 $ neutron shield
29 12 -1.687 198 -199 260 -202 #37 #38 #39 #99 #260 #261
#262 #263 #265 #266 #267 #268 #244 imp:n,p=1 $ neutron
shield
36 8 -7.92 149 -166 202 -201 #265 #266 #267 #268 imp:n,p=1 $ SS Skin
over NS
6 8 -7.92 (-166 199 260 -202)#37 #38 :
(149 -198 260 -202) #39 #99 imp:n,p=1 $ top & bot ss plate
on NS
30 0 150 -149 -201 260 imp:n,p=1 $ void space between BL & NS
31 0 161 -14 260 -251 imp:n,p=1 $ void btw side of TL and csk
32 0 155 -150 260 -251 imp:n,p=1 $ void btw side of BL and csk
33 0 155 -1 -260 imp:n,p=1 $ void btw csk bottom and BL
34 0 166 -161 260 -201 imp:n,p=1 $ void btw top of NS and TL
35 0 167 -2 -255 imp:n,p=1 $ canister plug
c ***** trunnion blocks with trunnion plugs *****
37 8 -7.92 (195 -344 345 -166 196 -341 260)#260 :
(195 -330 260 -341 -196) #260 imp:n,p=1 $ TR trun block
260 17 -0.90 195 -336 260 -341 imp:n,p=1 $ PP trunnion plug
265 8 -7.92 -334 -300 341 imp:n,p=1 $ Fe trunnion plug
38 8 -7.92 (-195 -344 345 -166 196 342 260)#261:
(-195 -330 260 342 -196) #261 imp:n,p=1 $ TL trun block
261 17 -0.90 -195 -336 260 342 imp:n,p=1 $ PP trunnion plug
266 8 -7.92 -334 301 -342 imp:n,p=1 $ Fe trunnion plug
39 8 -7.92 (195 -344 345 149 -197 -341 260)#262 :
(195 -331 260 -341 197) #262 imp:n,p=1 $ BR trun block
262 17 -0.90 195 -337 260 -341 imp:n,p=1 $ PP trunnion plug
267 8 -7.92 -335 -300 341 imp:n,p=1 $ Fe trunnion plug
99 8 -7.92 (-195 -344 345 149 -197 342 260)#263:
(-195 -331 260 342 197) #263 imp:n,p=1 $ BL trun block
263 17 -0.90 -195 -337 260 342 imp:n,p=1 $ PP trunnion plug
268 8 -7.92 -335 301 -342 imp:n,p=1 $ Fe trunnion plug
c ***** transport key/pad on cask under-side
244 8 -7.92 (-348 -349 351 -352 -202 256):(-353 -354 355 -356 260 -256)
imp:n,p=1 $ key plus pad on body
c **** impact limiters ****
c bottom limiter
80 8 -7.92 (156 -155 -254):(155 -151 -254 251) imp:n,p=1 $ inside skin
81 8 -7.92 (153 -152 -250):(152 -151 -250 253) imp:n,p=1 $ outside
skin
82 8 -7.92 151 -150 -250 251 imp:n,p=1 $ outside skin
83 15 -0.125 156 -151 -253 254 imp:n,p=1 $ balsa instead of
redwood
84 15 -0.125 154 -156 -253 252 imp:n,p=1 $ balsa instead of
redwood
85 15 -0.125 154 -156 -252 imp:n,p=1 $ balsa instead of
redwood
86 15 -0.125 152 -154 -253 252 imp:n,p=1 $ balsa instead of
redwood
87 15 -0.125 152 -154 -252 imp:n,p=1 $ balsa
c top limiter
90 8 -7.92 (14 -165 -254):(160 -14 -254 251) imp:n,p=1 $ inside steel
91 8 -7.92 (162 -163 -250):(160 -162 -250 253) imp:n,p=1 $ outside
steel
92 8 -7.92 -160 161 -250 251 imp:n,p=1 $ outside steel

```

```

93 15 -0.125      160 -165 -253 254      imp:n,p=1 $ balsa instead of
redwood
94 15 -0.125      165 -164 -253 252      imp:n,p=1 $ balsa instead of
redwood
95 15 -0.125      165 -164 -252          imp:n,p=1 $ balsa instead of
redwood
96 15 -0.125      164 -162 -253 252      imp:n,p=1 $ balsa instead of
redwood
97 15 -0.125      164 -162 -252          imp:n,p=1 $ balsa
c **** fuel regions
40 4  -2.511      5  -39 -28          imp:n,p=1 $ FUEL region 1 (bottom)
401 4 -2.511      39 -40 -28         imp:n,p=1 $ FUEL region 2
41 4  -2.511      40 -41 -28         imp:n,p=1 $ FUEL region 3
42 4  -2.511      41 -42 -28         imp:n,p=1 $ FUEL region 4
43 4  -2.511      42 -43 -28         imp:n,p=1 $ FUEL region 5
44 4  -2.511      43 -44 -28         imp:n,p=1 $ FUEL region 6
45 4  -2.511      44 -45 -28         imp:n,p=1 $ FUEL region 7
46 4  -2.511      45 -46 -28         imp:n,p=1 $ FUEL region 8
47 4  -2.511      46 -47 -28         imp:n,p=1 $ FUEL region 9
48 4  -2.511      47 -48 -28         imp:n,p=1 $ FUEL region 10
481 4 -2.511      48 -49 -28        imp:n,p=1 $ FUEL region 11
49 4  -2.511      49 -7  -28         imp:n,p=1 $ FUEL region 12 (top)
c ***** outside cells above/below cask
140 0          170 -60 -172      imp:n,p=0 $ air beneath cask-pt2
142 0          -153 60 -250      imp:n,p=1 $ air beneath cask-pt1
145 0          163 -61 -250      imp:n,p=1 $ air above cask-pt1
146 0          61 -171 -172      imp:n,p=0 $ air above cask-pt2
c ***** Cells outside radial cask surface
601 0      #265 #266 #267 #268 150 -161 201 -62  imp:n,p=1 $ inner air
(void)
602 0          150 -161 62 -63      imp:n,p=1 $ inner air (void)
603 0      (60 -61 250 -65):(150 -161 63 -250) imp:n,p=1 $ inner air (void)
606 0          60 -61 65 -64          imp:n,p=1 $ inner air (void)
605 0          60 -61 -172 64          imp:n,p=0 $ outer air (void)
190 0          -170:171:172          imp:n,p=0 $ problem boundary

c ***** BLOCK 2: SURFACE CARDS *****
c **** Horizontal cask planes
1 pz -237.26      $ cask bottom - ground surface
2 pz -220.75      $ top of csk bottom, canister bottom
5 pz -182.88      $ top bottom basket/bottom of fuel
7 pz 182.88       $ bottom of plenum basket/top of fuel
8 pz 224.72       $ top of plenum basket
11 pz 245.90      $ top of top fitting
12 pz 279.65      $ cask top - bot of lid
14 pz 291.08      $ cask top - top of Fe
c 17 pz 268.89    $ top of GS, slice cone
17 pz 270.74      $ top of GS, slice cone
18 pz -201.65     $ top of canister bottom
19 pz 253.77      $ bottom of canister top
20 pz 276.43      $ top of canister
31 pz 244.00      $ top of alum, bot of void
148 pz -178.155   $ Al/Void Bndry btw BL and NS
149 pz -176.30    $ bottom of neutron shield
150 pz -177.58    $ top of bottom limiter
151 pz -178.22    $ inside skin bottom limiter
152 pz -331.24    $ inside skin bottom limiter

```

153	pz	-331.88		\$ bottom of bottom limiter
154	pz	-275.94		\$ top of balsa disk bottom limiter
155	pz	-241.71		\$ top of inside skin bottom limiter
156	pz	-242.34		\$ Inside skin BL
160	pz	227.64		\$ inside skin top limiter
161	pz	227.01		\$ bottom of top limiter
162	pz	380.68		\$ inside skin top limiter
163	pz	381.25		\$ top of top limiter
164	pz	327.98		\$ bottom of balsa disc top limiter
165	pz	291.72		\$ top of inside skin top limiter
166	pz	226.30		\$ top of neutron shield
167	pz	-229.64		\$ bottom of canidter plug
300	px	118.12		\$ outside of trunion plug
301	px	-118.12		\$ outside of trunion plug
340	pz	166.823		\$ flat trun cutout
341	px	109.86		\$ trunnion block
342	px	-109.86		\$ trunnion block
343	pz	-120.573		\$ flat trun cutout
344	py	34.29		\$ Trunion block
345	py	-34.29		\$ Trunion block
348	p	-3.014893	1.0 0. 0.	\$ keyway surface
349	p	3.014893	1.0 0. 0.	\$ keyway syrface
351	pz	9.80		\$ bottom of key
352	pz	40.44		\$ top of key
353	p	-2.050304	1.0 0. 0.	\$ key pad surface
354	p	2.050304	1.0 0. 0.	\$ key pad surface
355	pz	-20.52		\$ bottom of key pad
356	pz	70.92		\$ top of key pad
195	px	0.0		\$ ambiguity surface
196	pz	183.08		\$ centerline of top trunnions
197	pz	-133.12		\$ centerline of bottom trunnions
198	pz	-172.49		\$ Inside steel plate on NS
199	pz	222.49		\$ Inside steel plate on NS
c	*****	cylindrical	cask	surfaces
25	cz	86.36		\$ cask inner surface outside of void (see 27)
21	cz	89.535		\$ outside inner shell inside gamma sheild
22	cz	97.79		\$ outside gamma sheild inside outer shell
222	cz	97.64		\$ lead gap at outer shell interface
251	cz	105.41		\$ Inside radius IL
260	cz	104.15		\$ inside NS
202	cz	115.72		\$ outside of neutron sheild
201	cz	116.20		\$ outside of SS Skin
27	cz	85.41		\$ outside radius of canister
28	cz	83.02		\$ inside radius of canister outside fuel rad
250	cz	155.00		\$ outside radius of impact limiter
252	cz	96.50		\$ radius of balsa disk
253	cz	154.4		\$ outside radius inside skin
254	cz	106.04		\$ inside skin
256	cz	107.96		\$ outside of key pad (1.5" thk)
255	cz	12.7		\$ canister plug
330	c/x	0 183.08	34.29	\$ trunnion block
331	c/x	0 -133.12	34.29	\$ trunnion block
334	c/x	0 183.08	31.75	\$ trunnion plug Fe
335	c/x	0 -133.12	31.75	\$ trunnion plug Fe
336	c/x	0 183.08	21.59	\$ trunnion plug PP
337	c/x	0 -133.12	21.59	\$ trunnion plug PP
c	*****	cone	surfaces	*****

```

c 332 kz -127.39 0.0566 $ tapering of STS
c 333 kz 173.68 0.0566 $ tapering of STS
332 kz -118.64 0.0566 $ tapering of STS
333 kz 168.63 0.0566 $ tapering of STS

```

```

c ***** surfaces for fuel regions
39 pz -164.59 $ top of fuel region 39
40 pz -146.30 $ top of fuel region 40
41 pz -109.73 $ top of fuel region 41
42 pz -73.15 $ top of fuel region 42
43 pz -36.53 $ top of fuel region 43
44 pz -0.0 $ top of fuel region 44
45 pz 36.53 $ top of fuel region 45
46 pz 73.15 $ top of fuel region 46
47 pz 109.73 $ top of fuel region 47
48 pz 146.30 $ top of fuel region 48
49 pz 164.59 $ top of fuel region 49

```

```

c ***** problem boundaries
170 pz -500.E2 $ bottom of air (problem boundary)
171 pz 500.E2 $ top of air (problem boundary)
172 cz 500.E2 $ radial air limit (problem boundary)

```

```

c ***** surfaces for detector segmentation
60 pz -334.095 $ bottom tally surface
61 pz 382.31 $ top tally surface
62 cz 125.0 $ radial tally surface (outer shell)
63 cz 152.0 $ radial tally surface (rail car edge)
64 cz 355.00 $ radial tally surface (2 m from IL)
65 cz 215.72 $ radial tally surface (1m from cask)
71 pz -190.0 $ segmentation plane
72 pz 200.0 $ segmentation plane
81 cz 25.00 $ segmentation cylinder
82 cz 50.00 $ segmentation cylinder
83 cz 75.00 $ segmentation cylinder
29 cz 101.45 $ segmentation cylinder
23 cz 124.47 $ segmentation cylinder
350 cz 182.88 $ segmentation cylinder

```

```

c ***** BLOCK 3: DATA CARDS *****

```

```

c
c

```

```

c --- volumetric neutron source in 12 axial zones for TN-61 cask
c 7x7 fuel assemblies; 35,000 MWd/Mt design basis; 12y cooling time

```

```

SDEF par=1 pos 0 0 0 axs=0 0 1 rad=d1 ext=d2 erg=d3 cel=d4
SI1 0 83.92 $ range of radius sampling: 0 to Rmax
SP1 -21 1 $ radial distribution: here r^1
SI2 -182.88 182.88 $ range of axial sampling
SP2 -21 0 $ axial distribution: here z^0
SI3 H 0.1 0.4 0.9 1.4 1.85 3.0 6.434 20 $ energy bins
SP3 0.0 .03776 .1929 .1769 .1310 .2331 .2098 .01842 $ bin prob.
SI4 L 40 401 41 42 43 44 45 46 47 48 481 49
SP4 0.0000924 0.008421 0.08446 0.1386 0.1529 0.1578
0.1562 0.1384 0.1071 0.05047 0.005463 0.0001396
SB4 0.05 0.05 0.1 0.1 0.1 0.1
0.1 0.1 0.1 0.1 0.05 0.05

```

```

c

```

```

c

```

```

c ---- Detector types and locations -- neutrons and NO secondary gammas
c -- doses on cask's radial surface (F2 segmented surface detectors)

```

```

c FM2      2.043E18      $ convert Sv/neutron to mrem/h for fuel zones
c          7.016E7 x 61 X 1.326 (NF) X 3600 X 1E5 = 2.043E18
c TF2 3j 6
FC2 Doses at contact averaged over subsurfaces
F2:n 201
FS2  -71 -39 -40 -41 -42 -43 -44 -45 -46 -47 -48 -49 -72 -8 -11
SD2  3.0E7 18552.00 13353.64 26699.98 26707.28 26736.49
      26670.78 26670.78 26736.49 26707.28 26699.98
      13353.64 25853.06 18048.22 15463.65 3.0E7
c FC12 Doses at the rail car edge averaged over subsurfaces
c F12:n 63
c FS12  -71 -39 -40 -41 -42 -43 -44 -45 -46 -47 -48 -49 -72 -8 -11
c SD12  3.0E7 24267.67 17467.76 34925.96 34935.52 34973.72
c          34887.76 34887.76 34973.72 34935.72 34925.96
c          17467.76 33818.11 23608.69 20227.84 3.0E7
FC12 Doses at 1 meters from cask averaged over subsurfaces
F12:n 65
FS12  -152 -154 -155 -71 -39 -40 -41 -42 -43 -44 -45 -46 -47
      -48 -49 -72 -8 -11 -165 -164 -162
SD12  1.0E8 76825.71 43985.79 72757.22 34517.57 24845.59 49677.59
      49691.17 49745.51 49623.25 49623.25 49745.51 49691.17
      49677.59 24845.59 48101.82 33580.26 28771.43
      59648.43 51783.15 71697.65 8.0E7
FC22 Doses at 2 meters from rail car averaged over subsurfaces
F22:n 64
FS22  -152 -154 -155 -71 -39 -40 -41 -42 -43 -44 -45 -46 -47
      -48 -49 -72 -8 -11 -165 -164 -162
SD22  1.0E8 126147.67 72224.59 119467.23 56677.79 40796.41 81570.51
      81592.81 81682.04 81481.29 81481.29 81682.04 81592.81
      81570.51 40796.41 78983.09 55138.72 47242.64
      97942.61 85027.83 117727.41 8.0E7
c
c -- doses along cask's top
FC32 Doses at top limiter surface averaged over subsurfaces
f32:n 61          $ surface tally
fs32  -81 -82 -83 -29 -23 -63 -350 -64
sd32  1963.50 5890.49 9817.48 14662.13 16338.41 23911.35
      32487.51 290848.35 7.8E7
c
c -- doses along cask's bottom
FC42 Doses at bottom limiter surface averaged over subsurfaces
f42:n 60          $ surface tally
fs42  -81 -82 -83 -29 -23 -63 -350 -64
sd42  1963.50 5890.49 9817.48 14662.13 16338.41 23911.35
      32487.51 290848.35 7.8E7
c
c mode n p
phys:n 20.0 0.0
cut:n j 0.0
c phys:p 0 1 1
esplt:n 0.5 0.1 0.5 0.01 0.25 0.001
wwp:n 5 3 5 0 0.5
nps 20000000
c void
c
c -----
c ambient neutron dose equiv. H*(10mm) Sv (from T-D3 of S&F)

```

```

c -----
de0  2.500E-08 1.000E-07 1.000E-06 1.000E-05 1.000E-04 1.000E-03
      1.000E-02 2.000E-02 5.000E-02 1.000E-01 2.000E-01 5.000E-01
      1.000E+00 1.500E+00 2.000E+00 3.000E+00 4.000E+00 5.000E+00
      6.000E+00 7.000E+00 8.000E+00 1.000E+01 1.400E+01 1.700E+01
      2.000E+01
df0  8.000E-12 1.040E-11 1.120E-11 9.200E-12 7.100E-12 6.200E-12
      8.600E-12 1.460E-11 3.500E-11 6.900E-11 1.260E-10 2.580E-10
      3.400E-10 3.620E-10 3.520E-10 3.800E-10 4.090E-10 3.780E-10
      3.830E-10 4.030E-10 4.170E-10 4.460E-10 5.200E-10 6.100E-10
      6.500E-10

```

```

c -----
c ambient photon dose equiv. H*(10mm) Sv (from T-D1 of S&F)
c -----
c de24  1.000E-02 1.500E-02 2.000E-02 3.000E-02 4.000E-02 5.000E-02
c      6.000E-02 8.000E-02 1.000E-01 1.500E-01 2.000E-01 3.000E-01
c      4.000E-01 5.000E-01 6.000E-01 8.000E-01 1.000E+00 1.500E+00
c      2.000E+00 3.000E+00 4.000E+00 5.000E+00 6.000E+00 8.000E+00
c      1.000E+01
c df24  7.690E-14 8.460E-13 1.010E-12 7.850E-13 6.140E-13 5.260E-13
c      5.040E-13 5.320E-13 6.110E-13 8.900E-13 1.180E-12 1.810E-12
c      2.380E-12 2.890E-12 3.380E-12 4.290E-12 5.110E-12 6.920E-12
c      8.480E-12 1.110E-11 1.330E-11 1.540E-11 1.740E-11 2.120E-11
c      2.520E-11

```

```

c ***** MATERIAL CARDS
c *****
c AIR: ANSI/ANS-6.4.3, Dry air; density = 0.0012 g/cm^3
c      Composition by mass fraction
c *****
m1  7014.50c -.75519
      8016.60c -.23179
      6000.60c -.00014
      18000.35c -.01288

```

```

c *****
c Fuel-Basket Nu-61b Cask
c      Density = 2.511 g/cm^3; Composition by atom fraction
c *****
m4  92238.50c 0.19053
      92235.50c 0.00773
      40000.60c 0.13149
      28000.50c 0.01470
      26000.50c 0.11116
      25055.50c 0.00331
      24000.50c 0.03318
      13027.50c 0.11140
      8016.60c 0.39652

```

```

c *****
c Top Fitting NU-61b Cask
c      Density = 0.836 g/cm^3; Composition by atom fraction
c *****
m5  26000.50c 0.45090
      28000.50c 0.05961
      25055.50c 0.01341

```

24000.50c 0.13457
40000.60c 0.11205
13027.50c 0.22945

C
C
C
C
C
m6

Plenum/Basket Nu-61b Cask
Density = 0.790 g/cm³; Composition by atom fraction

26000.50c 0.32657
28000.50c 0.04318
40000.60c 0.25966
25055.50c 0.00971
24000.50c 0.09746
13027.50c 0.26343

C
C
C
C
C
m7

Bottom/Basket Nu-61b
Density = 1.284 g/cm³; Composition by atom fraction

26000.50c 0.51974
28000.50c 0.06872
25055.50c 0.01545
24000.50c 0.15512
13027.50c 0.15415
40000.60c 0.08682

C
C
C
C
C
m8

Basket Periphery (SS304) TN-68 (Table 5.3-1)
Density = 7.92 g/cm³; Composition by atom fraction

26000.50c 0.68826
25055.50c 0.02013
24000.50c 0.20209
28000.50c 0.08952

C
C
C
C
C
m9

Carbon Steel TN-68 (Table 5.3-1)
Density = 7.8212 g/cm³; Composition by atom fraction

26000.50c 0.95510
6000.60c 0.04490

C
C
C
C
C
m10

Outer Basket/Rails TN-68 (Table 5.3-1)
Density = 2.702 g/cm³; Composition by atom fraction

13027.50c 1.00000

C
C
C
C
C
m12

Resin/Aluminum Composite for TN-68 (Table 5.3-1)
Density = 1.687 g/cm³; Composition by atom fraction

13027.50c 0.10331
6012.50c 0.24658
8016.60c 0.21985
1001.50c 0.42207
5010.60c 0.00164

```

5011.60c 0.00655
c
c
c *****
c Balsa for Impact Limiter (Standard Composition SCALE4.4)
c density = 0.125 g/cm^3; Composition by atom fraction
c *****
m15 6012.50c 0.2857
      8016.60c 0.2381
      1001.50c 0.4762
c
c *****
c Lead for Gamma Shield (Standard Composition SCALE4.4)
c density = 11.34 g/cm^3; Composition by atom fraction
c *****
m16 82000.50c 1.0
c
c
c *****
c Polypropylene Disk TN-68 (Table 5.3-1)
c Density = 0.90 g/cm^3; Composition by atom fraction
c *****
m17 6012 .33480
      1001 .66520
c
c prdmp 2j 1
c print

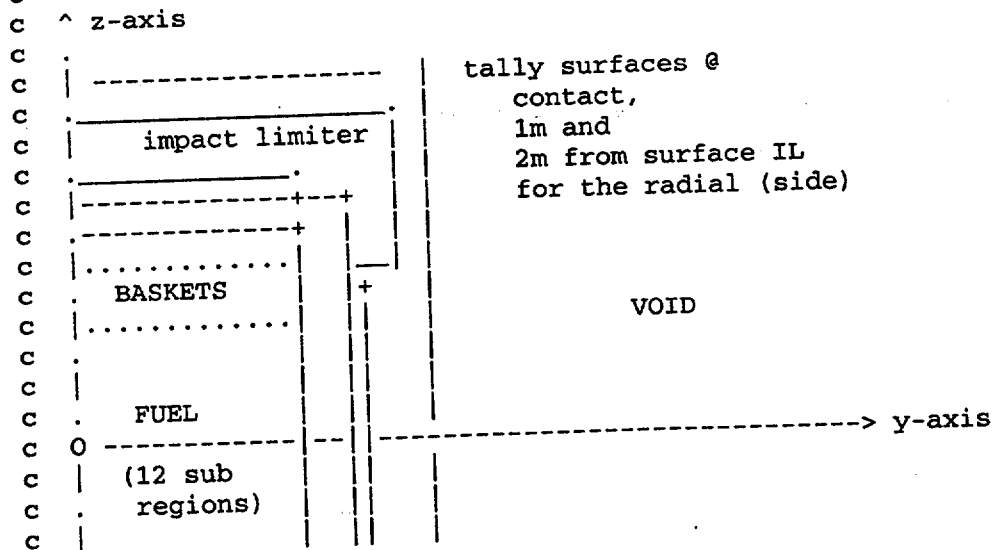
```

5.6.3 MCNP Primary Gamma Input File

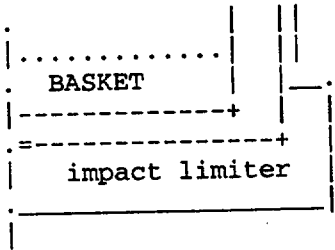
```

TransNuclear NU-61B cask: Near-Field model
c
c This model calculates doses for fuel gammas
c at the side of the cask
c *****
c BLOCK 1: CELL CARDS *****
c GEOMETRY (r-z)
c

```



C
C
C
C
C
C
C
C
C
C
C
C



M Mason 4/01

***** Cask cells

1	8	-7.92	1	-2	-260	#35	imp:n,p=1	\$ Fe cask bottom							
2	8	-7.92	2	-12	25	-371	imp:n,p=20	\$ Inner shell							
65	8	-7.92	2	-12	371	-21	imp:n,p=45	\$ Inner shell							
3	7	-1.284	18	-5	-28		imp:n,p=1	\$ bottom basket							
4	6	-0.790	7	-8	-28		imp:n,p=1	\$ top plenum basket							
5	5	-0.836	8	-11	-28		imp:n,p=1	\$ top fitting							
8	1	-0.0013	11	-19	-28		imp:n,p=1	\$ Void between top and canister							
9	1	-0.0013	20	-12	-27		imp:n,p=2	\$ Void between canister and lid							
10	8	-7.92	2	-18	-27		imp:n,p=2	\$ bottom of canister							
11	8	-7.92	12	-14	-260		imp:n,p=2	\$ Fe cask lid - part1							
12	8	-7.92	19	-20	-27		imp:n,p=2	\$ top of canister							
25	8	-7.92	18	-19	28	-370	imp:n,p=2	\$ The canister							
66	8	-7.92	18	-19	370	-27	imp:n,p=4	\$ The canister							
26	1	-0.0013	2	-12	27	-25	imp:n,p=8	\$ Void between canister and inner shell							
shell															
27	16	-11.34	333	-12	21	-372	332	-17	2	imp:n,p=100	\$ Gamma shield				
64	16	-11.34	333	-12	372	-373	332	-17	2	imp:n,p=250	\$ Gamma shield				
63	16	-11.34	333	-12	373	-374	332	-17	2	imp:n,p=600	\$ Gamma shield				
62	16	-11.34	2	-17	374	-222				imp:n,p=1500	\$ Gamma shield				
662	1	-0.0013	2	-17	222	-22				imp:n,p=1500	\$ Gamma Shield gap (.06")				
16	8	-7.92	21	2	-12	-22	#27	#64	#63	#62	#662	imp:n,p=250	\$ Gamma		
shield CS															
28	8	-7.92	2	-12	22	-375				imp:n,p=4000	\$ Outer shell				
67	8	-7.92	2	-12	375	-376				imp:n,p=10000	\$ Outer shell				
68	8	-7.92	2	-12	376	-260				imp:n,p=25000	\$ Outer shell				
c	29	12	-1.687	149	-166	260	-202	#37	#38	#39	#99	#240	#241	#242	#243
c				#260	#261	#262	#263			imp:n,p=60000	\$ neutron shield				
	29	12	-1.687	198	-199	260	-202	#37	#38	#39	#99	#260	#261		
				#262	#263	#265	#266	#267	#268	#244	imp:n,p=6E4	\$ neutron			
shield															
36	8	-7.92	149	-166	202	-201	#265	#266	#267	#268	imp:n,p=150000	\$ SS Skin			
over NS															
6	8	-7.92		(-166	199	260	-202)	#37	#38	:					
				(149	-198	260	-202)	#39	#99	imp:n,p=1.5E5	\$ top & bot ss				
plate on NS															
30	0	150	-149	-201	260					imp:n,p=25000	\$ void space between BL &				
NS															
31	0	161	-14	260	-251					imp:n,p=25000	\$ void btw side of TL and				
csk															
32	0	155	-150	260	-251					imp:n,p=25000	\$ void btw side of BL and				
csk															
33	0	155	-1	-260						imp:n,p=25000	\$ void btw csk bottom and				
BL															
34	0	166	-161	260	-201					imp:n,p=25000	\$ void btw top of NS' and				
TL															
35	0	167	-2	-255						imp:n,p=2	\$ canister plug				

```

c ***** trunnion blocks with trunnion plugs *****
37 8 -7.92 (195 -344 345 -166 196 -341 260)#260 :
      (195 -330 260 -341 -196) #260 imp:n,p=1.5E5 $ TR trun block
260 17 -0.90 195 -336 260 -341 imp:n,p=1.5E5 $ PP trunnion plug
265 8 -7.92 -334 -300 341 imp:n,p=1.5E5 $ Fe trunnion plug
38 8 -7.92 (-195 -344 345 -166 196 342 260)#261:
      (-195 -330 260 342 -196) #261 imp:n,p=1.5E5 $ TL trun block
261 17 -0.90 -195 -336 260 342 imp:n,p=1.5E5 $ PP trunnion plug
266 8 -7.92 -334 301 -342 imp:n,p=1.5E5 $ Fe trunnion plug
39 8 -7.92 (195 -344 345 149 -197 -341 260)#262 :
      (195 -331 260 -341 197) #262 imp:n,p=1.5E5 $ BR trun block
262 17 -0.90 195 -337 260 -341 imp:n,p=1.5E5 $ PP trunnion plug
267 8 -7.92 -335 -300 341 imp:n,p=1.5E5 $ Fe trunnion plug
99 8 -7.92 (-195 -344 345 149 -197 342 260)#263:
      (-195 -331 260 342 197) #263 imp:n,p=1.5E5 $ BL trun block
263 17 -0.90 -195 -337 260 342 imp:n,p=1.5E5 $ PP trunnion plug
268 8 -7.92 -335 301 -342 imp:n,p=1.5E5 $ Fe trunnion plug
c ***** transport key/pad on cask under-side
244 8 -7.92 (-348 -349 351 -352 -202 256):(-353 -354 355 -356 260 -256)
      imp:n,p=6E4 $ key plus pad on body
c **** impact limiters ****
c bottom limiter
80 8 -7.92 (156 -155 -254):(155 -151 -254 251) imp:n,p=25000 $ inside
skn
81 8 -7.92 (153 -152 -250):(152 -151 -250 253) imp:n,p=25000 $ outside
skn
82 8 -7.92 151 -150 -250 251 imp:n,p=25000 $ outside skin
83 15 -0.125 156 -151 -253 254 imp:n,p=25000 $ balsa instead of
redwood
84 15 -0.125 154 -156 -253 252 imp:n,p=10000 $ balsa instead of
redwood
85 15 -0.125 154 -156 -252 imp:n,p=500 $ balsa instead of
redwood
86 15 -0.125 152 -154 -253 252 imp:n,p=1000 $ balsa instead of
redwood
87 15 -0.125 152 -154 -252 imp:n,p=1 $ balsa
c top limiter
90 8 -7.92 (14 -165 -254):(161 -14 -254 251) imp:n,p=25000 $ inside skn
91 8 -7.92 (162 -163 -250):(161 -162 -250 253) imp:n,p=25000 $ outside
skn
92 8 -7.92 160 -161 -250 251 imp:n,p=1 $ outside skin
93 15 -0.125 161 -165 -253 254 imp:n,p=25000 $ balsa instead of
redwood
94 15 -0.125 165 -164 -253 252 imp:n,p=10000 $ balsa instead of
redwood
95 15 -0.125 165 -164 -252 imp:n,p=20 $ balsa instead of
redwood
96 15 -0.125 164 -162 -253 252 imp:n,p=5000 $ balsa instead of
redwood
97 15 -0.125 164 -162 -252 imp:n,p=1 $ balsa
c 98 0 161 -14 260 -251 imp:n,p=25000 $ space btw lid and
TL
c 98 10 -2.702 (14 -166 -21):(-14 13 29 -21) imp:n,p=1 $ al spacer
c **** fuel regions
40 4 -2.511 5 -39 -28 imp:n,p=1 $ FUEL region 1 (bottom)
401 4 -2.511 39 -40 -28 imp:n,p=1 $ FUEL region 2
41 4 -2.511 40 -41 -28 imp:n,p=1 $ FUEL region 3

```

```

42 4 -2.511 41 -42 -28 imp:n,p=1 $ FUEL region 4
43 4 -2.511 42 -43 -28 imp:n,p=1 $ FUEL region 5
44 4 -2.511 43 -44 -28 imp:n,p=1 $ FUEL region 6
45 4 -2.511 44 -45 -28 imp:n,p=1 $ FUEL region 7
46 4 -2.511 45 -46 -28 imp:n,p=1 $ FUEL region 8
47 4 -2.511 46 -47 -28 imp:n,p=1 $ FUEL region 9
48 4 -2.511 47 -48 -28 imp:n,p=1 $ FUEL region 10
481 4 -2.511 48 -49 -28 imp:n,p=1 $ FUEL region 11
49 4 -2.511 49 -7 -28 imp:n,p=1 $ FUEL region 12 (top)
c ***** outside cells above/below cask
140 0 170 -60 -172 imp:n,p=0 $ air beneath cask-pt2
142 0 -153 60 -250 imp:n,p=1 $ air beneath cask-pt1
145 0 163 -61 -250 imp:n,p=1 $ air above cask-pt1
146 0 61 -171 -172 imp:n,p=0 $ air above cask-pt2
c ***** Cells outside radial cask surface
601 0 #265 #266 #267 #268 150 -161 201 -62 imp:n,p=150000 $ inner air
(void)
602 0 150 -161 62 -63 imp:n,p=150000 $ inner air (void)
603 0 (60 -61 250 -65):(150 -161 63 -250) imp:n,p=150000 $ inner air (void)
606 0 60 -61 65 -64 imp:n,p=150000 $ inner air (void)
605 0 60 -61 -172 64 imp:n,p=0 $ outer air (void)
190 0 -170:171:172 imp:n,p=0 $ problem boundary

c ***** BLOCK 2: SURFACE CARDS *****
c ***** Horizontal cask planes
1 pz -237.26 $ cask bottom - ground surface
2 pz -220.75 $ top of csk bottom, canister bottom
5 pz -182.88 $ top bottom basket/bottom of fuel
7 pz 182.88 $ bottom of plenum basket/top of fuel
8 pz 224.72 $ top of plenum basket
11 pz 245.90 $ top of top fitting
12 pz 279.65 $ cask top - bot of lid
14 pz 291.08 $ cask top - top of Fe
c 17 pz 268.89 $ top of GS, slice cone
17 pz 270.74 $ top of GS, slice cone
18 pz -201.65 $ top of canister bottom
19 pz 253.77 $ bottom of canister top
20 pz 276.43 $ top of canister
31 pz 244.00 $ top of alum, bot of void
148 pz -178.155 $ Al/Void Bndry btw BL and NS
149 pz -176.30 $ bottom of neutron shield
150 pz -177.58 $ top of bottom limiter
151 pz -178.22 $ inside skin bottom limiter
152 pz -331.24 $ inside skin bottom limiter
153 pz -331.88 $ bottom of bottom limiter
154 pz -275.94 $ top of balsa disk bottom limiter
155 pz -241.71 $ top of inside skin bottom limiter
156 pz -242.34 $ Inside skin BL
160 pz 227.64 $ inside skin top limiter
161 pz 227.01 $ bottom of top limiter
162 pz 380.68 $ inside skin top limiter
163 pz 381.25 $ top of top limiter
164 pz 327.98 $ bottom of balsa disc top limiter
165 pz 291.72 $ top of inside skin top limiter
166 pz 226.30 $ top of neutron shield
167 pz -229.64 $ bottom of canidter plug
300 px 118.12 $ outside of trunion plug

```

301	px	-118.12		\$ outside of trunion plug
340	pz	166.823		\$ flat trun cutout
341	px	109.86		\$ trunion block
342	px	-109.86		\$ trunion block
343	pz	-120.573		\$ flat trun cutout
344	py	34.29		\$ Trunion block
345	py	-34.29		\$ Trunion block
348	p	-3.014893	1.0 0. 0.	\$ keyway surface
349	p	3.014893	1.0 0. 0.	\$ keyway surface
351	pz	9.80		\$ bottom of key
352	pz	40.44		\$ top of key
353	p	-2.050304	1.0 0. 0.	\$ key pad surface
354	p	2.050304	1.0 0. 0.	\$ key pad surface
355	pz	-20.52		\$ bottom of key pad
356	pz	70.92		\$ top of key pad
195	px	0.0		\$ ambiguity surface
196	pz	183.08		\$ centerline of top trunnions
197	pz	-133.12		\$ centerline of bottom trunnions
198	pz	-172.49		\$ Inside steel plate on NS
199	pz	222.49		\$ Inside steel plate on NS
c ***** cylindrical cask surfaces				
25	cz	86.36		\$ cask inner surface outside of void (see 27)
371	cz	88.0		\$ split of inner surface
21	cz	89.535		\$ outside inner shell inside gamma shield
372	cz	92.1		\$ gamma shield split
373	cz	94.2		\$ gamma shield split
374	cz	96.0		\$ gamma shield split
22	cz	97.79		\$ outside gamma shield inside outer shell
222	cz	97.64		\$ lead gap at outer shell interface
375	cz	100.5		\$ split of outer shell
376	cz	103.0		\$ split of outer shell
251	cz	105.41		\$ Inside radius BL
260	cz	104.15		\$ inside NS
202	cz	115.72		\$ outside of neutron shield
201	cz	116.20		\$ outside of SS Skin
27	cz	85.41		\$ outside radius of canister
28	cz	83.02		\$ inside radius of canister outside fuel rad
370	cz	83.75		\$ Split canister
250	cz	155.00		\$ outside radius of impact limiter
252	cz	96.5		\$ radius of balsa disk
253	cz	154.4		\$ outside radius inside skin
254	cz	106.04		\$ inside skin
255	cz	12.7		\$ canister plug
256	cz	107.96		\$ outside of key pad (1.5" thk)
330	c/x	0 183.08 34.29		\$ trunion block
331	c/x	0 -133.12 34.29		\$ trunion block
334	c/x	0 183.08 31.75		\$ trunion plug Fe
335	c/x	0 -133.12 31.75		\$ trunion plug Fe
336	c/x	0 183.08 21.59		\$ trunion plug PP
337	c/x	0 -133.12 21.59		\$ trunion plug PP
c ***** cone surfaces *****				
332	kz	-118.64	0.0566	\$ tapering of STS
333	kz	168.63	0.0566	\$ tapering of STS
c ***** surfaces for fuel regions				
39	pz	-164.59		\$ top of fuel region 39
40	pz	-146.30		\$ top of fuel region 40
41	pz	-109.73		\$ top of fuel region 41

```

42 pz -73.15      $ top of fuel region 42
43 pz -36.53      $ top of fuel region 43
44 pz -0.0        $ top of fuel region 44
45 pz 36.53       $ top of fuel region 45
46 pz 73.15       $ top of fuel region 46
47 pz 109.73      $ top of fuel region 47
48 pz 146.30      $ top of fuel region 48
49 pz 164.59      $ top of fuel region 49

```

```

c ***** problem boundaries
170 pz -500.E2    $ bottom of air (problem boundary)
171 pz 500.E2     $ top of air (problem boundary)
172 cz 500.E2     $ radial air limit (problem boundary)

```

```

c ***** surfaces for detector segmentation
60 pz -334.095   $ bottom tally surface
61 pz 382.31     $ top tally surface
62 cz 125.0      $ radial tally surface (outer shell)
63 cz 152.0      $ radial tally surface (rail car edge)
64 cz 355.00     $ radial tally surface (2 m from IL)
65 cz 215.72     $ radial tally surface (1m from cask)
71 pz -190.0     $ segmentation plane
72 pz 200.0      $ segmentation plane
81 cz 25.00      $ segmentation cylinder
82 cz 50.00      $ segmentation cylinder
83 cz 75.00      $ segmentation cylinder
29 cz 101.45     $ segmentation cylinder
23 cz 124.47     $ segmentation cylinder
350 cz 182.88    $ segmentation cylinder

```

c ***** BLOCK 3: DATA CARDS *****

```

c
c
c --- gamma-ray source for fuel in TN61 12 yr cooled-- 12 axial cylindrical
zones (inner)
c 7x7 fuel assemblies; 35,000 MWD/Mt design basis; 12y cooling time
SDEF par=2 pos= 0 0 0 axs=0 0 1 rad=d1 ext=d2 erg d6 cel=d7
SI1 0 83.92      $ range of radius sampling: 0 to Rmax
SP1 -21 1        $ radial distribution: here r^1
SI2 -182.88 182.88 $ range of axial sampling
SP2 -21 0        $ axial distribution: here z^0
SI6 H 0.01 0.05 0.1 0.2 0.3 0.4 0.6 0.8 1.0 1.33 1.66 $ energy bins
- fuel
SP6 0.0 .2709 .0759 .0534 .0159 .0104 .0280 $ bin probs.
- fuel
.5111 .0151 .0165 .0028
SI7 L 40 401 41 42 43 44 45 46 47 48 481 49 $ fuel zones
SP7 0.01178 0.03873 0.10750 0.11836 0.12 0.12 $ prob. emission per fuel
zone
0.11912 0.11515 0.10766 0.08973 0.03165 0.01205

```

```

c SB4 0.05 0.05 0.1 0.1 0.1 0.1
c 0.1 0.1 0.1 0.1 0.05 0.05

```

```

c
c
c ---- Detector types and locations -- neutrons and NO secondary gammas
c -- doses on cask's radial surface (F2 segmented surface detectors)
c FM2 2.332E25 $ convert Sv/neutron to mrem/h for fuel zones
c 1.071E15 x 61 X 0.9917 (NF) X 3600 X 1E5 = 2.332E25
c TF2 3j 6

```

FC2 Doses at contact averaged over subsurfaces

F2:p 201
FS2 -71 -39 -40 -41 -42 -43 -44 -45 -46 -47 -48 -49 -72 -8 -11
SD2 3.0E7 18552.00 13353.64 26699.98 26707.28 26736.49
26670.78 26670.78 26736.49 26707.28 26699.98
13353.64 25853.06 18048.22 15463.65 3.0E7

FC12 Doses at 1 meters from cask averaged over subsurfaces

F12:p 65
FS12 -152 -154 -155 -71 -39 -40 -41 -42 -43 -44 -45 -46 -47
-48 -49 -72 -8 -11 -165 -164 -162
SD12 1.0E8 76825.71 43985.79 72757.22 34517.57 24845.59 49677.59
49691.17 49745.51 49623.25 49623.25 49745.51 49691.17
49677.59 24845.59 48101.82 33580.26 28771.43
59648.43 51783.15 71697.65 8.0E7

FC22 Doses at 2 meters from rail car averaged over subsurfaces

F22:p 64
FS22 -152 -154 -155 -71 -39 -40 -41 -42 -43 -44 -45 -46 -47
-48 -49 -72 -8 -11 -165 -164 -162
SD22 1.0E8 126147.67 72224.59 119467.23 56677.79 40796.41 81570.51
81592.81 81682.04 81481.29 81481.29 81682.04 81592.81
81570.51 40796.41 78983.09 55138.72 47242.64
97942.61 85027.83 117727.41 8.0E7

c
c

mode p

phys:p 20.0 0.0

c cut:n j 0.0

c phys:p 0 1 1

c esplt:n 0.5 0.1 0.5 0.01 0.25 0.001

c wwp:n 5 3 5 0 0.5

nps 300000000

c void

c

c -----
c ambient photon dose equiv. H*(10mm) Sv (from T-D1 of S&F)
c -----

de0 1.000E-02 1.500E-02 2.000E-02 3.000E-02 4.000E-02 5.000E-02
6.000E-02 8.000E-02 1.000E-01 1.500E-01 2.000E-01 3.000E-01
4.000E-01 5.000E-01 6.000E-01 8.000E-01 1.000E+00 1.500E+00
2.000E+00 3.000E+00 4.000E+00 5.000E+00 6.000E+00 8.000E+00
1.000E+01

df0 7.690E-14 8.460E-13 1.010E-12 7.850E-13 6.140E-13 5.260E-13
5.040E-13 5.320E-13 6.110E-13 8.900E-13 1.180E-12 1.810E-12
2.380E-12 2.890E-12 3.380E-12 4.290E-12 5.110E-12 6.920E-12
8.480E-12 1.110E-11 1.330E-11 1.540E-11 1.740E-11 2.120E-11
2.520E-11

c

c ***** MATERIAL CARDS

c *****

c AIR: ANSI/ANS-6.4.3, Dry air; density = 0.0012 g/cm³

c Composition by mass fraction

c *****

m1 7014 -.75519

8016 -.23179

6000 -.00014

18000 -.01288

c

```

c
c *****
c Fuel-Basket Nu-61b Cask
c Density = 2.511 g/cm^3; Composition by atom fraction
c *****
m4 92238 0.19053
    92235 0.00773
    40000 0.13149
    28000 0.01470
    26000 0.11116
    25055 0.00331
    24000 0.03318
    13027 0.11140
    8016 0.39652

c
c *****
c Top Fitting NU-61b Cask
c Density = 0.836 g/cm^3; Composition by atom fraction
c *****
m5 26000 0.45090
    28000 0.05961
    25055 0.01341
    24000 0.13457
    40000 0.11205
    13027 0.22945

c
c *****
c Plenum/Basket Nu-61b Cask
c Density = 0.790 g/cm^3; Composition by atom fraction
c *****
m6 26000 0.32657
    28000 0.04318
    40000 0.25966
    25055 0.00971
    24000 0.09746
    13027 0.26343

c
c *****
c Bottom/Basket Nu-61b
c Density = 1.284 g/cm^3; Composition by atom fraction
c *****
m7 26000 0.51974
    28000 0.06872
    25055 0.01545
    24000 0.15512
    13027 0.15415
    40000 0.08682

c
c *****
c Basket Periphery (SS304) TN-68 (Table 5.3-1)
c Density = 7.92 g/cm^3; Composition by atom fraction
c *****
m8 26000 0.68826
    25055 0.02013
    24000 0.20209
    28000 0.08952

c

```

```

c *****
c Carbon Steel TN-68 (Table 5.3-1)
c Density = 7.8212 g/cm^3; Composition by atom fraction
c *****
c m9 26000 0.95510
c 6000 0.04490
c
c *****
c Outer Basket/Rails TN-68 (Table 5.3-1)
c Density = 2.702 g/cm^3; Composition by atom fraction
c *****
c m10 13027 1.00000
c
c *****
c Resin/Aluminum Composite for TN-68 (Table 5.3-1)
c Density = 1.687 g/cm^3; Composition by atom fraction
c *****
c m12 13027 0.10331
c 6012 0.24658
c 8016 0.21985
c 1001 0.42207
c 5010 0.00164
c 5011 0.00655
c
c *****
c Balsa for Impact Limiter (Standard Composition SCALE4.4)
c density = 0.125 g/cm^3; Composition by atom fraction
c *****
c m15 6012 0.2857
c 8016 0.2381
c 1001 0.4762
c
c *****
c Lead for Gamma Shield (Standard Composition SCALE4.4)
c density = 11.34 g/cm^3; Composition by atom fraction
c *****
c m16 82000 1.0
c
c *****
c Polypropylene Disk TN-68 (Table 5.3-1)
c Density = 0.90 g/cm^3; Composition by atom fraction
c *****
c m17 6012 .33480
c 1001 .66520
c
c prdmp 2j 1
c print

```

TABLE 5.1-1

NUHOMS® MP-197/61BT SHIELD MATERIALS

<u>Component</u>	<u>Material</u>	<u>Density (g/cm³)</u>	<u>Thickness (inches)</u>
Cask Body Wall	Stainless Steel	7.92	3.75
	Lead	11.34	3.25
Cask Lid	Stainless Steel	7.92	4.50
Cask Bottom	Stainless Steel	7.92	6.50
Resin ^a	Polyester Resin Styrene Aluminum Hydrate Zinc Borate	1.58	4.56
Aluminum Box	Aluminum	2.7	0.12
Outer Shell	Stainless Steel	7.92	0.19
Basket ^b	Stainless Steel	7.92	Homogenized into source region
	Aluminum	2.7	
	Neutron Poison Material ^b		
Rails	Stainless Steel	7.92	0.44"
Impact Limiter	Stainless Steel	7.92	0.25
	Redwood	0.387	19.25 ^c
	Balsa Wood	0.125	15.25 ^c
Canister Wall	Stainless Steel	7.92	0.5"
Canister Lids	Stainless Steel	7.92	8.92"
Canister Bottom	Stainless Steel	7.92	7.5"

Notes:

- ^a The neutron shielding is borated polyester resin compound with a density of 1.58 g/cc.
- ^b This is modeled as plain aluminum for shielding purposes .
- ^c Thickness of wood is variable, redwood modeled as balsa.

TABLE 5.1-2

SUMMARY OF DOSE RATES
(Exclusive Use)

Normal Conditions	Package Surface mSv/h (mrem/h)			Vehicle Edge mSv/h (mrem/h)			2 Meter from Vehicle mSv/h (mrem/h)			
	Radiation	Top	Side	Bottom	Top	Side	Bottom	Top	Side	Bottom
Gamma	0.009 (0.9)	0.13 (13)	0.013 (1.3)	-	0.054 (5.4)	-	-	-	0.029 (2.9)	-
Neutron	0.009 (0.9)	1.25 (125) ¹	0.020 (2.0)	-	0.170 (17.0)	-	-	-	0.071 (7.1)	-
Total	0.018 (1.8)	1.38(137)	0.033 (3.3)	-	0.22 (22)	-	-	-	0.1 (10)	-
Limit	10 (1000)	10 (1000)	10 (1000)		2 (200)				0.1 (10)	

Hypothetical Accident Conditions	1 Meter from Package Surface mSv/h (mrem/h)			
	Radiation	Top	Side	Bottom
Gamma	< 0.008 (0.8)	0.15 (15)	< 0.011 (1.1)	
Neutron	< 0.009 (0.9)	4.25 (425)	< 0.020 (2.0)	
Total	< 0.017 (1.7)	4.41 (440)	< 0.031 (3.1)	
Limit	10 (1000)	10 (1000)	10 (1000)	

(1) Dose around key-way on cask.

TABLE 5.2-1

BWR FUEL ASSEMBLY DESIGN CHARACTERISTICS

Transnuclear, ID	7 x 7 - 49/0	8 x 8 - 63/1	8 x 8 - 62/2	8 x 8 - 60/4	8 x 8 - 60/1	9 x 9 - 74/2	10x10- 92/2
GE Designations	GE2 GE3	GE4	GE-5 GE-Pres GE-Barrier GE8 Type I	GE8 Type II	GE9 GE10	GE11 GE13	GE12
Max Length (in) ^a	176.2	176.2	176.2	176.2	176.2	176.2	176.2
Max Width (in) ^a	5.44	5.44	5.44	5.44	5.44	5.44	5.44
Rod Pitch (in)	0.738	0.640	0.640	0.640	0.640	0.566	0.510
No of Fueled Rods	49	63	62	60	60	66 full 8 partial	78 full 14 partial
Maximum Active Fuel Length (in)	144	146	150	150	150	146" full 90" partial	150" full 93" partial
Fuel Rod OD (in)	0.563	0.493	0.483	0.483	0.483	0.440	0.404
Clad Thickness (in)	0.032	0.034	0.032	0.032	0.032	0.028	0.026
Fuel Pellet OD (in)	0.487	0.416	0.410	0.410	0.411	0.376	0.345
No of Water Rods	0	1	2	4	1	2	2
Water Rod OD (in)	---	0.493	0.591	2 @ 0.591 2 @ 0.483	1.340	0.980	0.980
Water Rod ID (in)	---	0.425	0.531	2 @ 0.531 2 @ 0.419	1.260	0.920	0.920
Maximum MTU/assembly ^b	0.1977	0.1880	0.1886	0.1825	0.1834	0.1766	0.1867
Minimum Plenum Volume (in ³)	2.066	1.595	1.273	1.273	1.291	1.184	0.995
Fill Gas	He	He	He	He	He	He	He
Maximum Initial Rod Pressurization (psig)	10	10	80	80	80	155	155

^a Unirradiated length and width.

^b The maximum MTU/assembly is calculated based on the theoretical density. The calculated value is higher than the actual.

TABLE 5.2-1

BWR FUEL ASSEMBLY DESIGN CHARACTERISTICS
(continued)

Transnuclear, ID	7 x 7 - 49/0	8 x 8 - 63/1	8 x 8 - 62/2	8 x 8 - 60/4	8 x 8 - 60/1	9 x 9 - 74/2	10x10- 92/2
GE Designations	GE2 GE3	GE4	GE-5 GE-Pres GE-Barrier GE8 Type I	GE8 Type II	GE9 GE10	GE11 GE13	GE12
Max Length (in) ^a	176.2	176.2	176.2	176.2	176.2	176.2	176.2
Plenum Length (in)	16.47	14.47	10.47	10.47'	10.47	14.47	10.47
Top Fitting Length (in)	8.34	8.34	8.34	8.34	8.34	8.34	8.34
Bottom Fitting Length (in)	7.39	7.39	7.39	7.39	7.39	7.39	7.39

TABLE 5.2-2

BWR FUEL ASSEMBLY HARDWARE CHARACTERISTICS

Item	Material	Average Mass (kg/assembly)
<u>Fuel Zone</u>		49.2
Cladding	Zircaloy	1.95
Spacers	Zircaloy	0.36
Spacer Springs	Inconel	
<u>Fuel-Gas Plenum Zone</u>		4.89
Cladding	Zircaloy	1.05
Springs	Stainless Steel	
<u>Top End Fitting Zone</u>		2.08
Upper Tie Plate	Stainless Steel	0.05
Lock Tab Washers & Nuts	Stainless Steel	0.43
Expansion Springs	Inconel	1.26
End Plugs	Zircaloy	
<u>Bottom End Fitting Zone</u>		0.05
Finger Springs	Inconel	1.26
End Plugs	Zircaloy	4.70
Lower Tie Plate	Stainless Steel	
<u>Channel</u>		37.1
Channel Sleeve	Zircaloy	0.13
Channel Spacer & Rivet ^a	Stainless Steel	
Channel Fastener ^a		0.46
Guard	Stainless Steel	0.13
Spring & Bolt	Inconel	105.1
<u>Total</u>		

^a The channel spacer, rivet and fastener are located at top end fitting zone.

TABLE 5.2-3

MATERIAL COMPOSITIONS FOR FUEL ASSEMBLY HARDWARE MATERIALS

<u>Material</u> ^a	<u>Element</u>	<u>Weight %</u>
Zircaloy	Zirconium	98.225
	Tin	1.5
	Chromium	0.1
	Nitrogen	0.05
	Cobalt	0.001
Stainless Steel (SS304)	Iron	69.5
	Chromium	19.0
	Nickel	9.5
	Manganese	1.92
	Cobalt	0.08
Inconel	Nickel	73
	Chromium	15
	Iron	7
	Titanium	2.5
	Silicon	1.85
	Cobalt	0.649

^a Material compositions are taken from the SCALE Standard Composition Library, however, cobalt impurities are taken from Reference 2.

TABLE 5.2-4

BWR FUEL ASSEMBLY SOURCE (with CHANNELS)
 BUNDLE AVERAGE ENRICHMENT 3.3 wt% U235,
 40,000 MWD/MTU, 10 YEAR COOLING TIME

<u>Total Gamma Source (γ/sec/assembly)</u>	
<u>TN Design ID</u>	<u>Total</u>
7x7-49-0	1.38E15
8x8-63-1	1.32E15
8x8-62-2	1.30E15
8x8-60-4	1.28E15
8x8-60-1	1.29E15
9x9-74-2	1.24E15
10x10-92-2	1.31E15

<u>Total (α, n) plus Spontaneous Fission Neutron Source</u> <u>(n/sec/assembly)</u>	
<u>TN Design ID</u>	<u>Total</u>
7x7-49-0	8.98E07
8x8-63-1	8.21E07
8x8-62-2	7.89E07
8x8-60-4	8.06E07
8x8-60-1	8.05E07
9x9-74-2	6.92E07
10x10-92-2	7.22E07

TABLE 5.2-5
 PRIMARY GAMMA SOURCE SPECTRUM
 SCALE 18 GROUP STRUCTURE
 GENERAL ELECTRIC 7x7, BUNDLE AVERAGE ENRICHMENT 2.65wt% U235,
 35,000 MWD/MTU, AND 12 YEAR COOLING TIME
 WITH CHANNELS

<u>Scale Group</u>	<u>Energy Interval, MeV</u>	<u>Active Fuel Zone</u>	<u>γ/sec/assembly</u>		
			<u>Plenum Zone^a</u>	<u>Top Fitting Zone^a</u>	<u>Bottom Fitting Zone^a</u>
28	8.00E+00 to 1.00E+01	4.07E+04			
29	6.50E+00 to 8.00E+00	1.92E+05			
30	5.00E+00 to 6.50E+00	9.78E+05			
31	4.00E+00 to 5.00E+00	2.44E+06			
32	3.00E+00 to 4.00E+00	3.76E+07			
33	2.50E+00 to 3.00E+00	4.03E+08			
34	2.00E+00 to 2.50E+00	4.44E+09			
35	1.66E+00 to 2.00E+00	3.04E+10			
36	1.33E+00 to 1.66E+00	2.90E+12	9.54E+10	3.03E+11	3.22E+11
37	1.00E+00 to 1.33E+00	1.72E+13	3.38E+11	1.07E+12	1.14E+12
38	8.00E-01 to 1.00E+00	1.57E+13			
39	6.00E-01 to 8.00E-01	5.32E+14			
40	4.00E-01 to 6.00E-01	2.92E+13			
41	3.00E-01 to 4.00E-01	1.09E+13			
42	2.00E-01 to 3.00E-01	1.65E+13			
43	1.00E-01 to 2.00E-01	5.55E+13			
44	5.00E-02 to 1.00E-01	7.90E+13			
45	1.00E-02 to 5.00E-02	2.82E+14			
	Total	1.04E+15	4.33E+11	1.38E+12	1.46E+12

^a Cobalt-60 is the gamma source of significance in the fuel assembly hardware.

TABLE 5.2-6
 NEUTRON SOURCE DISTRIBUTION
 GENERAL ELECTRIC 7x7,
 BUNDLE AVERAGE ENRICHMENT 2.65wt% U-235,
 35,000 MWD/MTU, AND 12 YEAR COOLING TIME
 WITH CHANNELS

TOTAL (α, n PLUS SPONTANEOUS FISSION) NEUTRON SOURCE
 SCALE STRUCTURE USING SPECTRA FOR URANIUM DIOXIDE

<u>Scale Group</u>	<u>Energy Interval, MeV</u>	<u>n/sec/assembly</u>
1	6.43E+00 to 2.00E+01	1.36E+06
2	3.00E+00 to 6.43E+00	1.55E+07
3	1.85E+00 to 3.00E+00	1.72E+07
4	1.40E+00 to 1.85E+00	9.67E+06
5	9.00E-01 to 1.40E+00	1.31E+07
6	4.00E-01 to 9.00E-01	1.42E+07
7	1.00E-01 to 4.00E-01	2.79E+06
	Total	7.38E+07

TABLE 5.2-7

SOURCE TERM SUMMARY

SAS2H Source Terms

Summary

Neutron and Gamma Source As a Function of Burnup, Water Density and Active Core Height

7x7 Fuel Assembly 40,000 MWd/MtU Average Burnup 10 Years Cool Time

Power (MW) 5 Cycle Length (days) 527.2

Output File Name	Zone	Frac Core Height	Peaking Factor	Burnup (MWd/MtU)	SAS2H Power (MW)	Water Density (g/cc)	Neutron Source (n/s)	Neutron Peaking Factor	Gamma Source (g/s)	Gamma Peaking Factor
7x7-9-36.output	12	0.95-1.0	0.2410	9640	1.205	0.3609	1.661E+04	0.0028	1.574E+13	0.2303
7x7-25-36.output	11	0.90-0.95	0.6330	25320	3.165	0.3631	6.500E+05	0.1093	4.275E+13	0.6255
7x7-36-37.output	10	0.8-0.9	0.8973	35891	4.486	0.3701	6.005E+06	0.5047	1.238E+14	0.9053
7x7-43-39.output	9	0.7-0.8	1.0766	43065	5.383	0.3861	1.274E+07	1.0707	1.499E+14	1.0964
7x7-46-41.output	8	0.6-0.7	1.1515	46061	5.758	0.4118	1.647E+07	1.3842	1.535E+14	1.1227
7x7-47-43.output	7	0.5-0.6	1.1912	47649	5.956	0.4375	1.859E+07	1.5624	1.663E+14	1.2164
7x7-48-47.output	6	0.4-0.5	1.2000	48000	6.000	0.4708	1.877E+07	1.5775	1.674E+14	1.2244
7x7-48-53.output	5	0.3-0.4	1.2000	48000	6.000	0.5251	1.819E+07	1.5288	1.671E+14	1.2223
7x7-47-59.output	4	0.2-0.3	1.1836	47345	5.918	0.5945	1.649E+07	1.3859	1.644E+14	1.2027
7x7-43-70.output	3	0.1-0.2	1.0750	43001	5.375	0.7008	1.005E+07	0.8447	1.484E+14	1.0854
7x7-31-75.output	2	0.05-0.1	0.7746	30985	3.873	0.7541	1.002E+06	0.1683	5.245E+13	0.7674
7x7-9-76.output	1	0.0-0.05	0.2357	9426	1.178	0.7603	1.100E+04	0.0018	1.542E+13	0.2256
Average/Total			0.9917	39670	4.959	0.5016	1.190E+08	1.0000	1.367E+15	1.0000

Uniform Case 0.0-1.0 1 40000 5 0.432 8.976E+07 1.382E+15
 Ratio to Non-Uniform Case 1.326 0.989

TABLE 5.3-1

MATERIALS INPUT FOR MCNP

Zone	Material	Density (g/cc)	Element/Nuclide	Library Identifier	Atomic Number Density (atoms/barn-cm)		
Fuel/Basket*	UO ₂	1.727	U-235	92235	1.502E-04		
			U-238	92238	3.703E-03		
			O	8016	7.706E-03		
	Zircaloy	0.394	Zr	40302	2.556E-03		
			Cr	24304	6.448E-04		
	SS304	0.293	Mn	25055	6.424E-05		
			Fe	26304	2.160E-03		
			Ni	28304	2.856E-04		
			Aluminum	0.097	Al	13027	2.165E-03
			Plenum/Basket*	0.329	Zr	40302	2.134E-03
Cr	24304	8.010E-04					
Mn	25055	7.980E-05					
Fe	26304	2.684E-03					
Ni	28304	3.548E-04					
Aluminum	0.097	Al	13027	2.165E-03			
		Top Fitting/Basket*	0.163	Zr	40302	1.057E-03	
				Cr	24304	1.270E-03	
				Mn	25055	1.265E-04	
				Fe	26304	4.254E-03	
Ni	28304			5.625E-04			
Aluminum	0.097	Al	13027	2.165E-03			
		Bottom Fitting/Basket*	0.188	Zr	40302	2.179E-03	
				Cr	24304	2.170E-04	
				Mn	25055	7.300E-03	
				Fe	26304	9.651E-04	
Ni	28304			1.219E-03			
Aluminum	0.0.097	Al	13027	2.165E-03			
		Basket Periphery (rails)	7.92	Cr	24304	1.743E-02	
				Mn	25055	1.736E-03	
				Fe	26304	5.936E-02	
				Ni	28304	7.721E-03	
Resin/Aluminum	Resin (1.58 g/cc) & Al (2.702 g/cc)			1.687	O	8016	2.245E-02
			Al	13027	1.055E-02		
			C	6012	2.518E-02		
			H	1001	4.310E-02		
			B-10	5010	1.662E-04		
			B-11	5011	6.692E-04		
(gamma shield)	Lead	11.34	Pb	82000	3.296E-02		
Impact Limiter	Balsa Wood	0.125	C	6012	2.787E-03		
			O	8016	2.323E-03		
			H	1001	4.646E-03		

* - One-half of basket mass in the region

TABLE 5.4-1

RESPONSE FUNCTIONS FOR GAMMA

<u>Photon Energy (MeV)</u>	<u>Response (10^{-12} Sv cm²)</u>
0.01	0.0769
0.015	0.846
0.02	1.01
0.03	0.785
0.04	0.614
0.05	0.526
0.06	0.504
0.08	0.532
0.10	0.611
0.15	0.890
0.20	1.18
0.30	1.81
0.40	2.38
0.50	2.89
0.60	3.38
0.80	4.29
1.0	5.11
1.5	6.92
2.0	8.48
3.0	11.1
4.0	13.3
5.0	15.4
6.0	17.4
8.0	21.2
10.0	25.2

TABLE 5.4-2

RESPONSE FUNCTIONS FOR NEUTRON

Neutron Energy (MeV)	Response (10^{-12} Sv cm ²)
2.5E-8	8.0
1.0E-7	10.4
1.0E-6	11.2
1.0E-5	9.2
1.0E-4	7.1
1.0E-3	6.2
1.0E-2	8.6
2.0E-2	14.6
5.0E-2	35.0
1.0E-1	69.0
2.0E-1	126
5.0E-1	258
1.0	340
1.5	362
2.0	352
3.0	380
4.0	409
5.0	378
6.0	383
7.0	403
8.0	417
10.0	446
14.0	520
17.0	610
20.0	650

FIGURE 5.1-1

NUHOMS®-MP197 CASK SHELDDING CONFIGURATION

**FIGURE WITHHELD AS SENSITIVE
UNCLASSIFIED INFORMATION**

FIGURE 5.2-1

AXIAL BURNUP PROFILE FOR DESIGN BASIS FUEL

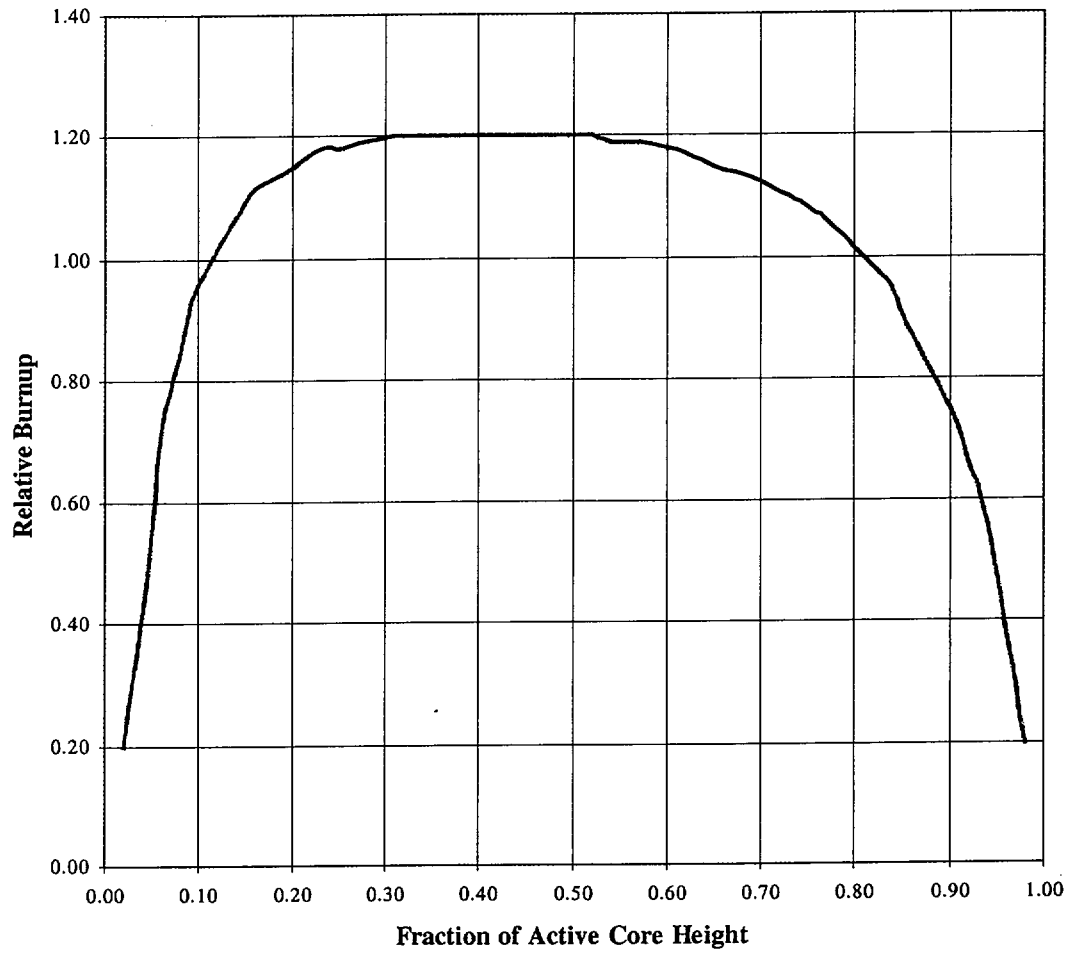


FIGURE 5.3-1

MCNP TOP HALF MODEL

**FIGURE WITHHELD AS SENSITIVE
UNCLASSIFIED INFORMATION**

All dimensions in cm.

FIGURE 5.3-2

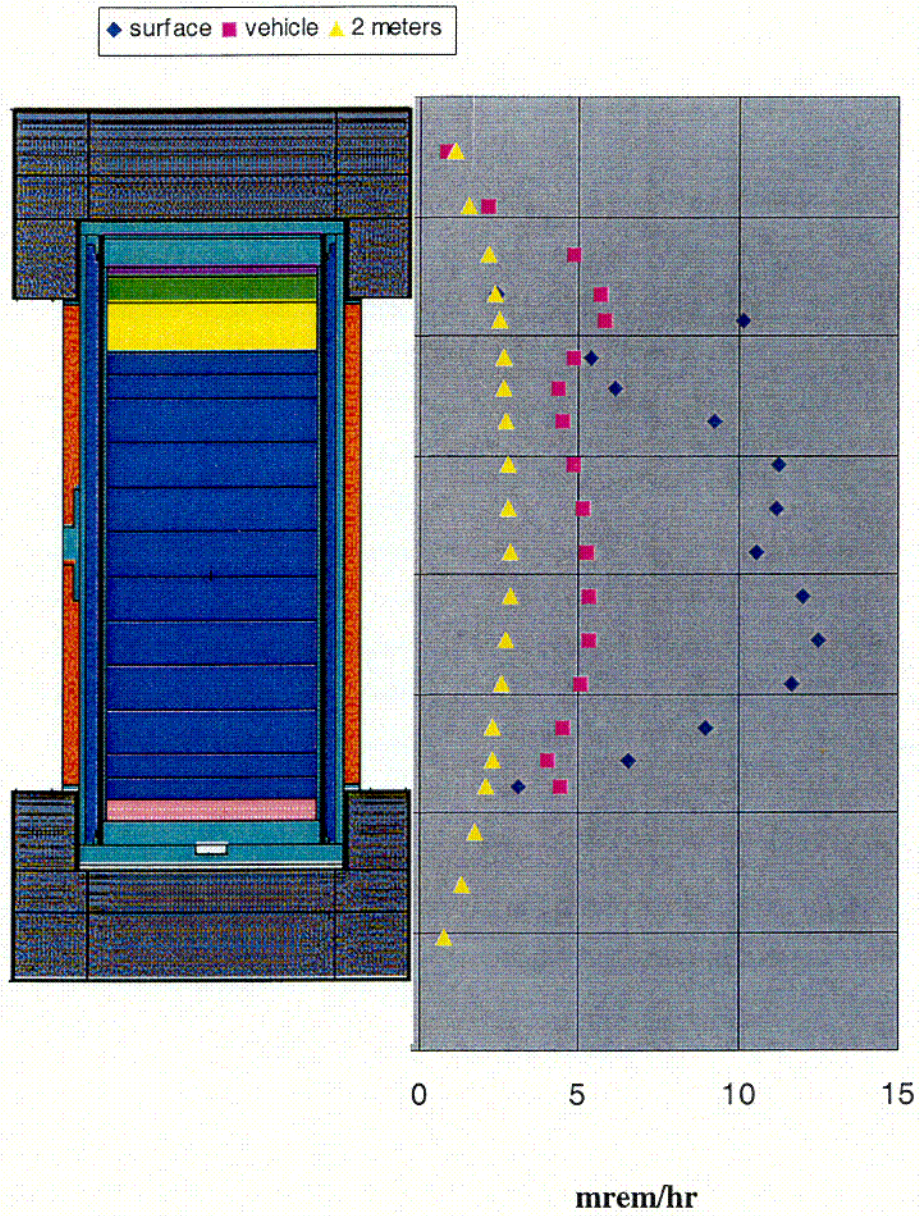
MCNP BOTTOM HALF MODEL

**FIGURE WITHHELD AS SENSITIVE
UNCLASSIFIED INFORMATION**

All dimensions in cm.

Rev0 4/01

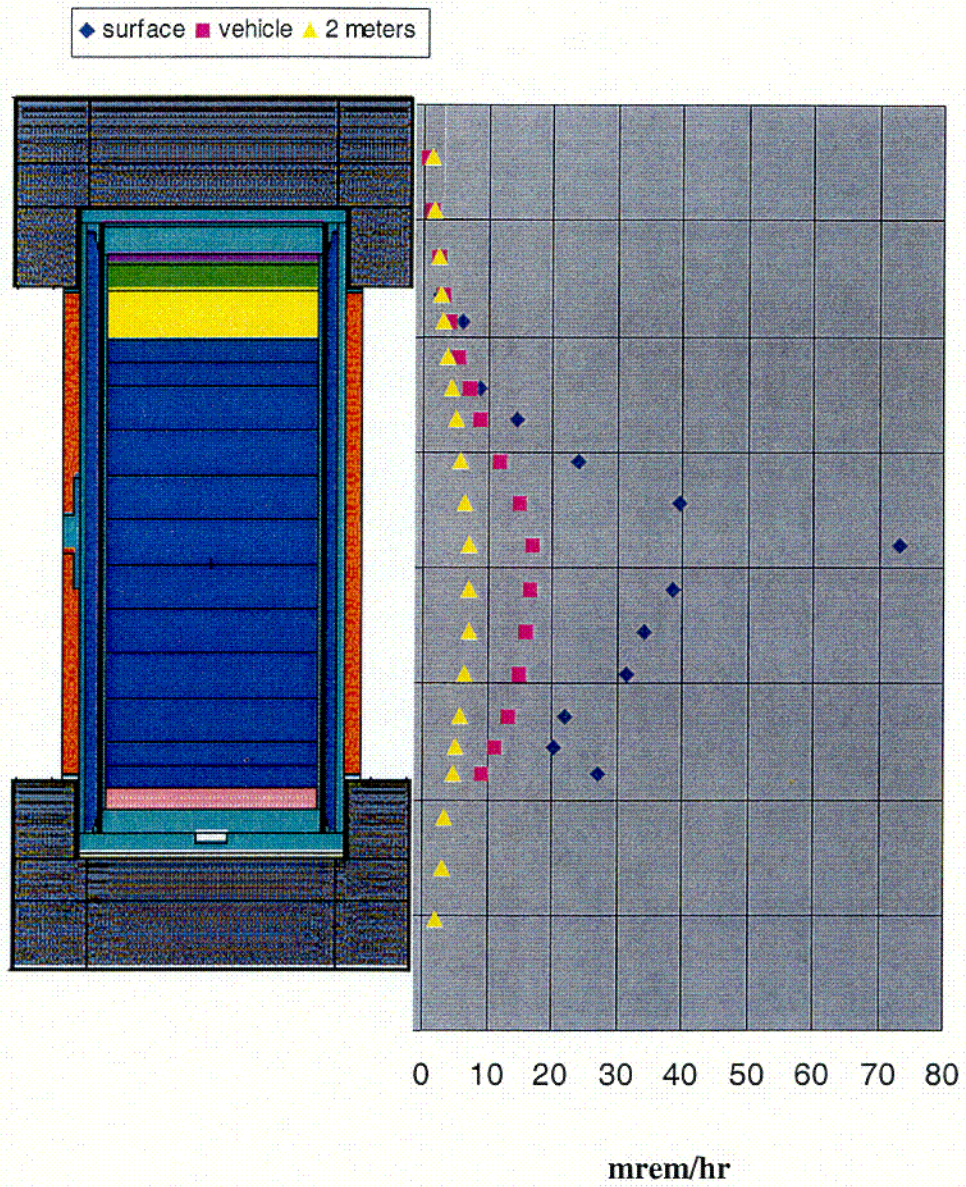
FIGURE 5.4-1
NUHOMS[®]-MP197 RADIAL GAMMA DOSE RATE PROFILE



C02

FIGURE 5.4-2

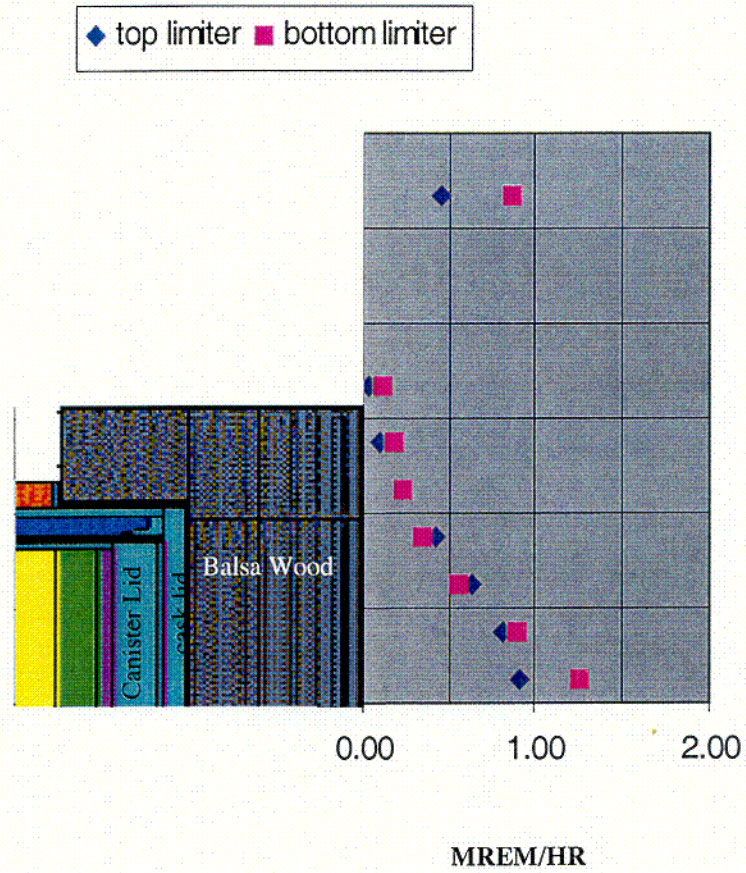
NUHOMS[®]-MP197 RADIAL NEUTRON DOSE RATE PROFILE



C03

FIGURE 5.4-3

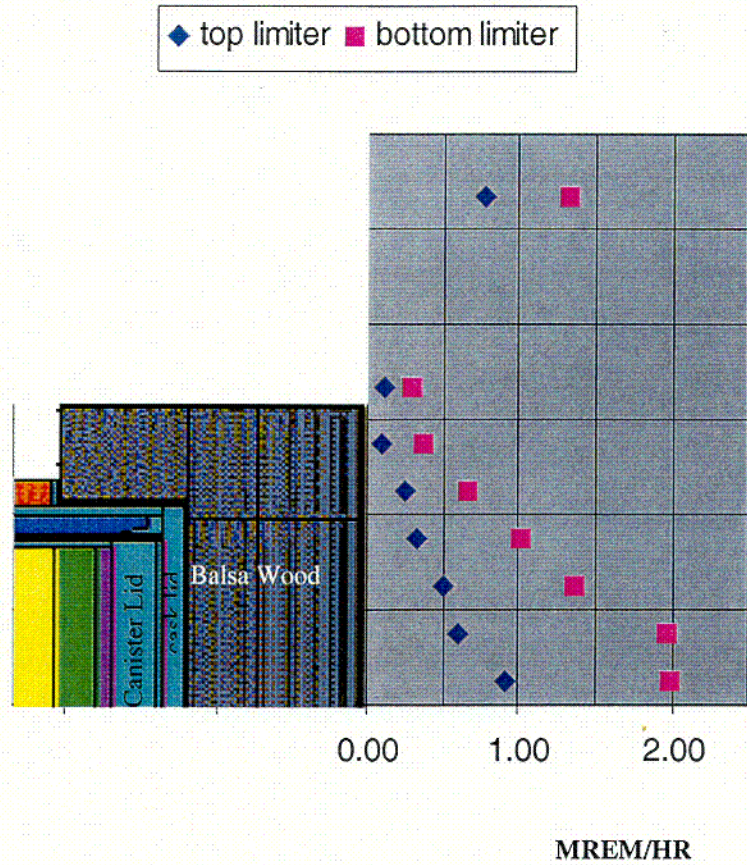
NUHOMS[®]-MP197 GAMMA DOSE RATE
IMPACT LIMITER SURFACE



204

FIGURE 5.4-4

NUHOMS[®]-MP197 NEUTRON DOSE RATE
IMPACT LIMITER SURFACE



C05